REGULATORS OF MAMMALIAN MEIOSIS

By
Tara M. Little

A dissertation submitted to Johns Hopkins University in conformity with the requirements for the degree of Doctor of Philosophy

Baltimore, Maryland
August 2020

Abstract

Meiosis is the process in which one diploid cell is divided into four haploid gametes. This process must be tightly regulated, as errors can result in infertility, genetic mutation, or miscarriage. In mammals, this process is sexually dimorphic. Spermatogenesis begins during puberty and continues cyclically throughout the lifetime of the male. In contrast, oocytes are formed during embryogenesis, then arrest until immediately prior to ovulation. Oocytes are also unique in that they undergo acentriolar division, instead relying on microtubule organizing centers. Due to these differences in timing and organization, many meiotic regulators function differently in each sex. This thesis explores the roles of three meiotic proteins, and how those roles differ between oocytes and spermatocytes. I examine the meiotic roles of polo-like kinase 1 (PLK1) in oogenesis and demonstrate that it is a critical regulator of microtubule organizing center (MTOC) and liquid-like spindle domain (LISD) organization. I also investigate the localization of another polo-like kinase, PLK4, during spermatogenesis. Additionally, I present preliminary data evaluating the possibly sexually dimorphic roles of both PLK4 and SAS4. Together, the results presented in this thesis supports the sexually dimorphic regulation of mammalian meiosis.

Advisor:

Philip Jordan, Ph.D.

Readers:

Valeria Culotta, Ph.D.

Yumi Kim, Ph.D.

Erika Matunis, Ph.D.

Photini Sinnis, M.D.

Alternate Readers:

Jennifer Kavran, Ph.D.

Sean Prigge, Ph.D.

Acknowledgements

In memory of Alice M. Twigg and Gladys M. Biser, who both inspired me to become a strong and stubborn woman.

I have been incredibly fortunate to have the support of many people throughout my journey at Johns Hopkins. It would be impossible to name everyone that has played a role in both my personal and professional development. I am forever grateful for all of those who have encouraged me.

I am immensely thankful for my advisor, Dr. Philip Jordan. I would not have attained this degree without his unwavering support, enthusiasm, and patience. His advice and insight have pushed me to become both a better scientist and a better person. I hope to emulate his mentorship and leadership throughout my career.

I also want to thank my thesis committee members and readers, Drs. Valeria Culotta, Erika Matunis, Yumi Kim, Sergi Rego, Photini Sinnis, Sean Prigge and Jennifer Kavran. All provided invaluable feedback on my projects and professional development. Drs. Pierre Coulombe and Michael Matunis supported me through an incredibly challenging time in my tenure. I owe many thanks to the dedicated BMB administrative staff, who work tirelessly to support all of the students in the program.

I have had the privilege of working alongside many amazing lab mates throughout my graduate career. Thank you to Jess, Grace, Steve, Marina, Alisa, Michelle, Maggie, Romina, Chris, Maria, Xueqi, Yujiao, Nat and Adina for your friendship and input over these last few years. I am forever indebted to Jingwen

Xu, Anagha Sadasivan, and Abhinaya Ganesan for their contributions towards my projects.

Some of my fondest memories at Hopkins are a result of time shared with my classmates. Thank you to Danielle Bouchard and Harry Liu for their comrade during our first year and beyond. I would also like to thank Abby Zieman, Justin Jacobs, Yajuan Guo, Fengrong Wang, Elizabeth Alexander, Rebecca Ursin, and Haobo Wang for their friendship as we all moved through the program.

I would not be half the person I am today without the unwavering support and love from my family. I would not have pursued science as a career if it were not for my cousin, Jamie, setting the example. My grandparents always encouraged me to pursue my dreams, regardless of how far-fetched they seemed. I want to thank all the members of my extended family for their support, as well.

My husband has stood with me from day one of this endeavor, always cheering me on through both the good and bad times. Thank you for never wavering in the face of the hectic schedules, heavy workloads, and large quantities of takeout over the past few years. I could not have done this without you by my side.

Finally, I want to thank two of the most important people in my life. I cannot accurately describe the credit I owe to my Mom and Dad. I am blessed to have the most amazing parents anyone could ask for. They have always pushed me to do my best, personally and professionally. They have supported me, even when they were not quite sure what I was thinking. I owe you both for everything that I have achieved.

Table of Contents

Abstract ..... **ii**

Acknowledgements ..... **iv**

Table of Contents ..... **vi**

Summary of Tables ..... **ix**

Summary of Figures ..... **x**

Background and Summary **1**

Chapter I: PLK1 is required for chromosome compaction and microtubule organization in mouse oocytes **6**

Abstract 6

Introduction 7

Materials and Methods 13

Results 17

Conditional knockout of Plk1 in oocytes results in infertility 17

Plk1 cKO oocytes fail to form polar bodies 18

Plk1 cKO oocytes show abnormal chromosome compaction 21

Plk1 cKO oocytes fail to form normal bipolar metaphase I spindles 24

Plk1 cKO oocytes display defects in MTOC and LISD distribution 24

Discussion 32

PLK1 and NEBD 32

Role for PLK1 during chromosome compaction before segregation 33

PLK1 is essential for acentriolar bipolar spindle formation in oocytes 34

Acknowledgements 41

Table I: Primers used in this study 46

Table II: Antibodies used in this study 47

Supplemental Table III: Cre efficiency 48
References 49
Chapter II: PLK4 localizes to the centrioles in mouse spermatocytes……..55
Abstract 55
Introduction 56
Materials and Methods 62
Results and Discussion 64
mCherry-PLK4 localizes to the MTOCs of oocytes 64
mCherry-PLK4 localizes to the centrioles of spermatocytes 64
Future Directions and Preliminary Conclusions 67
Acknowledgements 74
Table I: Primers used in this study 75
Table II: Antibodies used in this study 76
References 77
Chapter III: The roles of PLK4 and SAS4 in mammalian meiosis 80
Abstract 80
Introduction 81
Materials and Methods 84
Preliminary Results 86
Sas4 cKO; Spo11-Cre males fail to develop mature spermatozoa 86
Sas4 cKO; Stra8-Cre spermatocytes undergo apoptosis in prophase 90
Sas4 cKO females are fertile 90
Plk4 cKO males develop undersized testes 95
Plk4 cKO oocytes successfully form a bipolar metaphase spindle 98
Discussion 98
Future Directions and Concluding Remarks 109

Supplementary Text III.1: yH2AX localization in *Sas4* cKO males.....111

Supplementary Table I: Primers used in this study.....114

Supplementary Table II: Antibodies used in this study 115

References 116

Appendix.....121

Master List of References 121

Curriculum Vitae 131

Summary of Tables

Supplemental Table I.1: Primers used in this study..... 46

Supplemental Table I.2: Antibodies used in this study 47

Supplemental Table I.3: Analysis of Cre excision efficiency..... 48

Supplemental Table II.1: Primers used in this study..... 75

Supplemental Table II.2: Antibodies used in this study 76

Supplemental Table III.1: Primers used in this study..... 114

Supplemental Table III.2: Antibodies used in this study 115

Summary of Figures

I.1: Structure of polo-like kinases 11

I.2: PLK1 localizes to the microtubule organizing centers and centromeres in oocytes 19

I.3: *Plk1* cKO follicle numbers and NEBD timing are equivalent to control, but oocytes fail to extrude the first polar body 22

I.4: *Plk1* cKO oocytes undergo abnormal chromosome compaction following NEBD 25

I.5: *Plk1* cKO oocytes form abnormal alpha-tubulin spindle structures during meiotic resumption 27

I.6: *Plk1* cKO oocytes fail to disperse C-NAP1 following meiotic resumption 30

I.7: *Plk1* cKO oocytes display abnormal localization of MTOC components 35

I.8: *Plk1* cKO oocytes display abnormal localization of LISD components 37

I.9: *Plk1* regulates chromosome condensation, MTOC fragmentation, and LISD recruitment in mammalian oocytes 42

Supplemental Figure I.1: Western blot analysis of PLK1 depletion 44

II.1: Centriole duplication is aligned with the cell cycle 57

II.2: mCherry-PLK4 localizes to the MTOCs in oocytes 65

II.3: *mCherry-Plk4; Spo11-Cre* males 68

II.4: mCherry-PLK4 localizes to the centrioles of spermatocytes 71

III.1: *Sas4* cKO; *Spo11-Cre* males develop normally sized testes 88

III.2: *Sas4* cKO; *Spo11-Cre* spermatocytes do not duplicate their centrioles 91

III.3: *Sas4* cKO; *Spo11-Cre* males do not produce mature spermatozoa 93

III.4: *Sas4* cKO; *Stra8-Cre* spermatocytes arrest in prophase I 96

III.5: *Sas4* cKO oocytes 101

III.6: PLK4 depletion results in decreased testes size 103

III.7: *Plk4* cKO oocytes 106

Supplementary Figure III.1: yH2AX localization in *Sas4* cKO males 112

Background and Summary

Background

During meiosis, one diploid mother cell is divided into four haploid daughter cells. This process requires the precise organization and regulation of cellular machinery to ensure that genetic information is properly divided. Dividing germ cells rely on subcellular structures to first separate homologous chromosomes in meiosis I, and then subsequently separate sister chromatids in meiosis II. Errors in meiosis can result in improperly divided gametes, causing infertility or miscarriage (Bazzi and Anderson, 2014; Bettencourt-Dias et al., 2005; Harris et al., 2011; Holubcová et al., 2015; Namgoong and Kim, 2018).

In mammals, this process is sexually dimorphic. Spermatocytes make use of canonical centrosomes, much like the mechanisms in mitotically dividing cells. The centrioles localize to the spindle poles and serve as a nucleation site for microtubules, which in turn form the metaphase spindle. In contrast, oocytes undergo acentriolar division, and instead rely on microtubule organizing centers (MTOCs). The stages of mammalian meiosis also occur at different times in males and females. The meiotic stages of spermatogenesis begin in puberty and continue in a cyclical manner throughout the lifetime of the organism. Oocytes, on the other hand, undergo most of prophase I while the female is still an embryo. The oocytes will then enter a late prophase arrest – referred to as a dictyate arrest – a few days after the female is born. Starting at puberty, a small number of oocytes will resume meiosis immediately prior to ovulation.

These differences in mechanisms and timing present unique challenges for each sex. Dividing spermatocytes need to properly duplicate and divide centrioles (Bettencourt-Dias et al., 2005; Sumiyoshi et al., 2002). Oocytes must maintain the integrity of both MTOCs and condensed chromatin during the extended dictyate arrest (Nagaoka et al., 2012; Schatten and Sun, 2015; Webster and Schuh, 2017). Based on these differences, it is hypothesized that mammalian oocytes and spermatocytes use different regulatory mechanisms to ensure that meiosis is completed properly.

Summary

The works presented in this thesis aim to further evaluate the differences between male and female meiosis. We investigate the roles of three different proteins, utilizing several mouse models with germ-cell specific conditional genetic mutations. The included data proposes previously unknown roles for these proteins, and further confirms the drastic sexual dimorphism in mammalian meiosis.

In Chapter I, I detail our studies of polo-like kinase 1 (PLK1) in oogenesis. Research into PLK1's meiotic roles have previously relied on RNA interference and chemical inhibition, which have produced conflicting results (Clift and Schuh, 2015; Lee and Rhee, 2011). We utilize a *Plk1* conditional knockout (cKO) mouse model to independently demonstrate that PLK1 is essential for multiple steps of oogenesis, including chromatin compaction, MTOC organization and LISD recruitment.

Another member of the polo-like kinase family, PLK4, is also known to have an important role in mitosis. PLK4 has been shown to regulate mitotic centriole biogenesis (Arquint and Nigg, 2016; Arquint et al., 2012; Moyer and Holland, 2019). PLK4 is known to localize to MTOCs in mammalian oocytes (Bury et al., 2017; Luo and Kim, 2015), but its localization in spermatocytes is unknown. In Chapter II, we aim to better understand its localization. We utilize a conditional overexpression mouse model (Basto et al., 2006) in which germ cells express high levels of a *mCherry-Plk4* transgene. We show that the tagged protein localizes to the centrioles of spermatocytes, indicating that PLK4 plays a role in centriolar regulation.

In Chapter III, I further investigate the meiotic regulation of both centrioles and MTOCs. We use a novel *Plk4* cKO mouse model to better evaluate roles of PLK4 in both males and females. We also use a *Sas4* cKO model to determine the meiotic roles of SAS4, a scaffolding protein that forms the foundation of centrioles in mitosis (Gopalakrishnan et al., 2011; Kuriyama, 2009; Leidel and Gönczy, 2003). Our preliminary results show that both PLK4 and SAS4 are necessary for spermatogenesis, while SAS4 does not appear to be essential for oogenesis.

References

Arquint, C., and Nigg, E.A. (2016). The PLK4-STIL-SAS-6 module at the core of centriole duplication. Biochem. Soc. Trans. *44*, 1253–1263.

Arquint, C., Sonnen, K.F., Stierhof, Y.-D., and Nigg, E.A. (2012). Cell-cycle-regulated expression of STIL controls centriole number in human cells. J. Cell Sci. *125*, 1342–1352.

Basto, R., Lau, J., Vinogradova, T., Gardiol, A., Woods, C.G., Khodjakov, A., and Raff, J.W. (2006). Flies without centrioles. Cell *125*, 1375–1386.

Bazzi, H., and Anderson, K.V. (2014). Acentriolar mitosis activates a p53-dependent apoptosis pathway in the mouse embryo. Proc. Natl. Acad. Sci. USA *111*, E1491–500.

Bettencourt-Dias, M., Rodrigues-Martins, A., Carpenter, L., Riparbelli, M., Lehmann, L., Gatt, M.K., Carmo, N., Balloux, F., Callaini, G., and Glover, D.M. (2005). SAK/PLK4 is required for centriole duplication and flagella development. Curr. Biol. *15*, 2199–2207.

Bury, L., Coelho, P.A., Simeone, A., Ferries, S., Eyers, C.E., Eyers, P.A., Zernicka-Goetz, M., and Glover, D.M. (2017). Plk4 and Aurora A cooperate in the initiation of acentriolar spindle assembly in mammalian oocytes. J. Cell Biol. *216*, 3571–3590.

Clift, D., and Schuh, M. (2015). A three-step MTOC fragmentation mechanism facilitates bipolar spindle assembly in mouse oocytes. Nat. Commun. *6*, 7217.

Gopalakrishnan, J., Mennella, V., Blachon, S., Zhai, B., Smith, A.H., Megraw, T.L., Nicastro, D., Gygi, S.P., Agard, D.A., and Avidor-Reiss, T. (2011). Sas-4 provides a scaffold for cytoplasmic complexes and tethers them in a centrosome. Nat. Commun. *2*, 359.

Harris, R.M., Weiss, J., and Jameson, J.L. (2011). Male hypogonadism and germ cell loss caused by a mutation in Polo-like kinase 4. Endocrinology *152*, 3975–3985.

Holubcová, Z., Blayney, M., Elder, K., and Schuh, M. (2015). Human oocytes. Error-prone chromosome-mediated spindle assembly favors chromosome segregation defects in human oocytes. Science *348*, 1143–1147.

Kuriyama, R. (2009). Centriole assembly in CHO cells expressing Plk4/SAS6/SAS4 is similar to centriogenesis in ciliated epithelial cells. Cell Motil. Cytoskeleton *66*, 588–596.

Lee, K., and Rhee, K. (2011). PLK1 phosphorylation of pericentrin initiates centrosome maturation at the onset of mitosis. J. Cell Biol. *195*, 1093–1101.

Leidel, S., and Gönczy, P. (2003). SAS-4 is essential for centrosome duplication in C elegans and is recruited to daughter centrioles once per cell cycle. Dev. Cell *4*, 431–439.

Luo, Y.-B., and Kim, N.-H. (2015). PLK4 is essential for meiotic resumption in mouse oocytes. Biol. Reprod. *92*, 101.

Moyer, T.C., and Holland, A.J. (2019). PLK4 promotes centriole duplication by phosphorylating STIL to link the procentriole cartwheel to the microtubule wall. Elife *8*.

Nagaoka, S.I., Hassold, T.J., and Hunt, P.A. (2012). Human aneuploidy: mechanisms and new insights into an age-old problem. Nat. Rev. Genet. *13*, 493–504.

Namgoong, S., and Kim, N.-H. (2018). Meiotic spindle formation in mammalian oocytes: implications for human infertility. Biol. Reprod. *98*, 153–161.

Schatten, H., and Sun, Q.-Y. (2015). Centrosome and microtubule functions and dysfunctions in meiosis: implications for age-related infertility and developmental disorders. Reprod Fertil Dev *27*, 934–943.

Sumiyoshi, E., Sugimoto, A., and Yamamoto, M. (2002). Protein phosphatase 4 is required for centrosome maturation in mitosis and sperm meiosis in C. elegans. J. Cell Sci. *115*, 1403–1410.

Webster, A., and Schuh, M. (2017). Mechanisms of aneuploidy in human eggs. Trends Cell Biol. *27*, 55–68.

Chapter I

PLK1 is required for chromosome compaction and microtubule organization in mouse oocytes

Tara M. Little and Philip W. Jordan

This chapter was published in Molecular Biology of the Cell (2020) and is reproduced here with minor edits.

Abstract

Errors during meiotic resumption in oocytes can result in chromosome missegregation and infertility. Several cell cycle kinases have been linked with roles in coordinating events during meiotic resumption, including polo-like kinases (PLKs). Mammals express four kinase-proficient PLKs (PLK1–4). Previous studies assessing the role of PLK1 have relied on RNA knockdown and kinase inhibition approaches, as *Plk1* null mutations are embryonically lethal. To further assess the roles of PLK1 during meiotic resumption, we developed a *Plk1* conditional knockout (cKO) mouse to specifically mutate *Plk1* in oocytes. Despite normal oocyte numbers and follicle maturation, *Plk1* cKO mice were infertile. From analysis of meiotic resumption, *Plk1* cKO oocytes underwent nuclear envelope breakdown with the same timing as control oocytes. However, *Plk1* cKO oocytes failed to form compact bivalent chromosomes, and localization of cohesin and condensin were defective. Furthermore, *Plk1* cKO oocytes either failed to organize α-tubulin or developed an abnormally small bipolar spindle. These abnormalities were attributed to aberrant release of the microtubule organizing center (MTOC) linker protein, C-NAP1, and the failure to recruit MTOC components and liquid-like spindle domain (LISD) factors. Ultimately, these defects result in meiosis I arrest before homologous chromosome segregation.

Introduction

Meiosis is a specialized cell division that results in the generation of haploid gametes from a diploid precursor germ cell. During meiosis, newly replicated homologous chromosomes become associated with one another via crossover recombination events. During the first meiotic division (meiosis I), homologous chromosomes segregate from one another, whereas sister chromatids remain paired until the second meiotic division (meiosis II). Errors during meiosis can lead to mutation, aneuploidy, and infertility.

Mammalian female meiosis possesses several unique features that are prone to error. First, meiosis is arrested at two different stages. Meiosis is initiated during embryogenesis, and arrests in late prophase, at a stage known as dictyate. During meiotic prophase, before arrest, chromosomes are subjected to induced DNA double-strand breaks that require repair via homologous recombination, which results in at least one crossover recombination event that stably links homologous chromosomes (Gray and Cohen, 2016). The amount of time for this first meiotic arrest differs from one oocyte to another. This is because meiotic prophase arrest is dictated by hormonal induced oocyte maturation, which is cyclical and results in one or a small subset of oocytes maturing for ovulation. It has been well documented that oocytes that remain arrested at dictyate for longer periods of time display depleted levels of proteins that are critical for meiotic resumption and chromosome segregation (Nagaoka *et al.*, 2012; Schatten and Sun, 2015; Webster and Schuh, 2017). For example, the structural maintenance of chromosome (SMC) complexes, cohesin and SMC5/6, have been implicated in

increased oocyte age-related errors in chromosome segregation (Burkhardt *et al.*, 2016; Hwang *et al.*, 2017; Jessberger, 2012; MacLennan *et al.*, 2015). Following meiotic resumption, oocytes undergo meiosis I where homologous chromosomes segregate, but sister chromatids remain associated with one another via centromeric cohesion (MacLennan *et al.*, 2015). Sister chromatids then align on a metaphase II plate but remain arrested unless the oocyte is fertilized (Mogessie *et al.*, 2018).

Another strikingly unique feature of oocytes is that they undergo meiotic divisions in an acentriolar manner. Instead, microtubule organizing centers (MTOCs), containing pericentrosomal components, including CEP192, gamma-tubulin, and NEDD1, are fragmented within the oocyte following nuclear envelope breakdown (NEBD) and the resumption of meiosis I (Baumann *et al.*, 2017; Clift and Schuh, 2015; Lee *et al.*, 2017; Ma *et al.*, 2017). Prior to meiotic resumption, MTOCs are held together by a linker protein, C-NAP1 (Sonn et al., 2011). C-NAP1 also links together centrioles in spermatocytes and mitotic cells (Vlijm et al., 2018; Zhang et al., 2015). In mitosis, PLK1 has been shown to phosphorylate C-NAP1 to induce centriole separation (Mardin et al., 2011).

In parallel to MTOC fragmentation, Aurora A kinase facilitates the distribution of a liquid-like meiotic spindle domain (LISD) by phosphorylating LISD component, TACC3 (So *et al.*, 2019). The LISD is essential for the stabilization of microtubules emanating from the MTOCs. The fragmented MTOCs then coalesce evenly into two MTOC structures on either side of the condensing bivalent chromosomes and form the bipolar spindle required to facilitate chromosome segregation

during meiosis I (Namgoong and Kim, 2018). It has been demonstrated that disassociation of C-NAP1 from the MTOC must occur before MTOC fragmentation and subsequent downstream steps (Clift and Schuh, 2015; Lee and Rhee, 2011).

The family of polo-like kinases (PLKs) consist of several closely related proteins with highly conserved structures (de Cárcer et al., 2011a). Each PLK has an N-terminal kinase domain and one to several C-terminal polo-box domains (Figure I.1). The polo-box domains contain tandem amino acid sequences that recognize serine and threonine motifs on target proteins (Almawi et al., 2020; Elia et al., 2003; Lee and Amon, 2003). Interactions at these domains have been shown to affect both localization and activation of the kinase (Elia et al., 2003). PLKs are found in all eukaryotic organisms. Mammals have 5 PLKs, each with unique functions. Mammalian PLK1-4 are known to play a role in mitotic division. PLK1 has been shown to regulate kinetochore and spindle organization in mitosis (de Cárcer et al., 2011a; Gheghiani et al., 2017; Li et al., 2008; Zhang et al., 2009). PLK2 regulates centriole duplication throughout developing embryos and in adult neuronal cells (Cizmecioglu et al., 2008; Cozza and Salvi, 2018; Ma et al., 2003). PLK3 is believed to be involved in cellular stress and the p53 apoptotic pathway (Aquino Perez et al., 2020; Bahassi et al., 2006; Xie et al., 2001). PLK4 regulates centriole duplication in mitotic cells, but has also been shown to be essential for meiotic resumption and acentriolar spindle formation in mammalian oocytes (Bettencourt-Dias et al., 2005; Bury et al., 2017; Ko et al., 2005; Luo and Kim, 2015; Moyer and Holland, 2019). In contrast, PLK5 is an inactive kinase which is believed to induce apoptosis in quiescent neuronal cells (de Cárcer et al., 2011b).

PLK2 and PLK3 null mice develop into adulthood, with significant mitotic defects (Ma et al., 2003; Myer et al., 2011). PLK1 and PLK4 null mutations are embryonically lethal (Lu et al., 2008; Rosario et al., 2010).

PLK1 and PLK4 have also been shown to regulate mammalian meiosis, although their roles are not as well understood as in mitosis. Through the use of chemical inhibitors, PLK1 has been shown to regulate meiotic chromosome condensation and spindle formation (Solc et al., 2015; Zhang et al., 2017). PLK1 is also believed to contribute to nuclear envelope breakdown (NEBD) in mammalian oocytes (Clift and Schuh, 2015). Chemical inhibition, genetic mutation and RNAi-based experiments have demonstrated that PLK4 is also essential for mammalian meiosis (Bury et al., 2017; Harris et al., 2011; Luo and Kim, 2015).

Since PLK1 null mutations are embryonically lethal, studies into PLK1's function in meiosis have been limited to RNA interference (RNAi) or chemical inhibitor-based depletion. Using these approaches, inhibition of PLK1 kinase function and has been shown to inhibit C-NAP1 disassociation from MTOCs, which causes defects in MTOC biogenesis and prevents the formation of conventional bipolar spindles (Clift and Schuh, 2015). While these studies are informative, these approaches are limited. Given the close structural similarity of the PLK family, it is possible that RNAi or inhibitors may affect other PLKs. Given the temporal dependence of RNAi and inhibitors, it is also possible that pre-treatment and post-treatment levels of PLK1 are sufficient to perform certain functions. A purely

Figure I.1: Members of the PLK family share a similar structure consisting of an N-terminal kinase domain and C-terminal polo-box domains (designated “PB”). The amino acid length of each protein is noted on the right side.

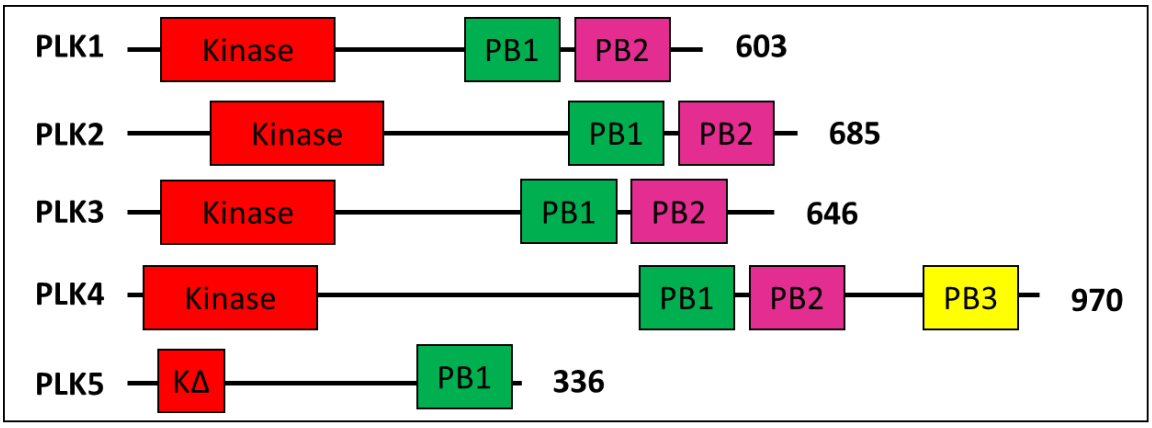
PLK1
Kinase
PB1
PB2
603
PLK2
Kinase
PB1
PB2
685
PLK3
Kinase
PB1
PB2
646
PLK4
Kinase
PB1
PB2
PB3
970
PLK5
KΔ
PB1
336

genetic model of depletion is necessary to better understand PLK1's roles in meiosis.

To further our collective understanding of the requirements for PLK1 during meiotic resumption in mammals, we utilized a *Plk1* conditional knockout approach to mutate *Plk1* specifically in mouse oocytes before meiotic resumption. We demonstrate the importance of PLK1 in ensuring female fertility and show novel findings with regard to chromosome architecture, and regulation of MTOC and LISD regulation.

Materials and Methods

Ethics Statement

All mice were bred at Johns Hopkins University (JHU, Baltimore, MD) in accordance with the National Institutes of Health and U.S. Department of Agriculture criteria. Protocols for their care and use were approved by the Institutional Animal Care and Use Committees of JHU.

Mice

mESC clones HEPD0663_7_E04 (C57BL/6N-A/a genetic background) bearing a "knockout first" allele of *Plk1* (*Plk1*tm1a(EUCOMM)Hmgu) were acquired from the Knockout Mouse Project (https://www.mousephenotype.org/data/genes/MGI:97621).

Chimeras were obtained by microinjection of HEPD0663_7_E04 mESCs into C57BL/6JN blastocyst-stage mouse embryos and assessed for germline transmission. Heterozygous progeny were bred with a C57BL/6J Flp recombinase deleter strain (B6.129S4-*Gt(ROSA)26Sor*tm1(FLP1)Dym/RainJ, JAX) to remove

the *SA-LacZ* and *Neo* selection cassette and produce the floxed exon 4 (designated *Plk1 flox*).

To produce offspring heterozygous for the deleted exon 4 (designated *Plk1 del*), heterozygous *Plk1 flox* males were mated to *Sox2-Cre* C57BL/6J (B6.Cg-Tg(Sox2-cre)1Amc/J, JAX) mice.

Further, heterozygous *Plk1 del* mice were bred to mice harboring the Cre transgenes that are specifically expressed in germ cells—*Spo11-Cre* (C57BL/6-Tg Spo11-cre)1Rsw/PecoJ), *Gdf9-Cre* (C57BL/6-Tg (Gdf9-icre)5092Coo/J), and *Zp3-Cre* (C57BL/6-Tg(Zp3-cre)93Knw/J)—which resulted in male progeny heterozygous for the *Plk1 del* allele and hemizygous for the germ cell–specific Cre transgene. These mice were bred to female homozygous *Plk1 flox* mice to derive *Plk1* cKO (*Plk1 flox/del, Cre*) and control (*Plk1 +/flox*) genotypes.

PCR genotyping

Primers used are described in Supplemental Table I.1. PCR conditions: 90°C for 2 min; 30 cycles of 90°C for 20 s, 58°C for annealing, 72°C for 1 min.

Oocyte harvesting and culture

Neonatal mice were harvested 1–2 d postpartum. Ovaries were dissected using methods previously described (Hwang *et al.*, 2018b).

Adult female mice were injected intraperitoneally with 5 IU of equine chorionic gonadotropin (Sigma) to stimulate ovarian follicle development. GV-staged oocytes were harvested from ovaries 44–48 h later. For metaphase II oocytes, mice were injected with 5 IU of equine chorionic, then injected with 5 IU of human chorionic gonadotropin (Sigma) 48 h later. Metaphase II oocytes were harvested

from the ampulla 12 h later. Oocytes were cultured in M2 medium supplemented with 5% fetal bovine serum (FBS; Life Technologies), and 3 mg/ml bovine serum albumin (BSA; Sigma-Aldrich). Oocyte-cumulus cell complexes were exposed to 300 IU/ml hyaluronidase (Sigma) in M2 medium supplemented with 3 mg/ml BSA to denude oocytes of surrounding cumulus cells.

For GVBD to metaphase I analyses, oocytes were harvested into M2 medium supplemented with 5% FBS, 3 mg/ml BSA, and 10 mM milrinone (Sigma-Aldrich). The oocytes were then washed and cultured in M2 medium supplemented with 5% FBS and 3 mg/ml BSA, and visually assessed for GVBD throughout a 6-h incubation. For premetaphase timepoints, oocytes were incubated for less time (0 h for dictyate, 2 h for NEBD, and 4 h for prometaphase). Metaphase-stage oocytes were harvested after a 6-h incubation.

Histology and microscopy

For histological assessment of oocytes, ovaries were fixed with Bouin's fixative, sectioned (5 μm thick), and stained with hematoxylin and eosin. Follicle stages were determined by visual assessment, as reported previously (Hwang *et al.*, 2017).

Oocyte chromatin spreads and whole-oocyte mounts for immunofluorescence microscopy analyses were performed using techniques previously described (Hwang *et al.*, 2018b). Primary antibodies used and dilutions are listed in Supplemental Table I.2. Secondary antibodies against mouse, rabbit, and human IgG and conjugated to Alexa 488, 568, or 633 (Life Technologies) were

used at 1:500 dilution. Preparations were then mounted with Vectashield + DAPI medium (Vector Laboratories) or Clearmount (Invitrogen).

Images were captured using a Zeiss Cell Observer Z1 linked to an ORCA-Flash 4.0 CMOS camera (Hamamatsu) and analyzed with the Zeiss ZEN 2012 blue edition image software. Photoshop (Adobe) was used to prepare figure images. Images shown are representative of defects and were chosen to demonstrate the observed phenotypes.

Meiotic substages of oocytes were determined visually using either SYCP3, alpha-tubulin, or DNA morphology. For quantification, metaphase-stage oocytes were identified by having condensed chromatin or bipolar alpha-tubulin localization. Quantification of MTOC and LISD components only included oocytes with at least one of those two characteristics.

Spindle dimensions were visualized with alpha-tubulin antibodies and measured using ImageJ (National Institutes of Health). Spindle length was defined as the distance from one spindle pole to the other. Spindle width was measured across the widest part of the spindle.

Graph preparation and statistical analysis was performed using GraphPad Prism (GraphPad Software). Two-tailed Mann-Whitney tests were performed to determine *P* values. The number of samples used for each quantification is included in the corresponding figure legend.

Results

Conditional knockout of Plk1 in oocytes results in infertility

We used a floxed *Plk1* allele (*Plk1 flox*) to assess the requirement for PLK1 during meiotic resumption in female mice (Figure I.2A; see *Materials and Methods*). Breeding heterozygous *Plk1 flox* mice to mice expressing the Cre recombinase transgene generated a knockout (KO) allele termed *Plk1 del* (Figure I.2A). We tested three germ cell–specific Cre transgenes, *Spo11-Cre*, *Gdf9-Cre*, and *Zp3-Cre*. *Spo11-Cre* is expressed during early prophase of meiosis, before the dictyate meiotic arrest (Hwang *et al.*, 2018a; Lyndaker *et al.*, 2013). In contrast, the *Gdf9-Cre* and *Zp3-Cre* are both expressed following the dictyate meiotic arrest, but before resumption of meiosis (Lan *et al.*, 2004). *Gdf9-Cre* is first expressed in primordial follicles by 3 d postpartum (dpp), and *Zp3-Cre* is first expressed in primary follicles by 5 dpp.

We first assessed PLK1 depletion in conditional knockout (cKO) oocytes compared with controls by assessing PLK1 localization via immunofluorescence microscopy during meiotic resumption. Consistent with previous studies (Clift and Schuh, 2015; Pahlavan *et al.*, 2000; So *et al.*, 2019; Solc *et al.*, 2015; Sun *et al.*, 2012; Wang *et al.*, 2017; Xiong *et al.*, 2008), PLK1 localizes to the developing spindle and kinetochores of the condensed bivalents (Figure I.2, B and D). Surprisingly, despite observing efficient deletion of the floxed third exon of *Plk1* (Supplemental Table I.1), cKO of *Plk1* using *Gdf9-Cre* or *Zp3-Cre* did not result in depletion of PLK1 protein (Supplemental Figure I.2, A and B). These observations demonstrate that mRNA levels and protein levels before conditional mutation of

the *Plk1 flox* allele are sufficient to maintain PLK1 protein levels during meiotic progression. In contrast, using the *Spo11-Cre* transgene resulted in the absence of PLK1 protein in *Plk1* cKO oocytes in metaphase I (Figure I.2, C and E and Supplemental Figure I.2, C and D). Therefore, we focused on *Plk1*, *Spo11-Cre* cKO mice in this study.

Breeding *Plk1* +/*flox, Spo11-Cre* females to wild-type males showed that mutation of the *Plk1 flox* allele mediated by *Spo11-Cre* was 90% efficient (Supplemental Table I.3). Because *Spo11-Cre* is expressed in early prophase, it is possible that defects could be occurring in newborn oocytes, before the dictyate arrest. Therefore, we assessed the meiotic stages of oocytes from newborn females and did not observe morphological differences with regard to prophase stage distribution, or synapsis and desynapsis morphology (Figure I.2, F and G).

Plk1 cKO oocytes fail to form polar bodies

Adult *Plk1, Spo11-Cre* cKO females failed to produce litters ($N = 5$). Despite this infertility, *Plk1* cKO females had normal ovarian morphology and equivalent oocyte numbers (Figure I.3, A and B). We isolated oocytes from control and *Plk1*, *Spo11-Cre* cKO mice and assessed synchronized meiotic resumption in vitro. We measured nuclear envelope breakdown (NEBD, also known as germinal vesicle breakdown, GVBD) and first polar body formation. NEBD was equivalent between controls and *Plk1*, *Spo11-Cre* cKO oocytes (Figure I.3C). To address whether oocytes would reach a metaphase II arrest stage, we assessed ovulated oocytes harvested from the ampulla. At this timepoint, control oocytes were arrested in

Figure I.2: PLK1 localizes to the microtubule organizing centers and centromeres in oocytes. (A) Schematic of mouse *Plk1* floxed allele containing loxP sites (red triangle), flanking exon 4 (gray box), and the resulting *Plk1* deletion allele after excision of exon 3 by Cre recombinase in early prophase. The purple round-sided rectangle represents the remaining Frt site following FLP-mediated recombination of the original conditional ready tm1a allele (see *Materials and Methods*). (B, C) Control (B) and *Plk1* cKO (C) oocytes immunolabeled with antibodies against PLK1 (green) and alpha-tubulin (α-TUB, red), and counterstained with DAPI (DNA, blue). Scale bar: 10 μm. (D, E) Chromatin spread preparation of control (D, scale bar: 5 μm) and *Plk1* cKO (E, scale bar: 5 μm) oocytes immunolabeled with antibodies against PLK1 (green) and centromeres/kinetochores (CEN, purple), and counterstained with DAPI (DNA, blue). (F) Chromatin spread preparations of control and *Plk1* cKO pachytene- and diplotene-stage oocytes harvested from newborn females (2 dpp). Spreads are stained with SYCP3 (green) and counterstained with DAPI (DNA, purple). Scale bar: 10 μm. (G) Quantification of meiosis I stages of oocytes harvested from newborn females (1–2 dpp). Six control mice and four *Plk1* cKO mice were assessed, with 100 oocytes counted per mouse. Mean and SD of each column are represented by the black bars. No significant difference between the control and *Plk1* cKO was observed according to a Mann-Whitney test (two-tailed).

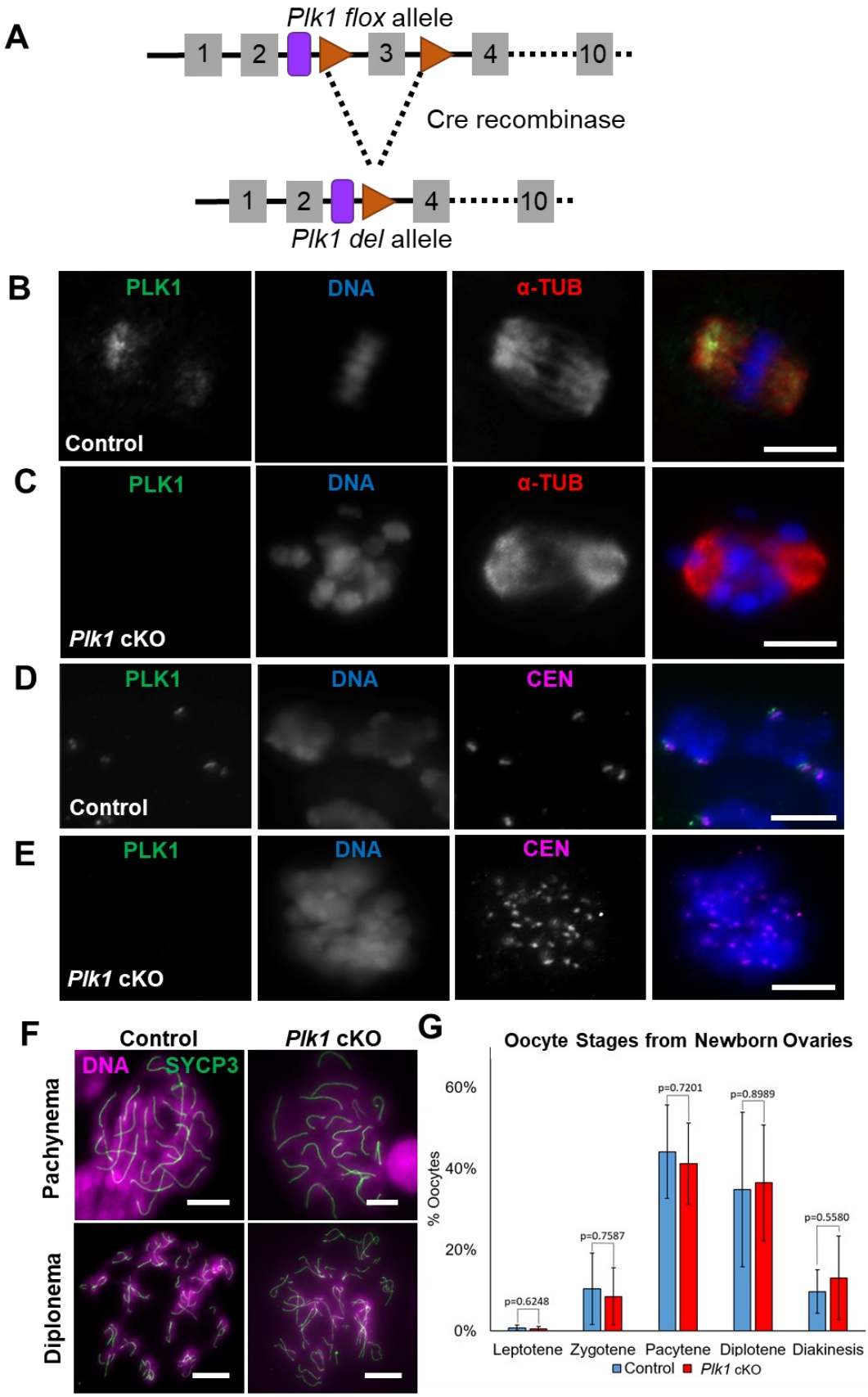
A
Plk1 flox allele
1
2
3
4
10
Cre recombinase
1
2
4
10
Plk1 del allele
B
PLK1
DNA
α-TUB
Control
C
PLK1
DNA
α-TUB
Plk1 cKO
D
PLK1
DNA
CEN
Control
E
PLK1
DNA
CEN
Plk1 cKO
F
Control
Plk1 cKO
DNA SYCP3
Pachynema
Diplonema
G
Oocyte Stages from Newborn Ovaries
% Oocytes
60%
40%
20%
0%
p=0.6248
p=0.7587
p=0.7201
p=0.8989
p=0.5580
Leptotene
Zygotene
Pacytene
Diplotene
Diakinesis
Control
Plk1 cKO

metaphase II with an attached polar body. In contrast, *Plk1*, *Spo11-Cre* cKO failed to extrude the first polar body (Figure I.3D). Assessment of oocytes via immunofluorescence microscopy indicated that *Plk1*, *Spo11-Cre* cKO oocytes failed to undergo metaphase-to-anaphase transition during meiosis I (Figure I.3E). Thus, our studies focused on the transition from NEBD to metaphase I.

Plk1 cKO oocytes show abnormal chromosome compaction

During meiotic resumption, homologous chromosomes associated via chiasmata (crossovers) condense and form easily discernible bivalent structures (Figure I.4A). We assessed bivalent formation, and compared axis morphology between the control and *Plk1*, *Spo11-Cre* cKO by analyzing cohesin and condensin localization in oocytes 6 h after meiotic resumption. From observing chromosome spread preparations, almost all control oocytes display bivalent chromosome morphology (Figure I.4, A and B). In contrast, 40% of *Plk1*, *Spo11-Cre* cKO oocytes failed to form compact chromosomes, instead having dispersed chromatin signal where resolution between separate chromosome pairs was not evident. We assessed axis formation in more detail by analyzing REC8 and SMC4, cohesin and condensin components, respectively. REC8-cohesin complexes form a single axial structure along the bivalent core (Figure I.4C). The expected axial localization of cohesin was observed for most chromatin spread preparations of control oocytes (Figure I.4, C and D). However, 40% of *Plk1*, *Spo11-Cre* cKO oocytes displayed only partial cohesin axis formation. Condensin forms two separate axes within the bivalent (Figure I.4E). The chromatin morphology defects observed for *Plk1*, *Spo11-Cre* cKO were further highlighted by assessing

Figure I.3: *Plk1* cKO follicle numbers and NEBD timing are equivalent to control, but oocytes fail to extrude the first polar body. (A) Cross sections of ovaries from adult control and *Plk1* cKO mice stained with hematoxylin and eosin. Scale bar: 250 μm. (B) Quantification of follicle stages from hematoxylin and eosin stained ovaries from control and *Plk1* cKO mice. Ten ovaries were counted per genotype. Mean and SD of the columns of each graph are represented by the black bars. No significant difference between the control and *Plk1* cKO was observed according to a Mann-Whitney test (two-tailed). (C) Timing of NEBD in oocytes from control and *Plk1* cKO mice. Oocytes (434) from 10 control mice and 401 oocytes from 10 *Plk1* cKO mice were assessed. Mean and SD of the columns of each graph are represented by the blue circles (control), pink squares (*Plk1* cKO), and corresponding bars. No significant difference between the control and *Plk1* cKO was observed according to a Mann-Whitney test (two-tailed). (D) Quantification of first polar body extrusion in control and *Plk1* cKO metaphase II oocytes collected from ampullas. Oocytes (84) from 5 control mice and 35 oocytes from 4 *Plk1* cKO mice were assessed. The majority of control oocytes scored without a polar body are likely a result of polar body loss during the collection and staining process. Bars represent 95% confidence intervals, and the *P* value (Mann-Whitney, two-tailed) for the indicated comparison is significant ($P < 0.0001$). (E) Examples of metaphase II control and *Plk1* cKO oocytes stained for alpha-tubulin (α-TUB, green) and DNA (DAPI, purple). Dotted circles indicate the outline of oocytes. Scale bar: 20 μm.

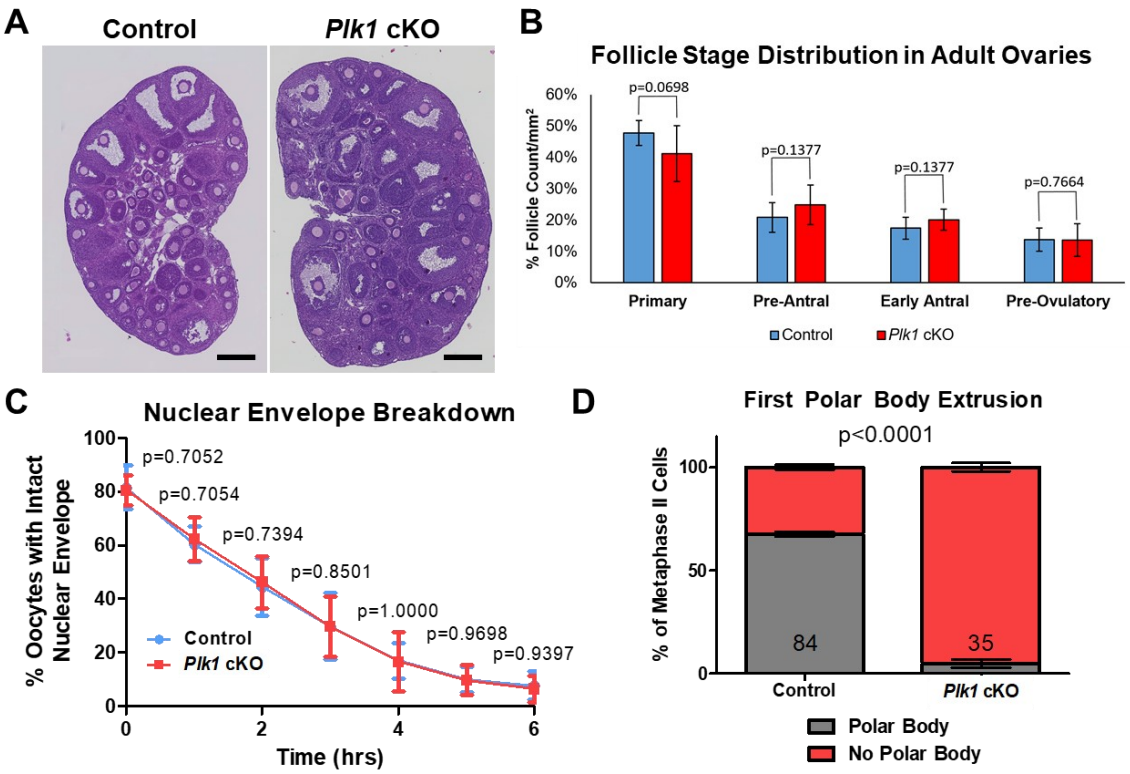
A
Control
Plk1 cKO
B
Follicle Stage Distribution in Adult Ovaries
% Follicle Count/mm²
60%
50%
40%
30%
20%
10%
0%
p=0.0698
p=0.1377
p=0.1377
p=0.7664
Primary
Pre-Antral
Early Antral
Pre-Ovulatory
Control
Plk1 cKO
C
Nuclear Envelope Breakdown
% Oocytes with Intact Nuclear Envelope
100
80
60
40
20
0
p=0.7052
p=0.7054
p=0.7394
p=0.8501
p=1.0000
p=0.9698
p=0.9397
Control
Plk1 cKO
0
2
4
6
Time (hrs)
D
First Polar Body Extrusion
p<0.0001
% of Metaphase II Cells
100
50
0
84
35
Control
Plk1 cKO
Polar Body
No Polar Body
E
α-TUB
DNA
Control
Plk1 cKO

condensin localization where the majority of oocytes had only partial condensin axial localization (55%), and a significant number with dispersed condensin localization throughout the chromatin (24%; Figure I.4, E and F).

Plk1 cKO oocytes fail to form normal bipolar metaphase I spindles

During meiotic resumption, acentriolar MTOC components fragment throughout the oocyte, then coalescence evenly on either side of the condensing bivalents to form the bipolar metaphase I spindle required to mediate chromosome segregation during meiosis I (Clift and Schuh, 2015). We first assessed bipolar spindle formation, using antibodies raised against alpha-tubulin, 6 h after meiotic resumption. From observing whole-oocyte preparations, almost all control oocytes developed a bipolar metaphase I spindle (Figure I.5, A and B). In contrast, 60% of *Plk1*, *Spo11-Cre* cKO oocytes formed a bipolar spindle, and the remaining 40% of oocytes did not harbor any alpha-tubulin signal. From further analyses of the bipolar spindle that formed in 60% of *Plk1*, *Spo11-Cre* cKO oocytes, we determined that the alpha-tubulin spindle length and width were reduced compared with the control oocytes (Figure I.5, C–E). Taken together, these data indicate that PLK1 is important for regulation of acentriolar MTOC dynamics following meiotic resumption in mouse oocytes, which is critical for the formation of bipolar spindles that are capable of mediating chromosome segregation during the metaphase-to-anaphase I transition.

Plk1 cKO oocytes display defects in MTOC and LISD distribution

Although we did observe bipolar spindles in 60% of the *Plk1*, *Spo11-Cre* cKO oocytes, these were morphologically abnormal, being both shorter in length

Figure I.4: *Plk1* cKO oocytes undergo abnormal chromosome compaction following NEBD. (A) Chromatin spread preparation of control (on the left, compact) and *Plk1* cKO (on the right, disperse) oocytes counterstained with DAPI (DNA). Scale bar: 10 μm. (B) Quantification of chromatin compaction. 151 oocytes from 19 control mice and 201 oocytes from 14 *Plk1* cKO mice were assessed. Bars represent 95% confidence intervals, and the *P* value (Mann-Whitney test, two-tailed) for the indicated comparison is significant (*P* = 0.0027). (C) Chromatin spreads of control and *Plk1* cKO oocytes immunolabeled with antibodies against REC8 (green), and counterstained with DAPI (DNA, purple). Scale bar: 5 μm. (D) Quantification of REC8 axis morphology. Oocytes (36) from 11 control mice and 28 oocytes from 9 *Plk1* cKO mice were assessed. Bars represent 95% confidence intervals, and the *P* value (Mann-Whitney test, two-tailed) for the indicated comparison is significant (*P* = 0.02). (E) Chromatin spreads of control and *Plk1* cKO oocytes immunolabeled with antibodies against SMC4 (green), and counterstained with DAPI (DNA, purple). Scale bar: 2 μm. (F) Quantification of SMC4 axis morphology. Oocytes (40) from 10 control mice and 26 oocytes from 9 *Plk1* cKO mice were assessed. Bars represent 95% confidence intervals, and the *P* value (Mann-Whitney test, two-tailed) for the indicated comparison is significant (*P* = 0.0003).

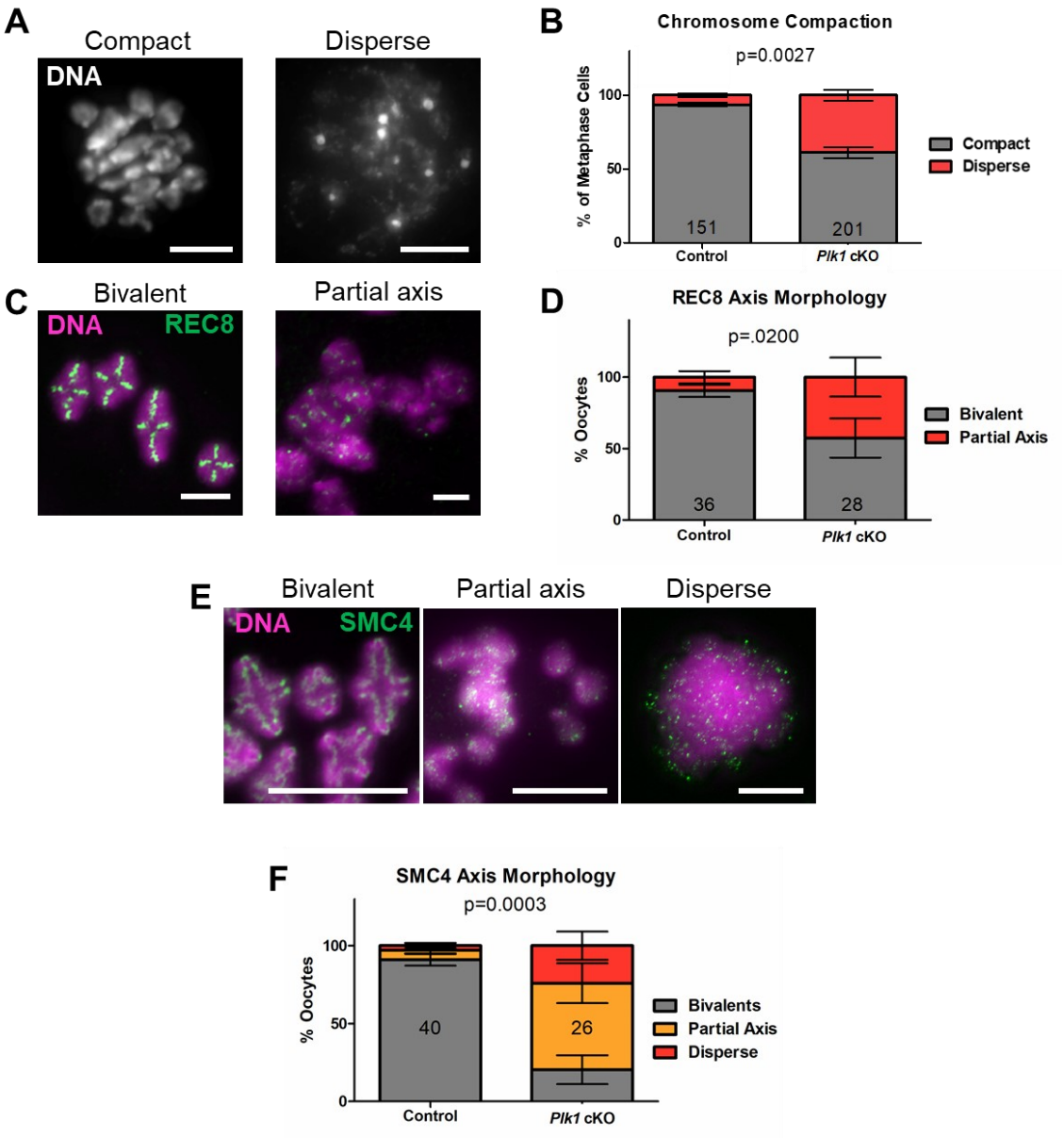
A
Compact
Disperse
DNA
B
Chromosome Compaction
p=0.0027
% of Metaphase Cells
100
50
0
151
201
Control
Plk1 cKO
Compact
Disperse
C
Bivalent
Partial axis
DNA
REC8
D
REC8 Axis Morphology
p=.0200
% Oocytes
100
50
0
36
28
Control
Plk1 cKO
Bivalent
Partial Axis
E
Bivalent
Partial axis
Disperse
DNA
SMC4
F
SMC4 Axis Morphology
p=0.0003
% Oocytes
100
50
0
40
26
Control
Plk1 cKO
Bivalents
Partial Axis
Disperse

Figure I.5: *Plk1* cKO oocytes form abnormal alpha-tubulin spindle structures during meiotic resumption. (A) Examples of control and *Plk1* cKO oocytes immunolabeled with antibodies against alpha-tubulin (α-TUB, green), and counterstained with DAPI (DNA, purple). Scale bar: 10 μm. (B) Quantification of alpha-tubulin localization. Oocytes (160) from 18 control mice and 224 oocytes from 14 *Plk1* cKO mice were assessed. Bars represent 95% confidence intervals, and the *P* value (Mann-Whitney test, two-tailed) for the indicated comparison is significant ($P = 0.0011$). (C) Examples of an average sized control spindle and small *Plk1* cKO spindles immunolabeled with antibodies against alpha-tubulin (α-TUB, green), and counterstained with DAPI (DNA, purple). Scale bar: 10 μm. (D) Box plot of spindle length from each spindle pole. Oocytes (33) from 9 control mice and 35 oocytes from 8 *Plk1* cKO mice were assessed. Whiskers represent minimum and maximum values, and the *P* value (Mann-Whitney test, two-tailed) for the indicated comparison is significant ($P < 0.0001$). (E) Box plot of the width of each spindle pole. Oocytes (33) from 9 control mice and 35 oocytes from 8 *Plk1* cKO mice were assessed. Whiskers represent minimum and maximum values, and the *P* value (Mann-Whitney test, two-tailed) for the indicated comparison is significant ($P = 0.0002$).

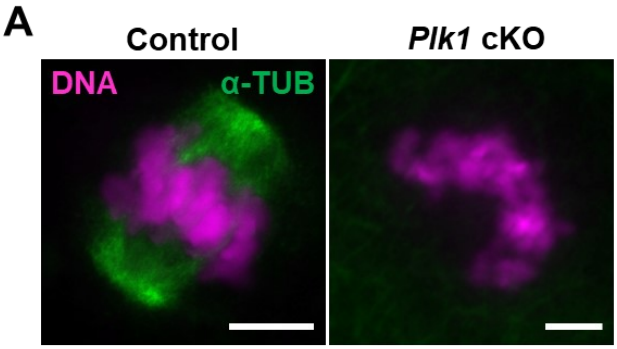
A
Control
Plk1 cKO
DNA
α-TUB

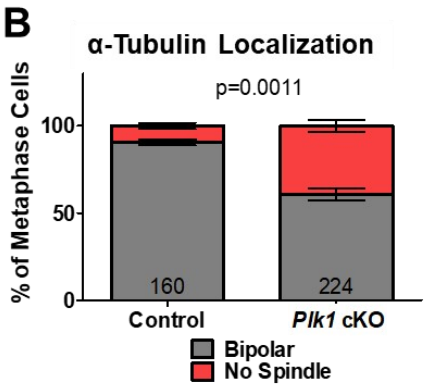
B
α-Tubulin Localization
p=0.0011
% of Metaphase Cells
100
50
0
160
224
Control
Plk1 cKO
Bipolar
No Spindle

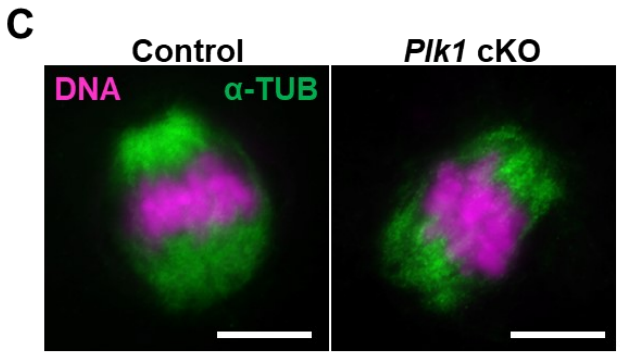
C
Control
Plk1 cKO
DNA
α-TUB

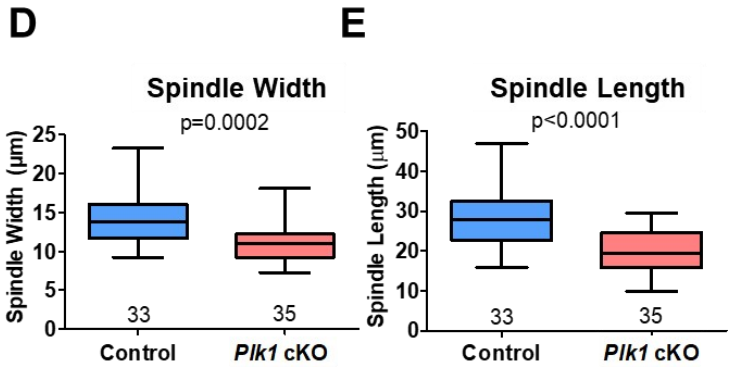
D
Spindle Width
p=0.0002
Spindle Width (μm)
25
20
15
10
5
0
33
35
Control
Plk1 cKO
E
Spindle Length
p<0.0001
Spindle Length (μm)
50
40
30
20
10
0
33
35
Control
Plk1 cKO

and width (Figure I.5). Therefore, we hypothesized that the regulation of acentriolar MTOCs may be perturbed in *Plk1*, *Spo11-Cre* cKO oocytes. We first assessed the localization of the centrosomal linker protein, C-NAP1. Before NEBD, C-NAP1 localizes as a dense focus at unfragmented acentriolar MTOCs in control and *Plk1*, *Spo11-Cre* cKO oocytes (Figure I.6, A and B). In control oocytes, C-NAP1 signal diminishes during prometaphase, and alpha-tubulin spindles begin to elongate and eventually form a bipolar spindle at metaphase I (Figure I.6A). In contrast, C-NAP1 remains as a dense focus in *Plk1*, *Spo11-Cre* cKO oocytes at prometaphase (Figure I.6, B and C). Notably, the prometaphase spindle in *Plk1* cKO oocytes appears smaller than those in control oocytes. This implies that the defects resulting in smaller metaphase spindles are already occurring in prometaphase.

Fragmentation of MTOCs following meiotic resumption in oocytes requires the dissociation of C-NAP1, during NEBD (Clift and Schuh, 2015; Lee and Rhee, 2011). Therefore, we hypothesized that the aberrancies in C-NAP1 dispersal following NEBD (Figure I.6) likely affects MTOC component localization in *Plk1*, *Spo11-Cre* cKO oocytes. We first assessed gamma-tubulin localization, which is a component of acentriolar MTOCs and spindle microtubules (Figure I.7, A and B; So *et al.*, 2019). Interestingly, the 44% of *Plk1*, *Spo11-Cre* cKO oocytes that had bipolar alpha-tubulin spindles lacked gamma-tubulin signals. In addition, 37% of *Plk1*, *Spo11-Cre* cKO oocytes had monopolar gamma-tubulin signals often with little or no alpha-tubulin signal. In contrast, 81% of control oocytes had bipolar gamma-tubulin signals.

Figure I.6: *Plk1* cKO oocytes fail to disperse C-NAP1 following meiotic resumption. (A, B) Control (A) and *Plk1* cKO (B) oocytes immunolabeled with antibodies against C-NAP1 (green) and alpha-tubulin (α-TUB, red), and counterstained with DAPI (DNA, blue). Solid squares indicate the source of zoomed images on the right. Dotted circles indicate the oocyte outline. Meiotic stages were determined based on alpha-tubulin and DAPI staining. Scale bar: 20 μm. (C) Quantification of C-NAP1 localization in pre-NEBD control (n = 73) and *Plk1* cKO (n = 107) oocytes, and post-NEBD control (n = 57) and *Plk1* cKO (n = 40) oocytes. Bars represent 95% confidence intervals, and the P value (Mann-Whitney test, two-tailed) for pre-NEBD was not significant (P = 0.6857), and for post-NEBD is significant (P = 0.0294).

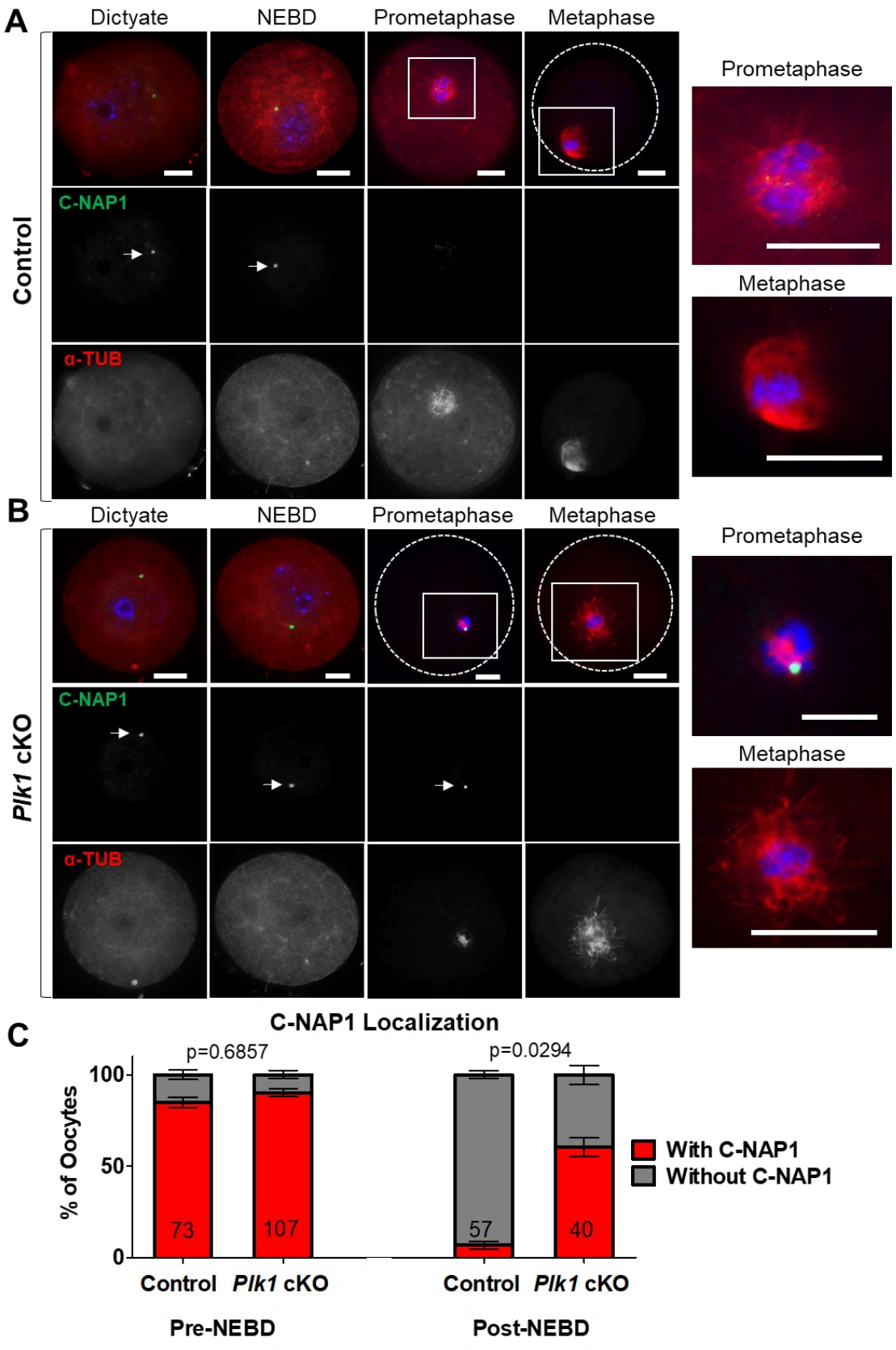
A
Dictyate
NEBD
Prometaphase
Metaphase
Control
C-NAP1
α-TUB
Prometaphase
Metaphase
B
Dictyate
NEBD
Prometaphase
Metaphase
Plk1 cKO
C-NAP1
α-TUB
Prometaphase
Metaphase
C
C-NAP1 Localization
p=0.6857
p=0.0294
% of Oocytes
100
50
0
73
107
57
40
With C-NAP1
Without C-NAP1
Control
Plk1 cKO
Control
Plk1 cKO
Pre-NEBD
Post-NEBD

We then assessed the localization of two components of acentriolar MTOCs, CEP192 and NEDD1, in oocytes with bipolar alpha-tubulin spindles. In control oocytes, CEP192 and NEDD1 distribute evenly at both alpha-tubulin spindle poles (Figure I.7, C–F). A CEP192 signal was absent in the majority (70%) of *Plk1*, *Spo11-Cre* cKO oocytes (Figure I.7, C and D). Similar results were obtained for NEDD1 with 74% of *Plk1*, *Spo11-Cre* cKO oocytes not harboring a NEDD1 signal (Figure I.7, E and F). These oocytes also had unorganized chromosomes, further supporting a chromosome compaction defect.

The MTOC assembly process is temporally coordinated with the organization of the LISD. Aurora A regulates the distribution of the LISD by phosphorylating TACC3, a critical LISD component (So *et al.*, 2019). While Aurora A localized to the alpha-tubulin spindle poles in control metaphase I oocytes, Aurora A was absent in most (78%) of the *Plk1* cKO oocytes (Figure I.8, A and B). In control oocytes, TACC3 localizes to the bipolar spindle (Figure I.8, C and D). However, the majority (78%) of *Plk1*, *Spo11-Cre* cKO oocytes did not have a TACC3 signal localized to any portion of the spindle.

Discussion

Plk1 and NEBD

PLKs have been associated with many stages of the cell cycle, including NEBD. Disassembly of nuclear pore complexes (NPCs) is known to be a key aspect of NEBD, required for nuclear envelope permeabilization (Champion *et al.*, 2017). PLK-1 in *Caenorhabditis elegans* and PLK1 in human cells has been shown to localize to the nuclear periphery, colocalizing with NPCs during late prophase. Mu-

tation of PLK-1 or kinase inhibition of mammalian PLK1 results in aberrant NEBD because PLK1 is required for phosphorylation of components of the NPC, which subsequently results in NPC disassembly (de Castro *et al.*, 2018; Linder *et al.*, 2017; Martino *et al.*, 2017).

NEBD is the first stage of meiotic resumption in oocytes. In a previous report, PLK1 kinase inhibition in mouse oocytes was shown to delay meiotic resumption with regard to NEBD (Solc *et al.*, 2015). Our results contrast this observation as NEBD was equivalent between controls and *Plk1*, *Spo11-Cre* cKO oocytes. However, the delay in NEBD caused by PLK1 kinase inhibition is small when comparing to CDK1 inhibition (Solc *et al.*, 2015). PLK1 is known to be involved in activation of CDK1 (Jackman *et al.*, 2003), but may not be essential for its role in NEBD in oocytes. Taken together, the NEBD role of PLK1 in mammalian oocytes is likely minor and does not result in the arrest of meiotic resumption. The discrepancy between the findings presented here and PLK1's previously-reported role in NEBD are likely due to off-target effects of PLK1 inhibitors on other PLKs. Due to their similar structures, the different PLKs can interact with and compensate for each other. Evidence of this has already been observed in the case of PLK2 and PLK4 in mitotic cells (Cizmecioglu et al., 2008). Therefore, compensation may also help explain the discrepancy in the role for PLK1 in NEBD in mouse oocytes.

Role for PLK1 during chromosome compaction before segregation

PLK1 has been shown to interact with and phosphorylate components of condensin in cultured human cancer cell lines, and these processes are important to facilitate proficient chromosome condensation and chromosome segregation

(Abe *et al.*, 2011; Kim *et al.*, 2014). In addition, PLK1 contributes to cohesin release during G2-phase in mitotically dividing cells, which is important for normal chromosome compaction (Haarhuis *et al.*, 2014). In budding yeast, it has been shown that the sole PLK homologue, Cdc5, is required for cohesin release, which coincides with PLK-dependent compaction of chromosomes before their segregation during meiosis I (Attner *et al.*, 2013; Challa *et al.*, 2019; Lee and Amon, 2003).

In mouse oocytes, PLK1 has been shown to accumulate at kinetochores, but there is also a PLK1 signal detected along bivalent chromosomes (Solc *et al.*, 2015). Here, we demonstrate *Plk1* cKO causes chromosomes to compact abnormally following NEBD, with cohesin and condensin axis formation defects. RNAi-mediated depletion or kinase inhibition of PLK1 resulted in delayed chromosome individualization after NEBD, with chromosomes remaining clumped together (Clift and Schuh, 2015). It was suggested that these observations were due to the MTOC fragmentation defects. However, based on previous studies linking PLK1 with chromatin dynamics, it is possible that PLK1 plays a direct role in the formation of individual bivalents in oocytes.

PLK1 is essential for acentriolar bipolar spindle formation in oocytes

Mammalian oocytes do not harbor centrioles, and instead rely on multiple acentriolar MTOCs that fragment from one another following NEBD, then subsequently coalesce evenly on each side of the condensed bivalents and form bipolar spindles (Clift and Schuh, 2015). Similar to work assessing the role of PLK1

Figure I.7: *Plk1* cKO oocytes display abnormal localization of MTOC components. (A) Examples of control and *Plk1* cKO metaphase I oocytes immunolabeled with antibodies against gamma-tubulin (γ-TUB, green) and alpha-tubulin (α-TUB, red), and counterstained with DAPI (DNA, blue). Scale bar: 10 μm. (B) Quantification of gamma-tubulin localization in metaphase I oocytes. Oocytes (133) from 3 control mice and 100 oocytes from 3 *Plk1* cKO mice were assessed. Bars represent 95% confidence intervals, and the *P* value (Mann-Whitney test, two-tailed) for the indicated comparison is significant ($P < 0.0001$). (C) Examples of control and *Plk1* cKO oocytes immunolabeled with antibodies against MTOC component, CEP192 (green), and alpha-tubulin (α-TUB, red), and counterstained with DAPI (DNA, blue). (D) Quantification of CEP192 localization. Oocytes (57) from 3 control mice and 47 oocytes from 3 *Plk1* cKO mice were assessed. Bars represent SD, and the *P* value (Mann-Whitney test, two-tailed) for the indicated comparison is significant ($P = 0.0012$). (E) Examples of control and *Plk1* cKO oocytes immunolabeled with antibodies against MTOC component, NEDD1 (green), and alpha-tubulin (α-TUB, red), and counterstained with DAPI (DNA, blue). (F) Quantification of NEDD1 localization. Oocytes (25) from 5 control mice and 21 oocytes from 5 *Plk1* cKO mice were assessed. Bars represent 95% confidence intervals, and the *P* value (Mann-Whitney test, two-tailed) for the indicated comparison is significant ($P = 0.002$).

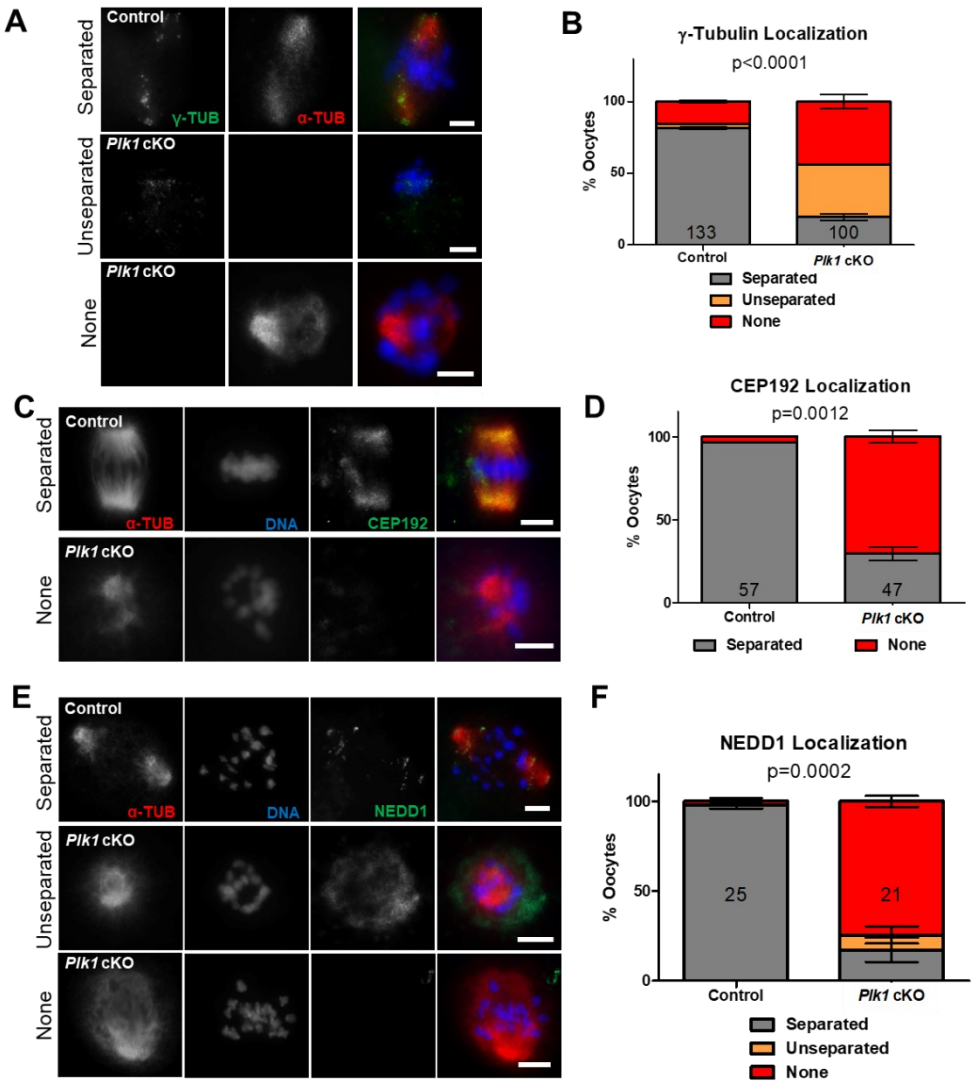
A
Control
γ-TUB
α-TUB
Separated
Plk1 cKO
Unseparated
Plk1 cKO
None
B
γ-Tubulin Localization
p<0.0001
% Oocytes
100
50
0
133
100
Control
Plk1 cKO
Separated
Unseparated
None
C
Control
α-TUB
DNA
CEP192
Separated
Plk1 cKO
None
D
CEP192 Localization
p=0.0012
% Oocytes
100
50
0
57
47
Control
Plk1 cKO
Separated
None
E
Control
α-TUB
DNA
NEDD1
Separated
Plk1 cKO
Unseparated
Plk1 cKO
None
F
NEDD1 Localization
p=0.0002
% Oocytes
100
50
0
25
21
Control
Plk1 cKO
Separated
Unseparated
None

Figure I.8: *Plk1* oocytes display abnormal localization of LISD components. (A) Examples of control and *Plk1* cKO metaphase I oocytes immunolabeled with antibodies against alpha-tubulin (α-TUB, red) and Aurora A (green), and counterstained with DAPI (DNA, blue). Scale bar: 10 μm. (B) Quantification of Aurora A localization in metaphase I oocytes. Oocytes (137) from 2 control mice and 37 oocytes from 3 *Plk1* cKO mice were assessed. Bars represent 95% confidence intervals, and the *P* value (Mann-Whitney test, two-tailed) for the indicated comparison is significant ($P = 0.0005$). (C) Examples of control and *Plk1* cKO oocytes immunolabeled with antibodies against LISD component, TACC3 (green), and alpha-tubulin (α-TUB, red), and counterstained with DAPI (DNA, blue). (D) Quantification of TACC3 localization. Oocytes (52) from 3 control mice and 37 oocytes from 3 *Plk1* cKO mice were assessed. Bars represent 95% confidence intervals, and the *P* value (Mann-Whitney test, two-tailed) for the indicated comparison is significant ($P < 0.0001$). Scale bars: 10 μm.

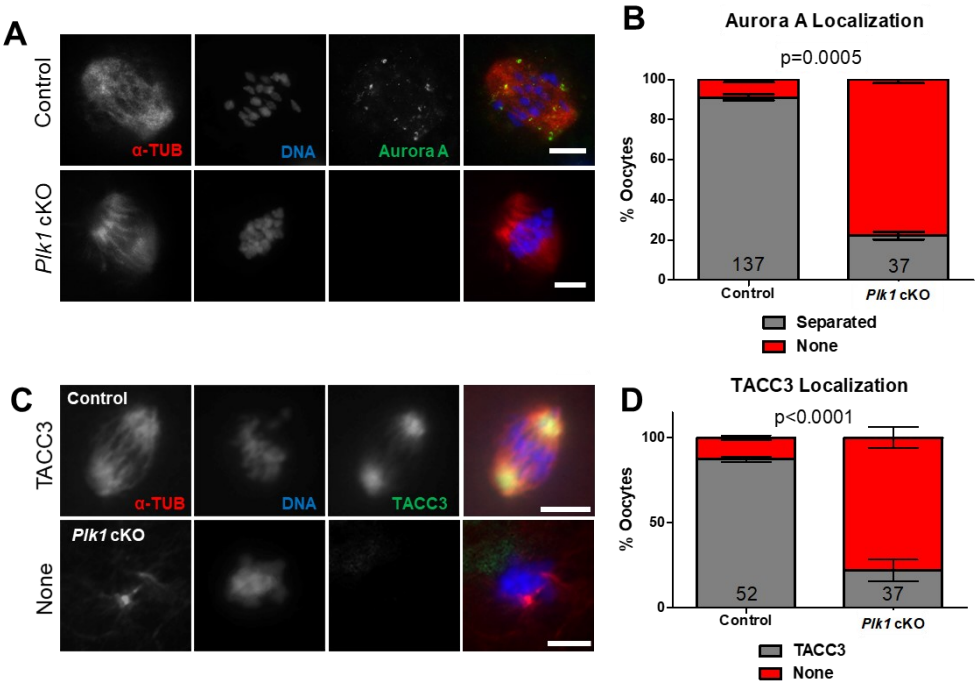
A
Control
α-TUB
DNA
Aurora A
Plk1 cKO
B
Aurora A Localization
p=0.0005
% Oocytes
100
80
60
40
20
0
137
37
Control
Plk1 cKO
Separated
None
C
TACC3
Control
α-TUB
DNA
TACC3
None
Plk1 cKO
D
TACC3 Localization
p<0.0001
% Oocytes
100
50
0
52
37
Control
Plk1 cKO
TACC3
None

in oocytes using siRNA and kinase inhibition approaches, we demonstrated that PLK1 is required for spindle integrity to ensure the formation of normal bipolar spindles capable of facilitating chromosome segregation during meiosis I (Clift and Schuh, 2015; Liao *et al.*, 2018; Solc *et al.*, 2015). Furthermore, using the *Plk1* cKO strategy, we complemented previous RNAi and kinase inhibitor approaches that showed that PLK1 is required for C-NAP1 dissociation during NEBD, which is critical for fragmentation of MTOC components (Clift and Schuh, 2015). In mitosis, both C-NAP1 dissociation and centrosome separation are initiated by PLK1 (Mardin *et al.*, 2011), demonstrating that although oocytes are acentriolar the importance of PLK1 in bipolar spindle formation is universal.

We showed that PLK1 is required for normal localization of acentriolar MTOC components gamma-tubulin, CEP192, and NEDD1. We observed a complete absence of gamma-tubulin at MTOCs in the majority of *Plk1* cKO oocytes, which is consistent with the observations made when PLK1 kinase activity was inhibited (Solc *et al.*, 2015). With regard to CEP192, we mostly observe a complete absence of the protein to MTOCs, whereas PLK1 inhibition led to monopolar localization of CEP192 (Clift and Schuh, 2015). The effects of PLK1 functional loss on NEDD1 had not previously been assessed in oocytes. However, in human cell lines PLK1 phosphorylates NEDD1 and increases its anchoring capacity for gamma-tubulin onto centrosomes (Zhang *et al.*, 2009). The formation of an abnormally small spindle in *Plk1* cKO oocytes may be due to an alternative microtubule assembly pathway. Prior studies have shown that kinetochore-dependent microtubule assembly may compensate for the loss of canonical

centrosomes in mammalian cells (Mishra *et al.*, 2010; Prosser and Pelletier, 2017). It is possible that such a pathway explains the presence of alpha-tubulin in oocytes without gamma-tubulin, as observed in our work and others (Solc *et al.*, 2015). Research in mammalian mitotic cells has demonstrated that microtubules can be nucleated and emanated from kinetochores when PLK1 is depleted (Torosantucci *et al.*, 2008). These kinetochore-based microtubules, driven by the RanGTP gradient, can organize themselves into spindle poles. This may explain the unstable bipolar spindles observed in *Plk1* cKO oocytes.

A recent, comprehensive study of factors required for bipolar spindle formation in oocytes discovered that TACC3 is a major component of a novel LISD (So *et al.*, 2019). The same study presented that Aurora A kinase, but not PLK1 kinase activity, is required for LISD maintenance. These experiments were designed to inhibit PLK1 and Aurora A at metaphase I stage oocytes, which is different from our experimental design using *Plk1* cKO oocytes. In mitotic cells, Aurora A and PLK1 are known to reciprocally activate each other throughout the cell cycle to regulate spindle assembly (Asteriti et al., 2015; Joukov and De Nicolo, 2018). Our results indicate that PLK1 does indeed play a role in LISD maintenance upstream of Aurora A. This is further supported by the observation that Aurora A and TACC3 are not recruited to the spindle in *Plk1* cKO oocytes. In support of our observations, a study using human cell lines determined that PLK1 inhibition resulted in down-regulation of TACC3 targeting to mitotic spindles (Fu *et al.*, 2013). Taken together, our results show that PLK1 activity is required for C-NAP1 dissociation, normal acentriolar MTOC fragmentation, and localization of MTOC

and LISD components that are important to ensure formation of a bipolar spindle (Figure I.9). These processes are critical for an oocyte to progress through meiosis I and be capable of fertilization, demonstrating that PLK1 is essential for female fertility in mammals.

Acknowledgements

We thank Steve Murray for helping coordinate obtaining the *Plk1* cKO mouse line, Karen Schindler, and Andrew Holland for antibodies, and Stephen Wellard and Grace Hwang for technical help.

Figure I.9: PLK1 regulates chromosome condensation, MTOC fragmentation, and LISD recruitment in mammalian oocytes. In control oocytes, PLK1 is responsible for dissociating C-NAP1 immediately after meiotic resumption. This allows MTOC components to fragment and then coalesce evenly on both sides of the condensed bivalents and form bipolar spindles. As oocytes enter metaphase, PLK1 is required for the recruitment of Aurora A (AURKA) to the MTOC and bipolar spindle. Aurora A then recruits TACC3, the major component of the LISD. In *Plk1* cKO oocytes, chromosomes do not properly condense following meiotic resumption. Furthermore, C-NAP1 is not dissociated in an efficient manner in *Plk1* cKO oocytes. This leads to MTOC (γ-tubulin, CEP192, and NEDD1) and LISD (Aurora A and TACC3) components failing to localize and cluster, and results in MTOC failure and abnormal spindle formation. Microtubules that do polymerize in *Plk1* cKO oocytes form a small, abnormal metaphase spindle, which is likely driven by a kinetochore-dependent microtubule assembly pathway (Torosantucci ***et al.***, 2008; Prosser and Pelletier, 2017). Ultimately, the defects observed in *Plk1* cKO oocytes lead to arrest in metaphase I.

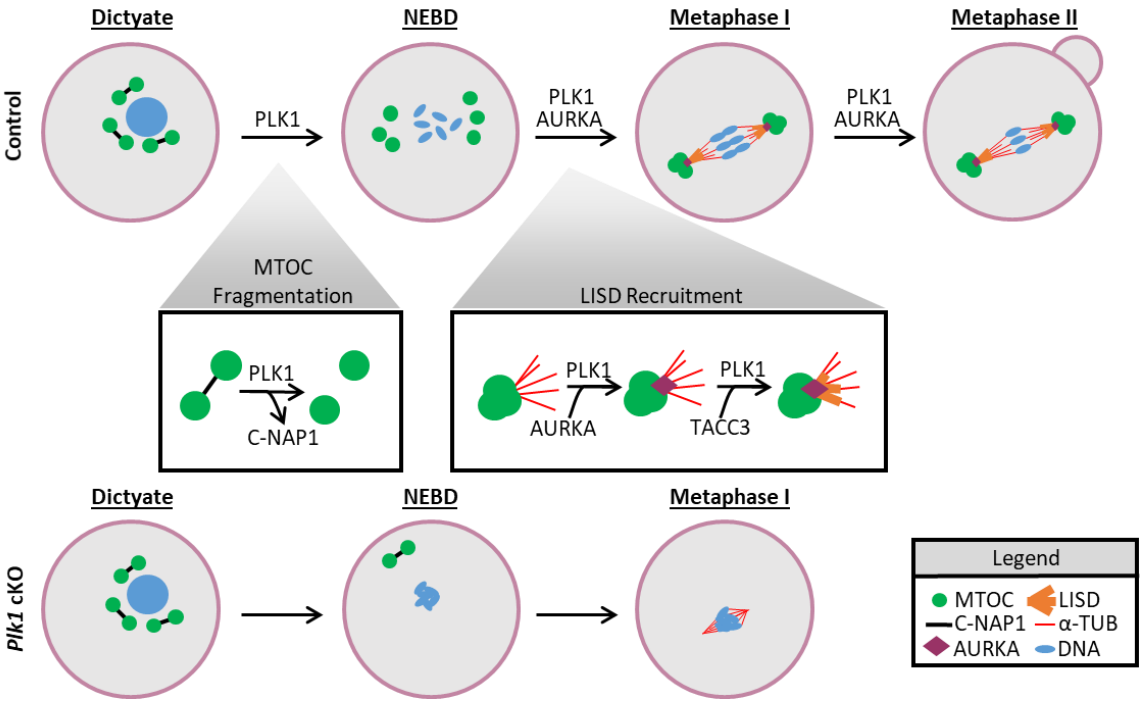
Dictyate
NEBD
Metaphase I
Metaphase II
Control
PLK1
PLK1
AURKA
PLK1
AURKA
MTOC
Fragmentation
LISD Recruitment
PLK1
C-NAP1
PLK1
AURKA
PLK1
TACC3
Dictyate
NEBD
Metaphase I
Plk1 cKO
Legend
MTOC
LISD
C-NAP1
α-TUB
AURKA
DNA

Supplemental Figure I.1: (A-D) Western blot analysis of PLK1 protein levels in extracts obtained from *Plk1 flox/del; Zp3-Cre* (A), *Plk1 flox/del; Gdf9-Cre* (B), and *Plk1 flox/del; Spo11-Cre* (C and D) oocytes. Protein size (kDa) and number of oocytes used per lane is indicated.

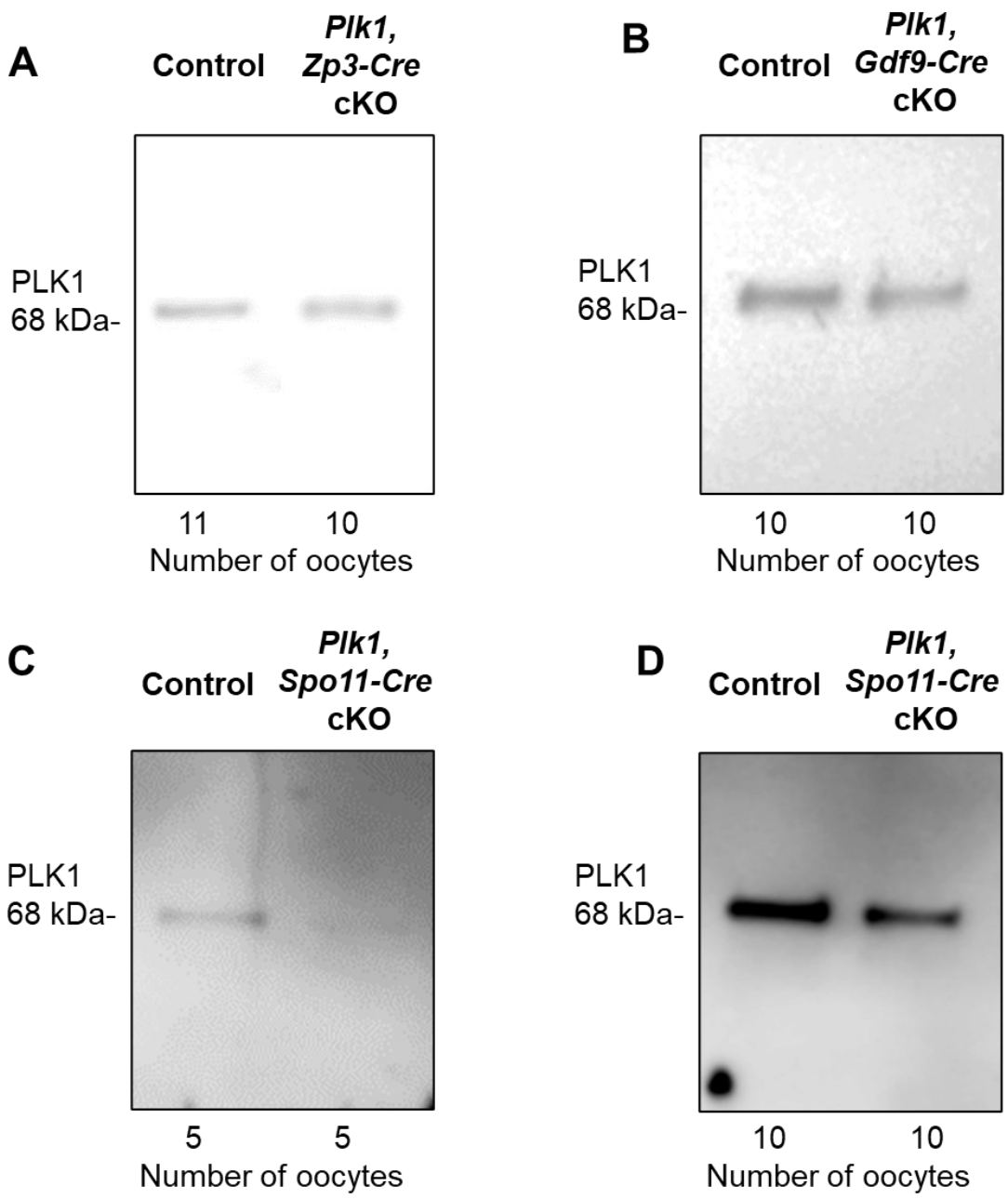
A
Control
Plk1, Zp3-Cre cKO
PLK1
68 kDa-
11
10
Number of oocytes
B
Control
Plk1, Gdf9-Cre cKO
PLK1
68 kDa-
10
10
Number of oocytes
C
Control
Plk1, Spo11-Cre cKO
PLK1
68 kDa-
5
5
Number of oocytes
D
Control
Plk1, Spo11-Cre cKO
PLK1
68 kDa-
10
10
Number of oocytes

Gene	Forward Primer (5'-…..-3')	Reverse Primer (5'-…..-3')	Product Size (bp)
Plk1^{del} and *Plk1*^{flox}	AGTATGGCAGGCAGCATCTC	ATGCTCCATGGAAAGTCAGG	*Del*: 341 *Flox*: 1174 *WT*: 1012
Cre Transgene	CCATCTGCCACCAGCCAG	TCGCCATCTTCCAGCAGG	420
Cre Internal Control	ACTGGGATCTTCGAACTCTTTGGAC	GATGTTGGGGCACTGCTCATTCACC	281

Supplemental Table I.1: Primers used in this study.

Primary Antibodies					
Antibody	**Host**	**Source**	**Cat. Number**	**IF Dilution**	**WB Dilution**
alpha-tubulin	Goat	LS Bio	LS-C204216	1:500	
alpha-tubulin	Mouse	Sigma-Aldrich	T9026	1:1000	1:10,000
alpha-tubulin	Rabbit	Thermo Scientific	PA5-29444	1:500	
Aurora A	Mouse	Thermo Scientific	MA5-15803	1:200	
centromere	Human	Antibodies Inc.	15-235	1:100	
CEP192	Goat	Dr. Andrew Holland		1:500	
C-NAP1	Rabbit	Proteintech Group	14498-1-AP	1:100	
gamma-tubulin	Mouse	Sigma-Aldrich	T6557	1:1000	
NEDD1	Mouse	Abcam	ab57336	1:750	
PLK1	Mouse	Abcam	ab17057	1:100	
PLK1	Rabbit	Genetex	GTX104302	1:100	1:5000
REC8	Rabbit	Dr. Karen Schindler		1:1000	
SMC4	Rabbit	Novus Biologicals	NBP1-86635	1:50	
SYCP3	Mouse	Santa Cruz Biotech	sc-74569	1:50	
SYCP3	Rabbit	Novus Biologicals	NB300-231	1:1000	
TACC3	Rabbit	Novus Biologicals	NBP2-67671	1:50	

Secondary Antibodies					
Antibody	**Host**	**Source**	**Cat. Number**	**IF Dilution**	**WB Dilution**
Mouse IgG (H+L), Alexa Fluor 488	Goat	Invitrogen	A-11001	1:500	
Mouse IgG (H+L), Alexa Fluor 568	Goat	Invitrogen	A-11031	1:500	
Rabbit IgG (H+L), Alexa Fluor 488	Goat	Invitrogen	A-11008	1:500	
Rabbit IgG (H+L), Alexa Fluor 568	Goat	Invitrogen	A-11011	1:500	
Human IgG (H+L), Alexa Fluor 633	Goat	Invitrogen	A-21091	1:500	
Goat IgG (H+L) Alexa Fluor 488	Donkey	Invitrogen	A-11055	1:500	
Goat IgG (H+L) Alexa Fluor 568	Donkey	Invitrogen	A-11057	1:500	
Goat IgG (H+L) Alexa Fluor 633	Donkey	Invitrogen	A-21082	1:500	
Mouse IgG (H+L), HRP	Rabbit	Invitrogen	31450		1:20,000
Rabbit IgG (H+L), HRP	Goat	Invitrogen	31466		1:20,000

Supplemental Table I.2: Antibodies used in this study.

	Offspring genotype distribution			
Breeding pairs	***Plk1 +/+***	***Plk1 +/flox***	***Plk1 +/del***	**Total**
♀ ***Plk1 +/flox, Zp3-Cre*** **x ♂wild-type**	44% (63 pups)	0% (0 pups)	56% (80 pups)	143 pups
♀ ***Plk1 +/flox, Spo11-Cre*** **x ♂ wild-type**	46% (67 pups)	10% (14 pups)	44% (63 pups)	144 pups

Supplemental Table I.3: Cre driver efficiency of *Zp3-Cre* and *Spo11-Cre* for excising exon 3 of the *Plk1 flox* allele via genotyping progeny of breeding pairs as indicated.

References

Abe, S., Nagasaka, K., Hirayama, Y., Kozuka-Hata, H., Oyama, M., Aoyagi, Y., Obuse, C., and Hirota, T. (2011). The initial phase of chromosome condensation requires Cdk1-mediated phosphorylation of the CAP-D3 subunit of condensin II. Genes Dev. *25*, 863–874.

Almawi, A.W., Langlois-Lemay, L., Boulton, S., Rodríguez González, J., Melacini, G., D'Amours, D., and Guarné, A. (2020). Distinct surfaces on Cdc5/PLK Polo-box domain orchestrate combinatorial substrate recognition during cell division. Sci. Rep. *10*, 3379.

Aquino Perez, C., Palek, M., Stolarova, L., von Morgen, P., and Macurek, L. (2020). Phosphorylation of PLK3 is controlled by protein phosphatase 6. Cells *9*.

Asteriti, I.A., De Mattia, F., and Guarguaglini, G. (2015). Cross-Talk between AURKA and Plk1 in Mitotic Entry and Spindle Assembly. Front. Oncol. *5*, 283.

Attner, M.A., Miller, M.P., Ee, L., Elkin, S.K., and Amon, A. (2013). Polo kinase Cdc5 is a central regulator of meiosis I. Proc. Natl. Acad. Sci. USA *110*, 14278–14283.

Bahassi, E.M., Myer, D.L., McKenney, R.J., Hennigan, R.F., and Stambrook, P.J. (2006). Priming phosphorylation of Chk2 by polo-like kinase 3 (Plk3) mediates its full activation by ATM and a downstream checkpoint in response to DNA damage. Mutat. Res. *596*, 166–176.

Baumann, C., Wang, X., Yang, L., and Viveiros, M.M. (2017). Error-prone meiotic division and subfertility in mice with oocyte-conditional knockdown of pericentrin. J. Cell Sci. *130*, 1251–1262.

Bettencourt-Dias, M., Rodrigues-Martins, A., Carpenter, L., Riparbelli, M., Lehmann, L., Gatt, M.K., Carmo, N., Balloux, F., Callaini, G., and Glover, D.M. (2005). SAK/PLK4 is required for centriole duplication and flagella development. Curr. Biol. *15*, 2199–2207.

Burkhardt, S., Borsos, M., Szydlowska, A., Godwin, J., Williams, S.A., Cohen, P.E., Hirota, T., Saitou, M., and Tachibana-Konwalski, K. (2016). Chromosome cohesion established by REC8-cohesin in fetal oocytes is maintained without detectable turnover in oocytes arrested for months in mice. Curr. Biol. *26*, 678–685.

Bury, L., Coelho, P.A., Simeone, A., Ferries, S., Eyers, C.E., Eyers, P.A., Zernicka-Goetz, M., and Glover, D.M. (2017). Plk4 and Aurora A cooperate in the initiation of acentriolar spindle assembly in mammalian oocytes. J. Cell Biol. *216*, 3571–3590.

Challa, K., Fajish V, G., Shinohara, M., Klein, F., Gasser, S.M., and Shinohara, A. (2019). Meiosis-specific prophase-like pathway controls cleavage-independent release of cohesin by Wapl phosphorylation. PLoS Genet. *15*, e1007851.

Champion, L., Linder, M.I., and Kutay, U. (2017). Cellular Reorganization during Mitotic Entry. Trends Cell Biol. *27*, 26–41.

Cizmecioglu, O., Warnke, S., Arnold, M., Duensing, S., and Hoffmann, I. (2008). Plk2 regulated centriole duplication is dependent on its localization to the centrioles and a functional polo-box domain. Cell Cycle *7*, 3548–3555.

Clift, D., and Schuh, M. (2015). A three-step MTOC fragmentation mechanism facilitates bipolar spindle assembly in mouse oocytes. Nat. Commun. *6*, 7217.

Cozza, G., and Salvi, M. (2018). The acidophilic kinases PLK2 and PLK3: structure, substrate targeting and inhibition. Curr Protein Pept Sci *19*, 728–745.

de Cárcer, G., Manning, G., and Malumbres, M. (2011a). From Plk1 to Plk5: functional evolution of polo-like kinases. Cell Cycle *10*, 2255–2262.

de Cárcer, G., Escobar, B., Higuero, A.M., García, L., Ansón, A., Pérez, G., Mollejo, M., Manning, G., Meléndez, B., Abad-Rodríguez, J., et al. (2011b). Plk5, a polo box domain-only protein with specific roles in neuron differentiation and glioblastoma suppression. Mol. Cell. Biol. *31*, 1225–1239.

de Castro, I.J., Gil, R.S., Ligammari, L., Di Giacinto, M.L., and Vagnarelli, P. (2018). CDK1 and PLK1 coordinate the disassembly and reassembly of the nuclear envelope in vertebrate mitosis. Oncotarget *9*, 7763–7773.

Elia, A.E.H., Rellos, P., Haire, L.F., Chao, J.W., Ivins, F.J., Hoepker, K., Mohammad, D., Cantley, L.C., Smerdon, S.J., and Yaffe, M.B. (2003). The molecular basis for phosphodependent substrate targeting and regulation of Plks by the Polo-box domain. Cell *115*, 83–95.

Fu, W., Chen, H., Wang, G., Luo, J., Deng, Z., Xin, G., Xu, N., Guo, X., Lei, J., Jiang, Q., et al. (2013). Self-assembly and sorting of acentrosomal microtubules by TACC3 facilitate kinetochore capture during the mitotic spindle assembly. Proc. Natl. Acad. Sci. USA *110*, 15295–15300.

Gheghiani, L., Loew, D., Lombard, B., Mansfeld, J., and Gavet, O. (2017). PLK1 activation in late G2 sets up commitment to mitosis. Cell Rep. *19*, 2060–2073.

Gray, S., and Cohen, P.E. (2016). Control of meiotic crossovers: from double-strand break formation to designation. Annu. Rev. Genet. *50*, 175–210.

Haarhuis, J.H.I., Elbatsh, A.M.O., and Rowland, B.D. (2014). Cohesin and its regulation: on the logic of X-shaped chromosomes. Dev. Cell *31*, 7–18.

Harris, R.M., Weiss, J., and Jameson, J.L. (2011). Male hypogonadism and germ cell loss caused by a mutation in Polo-like kinase 4. Endocrinology *152*, 3975–3985.

Hwang, G., Sun, F., O'Brien, M., Eppig, J.J., Handel, M.A., and Jordan, P.W. (2017). SMC5/6 is required for the formation of segregation-competent bivalent chromosomes during meiosis I in mouse oocytes. Development *144*, 1648–1660.

Hwang, G., Verver, D.E., Handel, M.A., Hamer, G., and Jordan, P.W. (2018a). Depletion of SMC5/6 sensitizes male germ cells to DNA damage. Mol. Biol. Cell *29*, 3003–3016.

Hwang, G.H., Hopkins, J.L., and Jordan, P.W. (2018b). Chromatin Spread Preparations for the Analysis of Mouse Oocyte Progression from Prophase to Metaphase II. J. Vis. Exp. *132*, e56736.

Jackman, M., Lindon, C., Nigg, E.A., and Pines, J. (2003). Active cyclin B1-Cdk1 first appears on centrosomes in prophase. Nat. Cell Biol. *5*, 143–148.

Jessberger, R. (2012). Age-related aneuploidy through cohesion exhaustion. EMBO Rep. *13*, 539–546.

Joukov, V., and De Nicolo, A. (2018). Aurora-PLK1 cascades as key signaling modules in the regulation of mitosis. Sci. Signal. *11*.

Kim, J.H., Shim, J., Ji, M.-J., Jung, Y., Bong, S.M., Jang, Y.-J., Yoon, E.-K., Lee, S.-J., Kim, K.G., Kim, Y.H., et al. (2014). The condensin component NCAPG2 regulates microtubule-kinetochore attachment through recruitment of Polo-like kinase 1 to kinetochores. Nat. Commun. *5*, 4588.

Ko, M.A., Rosario, C.O., Hudson, J.W., Kulkarni, S., Pollett, A., Dennis, J.W., and Swallow, C.J. (2005). Plk4 haploinsufficiency causes mitotic infidelity and carcinogenesis. Nat. Genet. *37*, 883–888.

Lan, Z.-J., Xu, X., and Cooney, A.J. (2004). Differential oocyte-specific expression of Cre recombinase activity in GDF-9-iCre, Zp3cre, and Msx2Cre transgenic mice. Biol. Reprod. *71*, 1469–1474.

Lee, B.H., and Amon, A. (2003). Role of Polo-like kinase CDC5 in programming meiosis I chromosome segregation. Science *300*, 482–486.

Lee, K., and Rhee, K. (2011). PLK1 phosphorylation of pericentrin initiates centrosome maturation at the onset of mitosis. J. Cell Biol. *195*, 1093–1101.

Lee, I.-W., Jo, Y.-J., Jung, S.-M., Wang, H.-Y., Kim, N.-H., and Namgoong, S. (2017). Distinct roles of Cep192 and Cep152 in acentriolar MTOCs and spindle formation during mouse oocyte maturation. FASEB J.

Li, H., Wang, Y., and Liu, X. (2008). Plk1-dependent phosphorylation regulates functions of DNA topoisomerase IIalpha in cell cycle progression. J. Biol. Chem. *283*, 6209–6221.

Liao, Y., Lin, D., Cui, P., Abbasi, B., Chen, C., Zhang, Z., Zhang, Y., Dong, Y., Rui, R., and Ju, S. (2018). Polo-like kinase 1 inhibition results in misaligned chromosomes and aberrant spindles in porcine oocytes during the first meiotic division. Reprod. Domest. Anim. *53*, 256–265.

Linder, M.I., Köhler, M., Boersema, P., Weberruss, M., Wandke, C., Marino, J., Ashiono, C., Picotti, P., Antonin, W., and Kutay, U. (2017). Mitotic Disassembly of Nuclear Pore Complexes Involves CDK1- and PLK1-Mediated Phosphorylation of Key Interconnecting Nucleoporins. Dev. Cell *43*, 141–156.e7.

Lu, L.-Y., Wood, J.L., Minter-Dykhouse, K., Ye, L., Saunders, T.L., Yu, X., and Chen, J. (2008). Polo-like kinase 1 is essential for early embryonic development and tumor suppression. Mol. Cell. Biol. *28*, 6870–6876.

Luo, Y.-B., and Kim, N.-H. (2015). PLK4 is essential for meiotic resumption in mouse oocytes. Biol. Reprod. *92*, 101.

Lyndaker, A.M., Lim, P.X., Mleczko, J.M., Diggins, C.E., Holloway, J.K., Holmes, R.J., Kan, R., Schlafer, D.H., Freire, R., Cohen, P.E., et al. (2013). Conditional inactivation of the DNA damage response gene Hus1 in mouse testis reveals separable roles for components of the RAD9-RAD1-HUS1 complex in meiotic chromosome maintenance. PLoS Genet. *9*, e1003320.

Ma, H., Marti-Gutierrez, N., Park, S.-W., Wu, J., Lee, Y., Suzuki, K., Koski, A., Ji, D., Hayama, T., Ahmed, R., et al. (2017). Correction of a pathogenic gene mutation in human embryos. Nature *548*, 413–419.

Ma, S., Charron, J., and Erikson, R.L. (2003). Role of Plk2 (Snk) in mouse development and cell proliferation. Mol. Cell. Biol. *23*, 6936–6943.

MacLennan, M., Crichton, J.H., Playfoot, C.J., and Adams, I.R. (2015). Oocyte development, meiosis and aneuploidy. Semin. Cell Dev. Biol. *45*, 68–76.

Mardin, B., Agircan, F., Lange, C., and Schiebel, E. (2011). Plk1 Controls the Nek2A-PP1[gamma] Antagonism in Centrosome Disjunction. Curr. Biol. *21*, 1145–1151.

Martino, L., Morchoisne-Bolhy, S., Cheerambathur, D.K., Van Hove, L., Dumont, J., Joly, N., Desai, A., Doye, V., and Pintard, L. (2017). Channel Nucleoporins Recruit PLK-1 to Nuclear Pore Complexes to Direct Nuclear Envelope Breakdown in C. elegans. Dev. Cell *43*, 157–171.e7.

Mishra, R.K., Chakraborty, P., Arnaoutov, A., Fontoura, B.M.A., and Dasso, M. (2010). The Nup107-160 complex and gamma-TuRC regulate microtubule polymerization at kinetochores. Nat. Cell Biol. *12*, 164–169.

Mogessie, B., Scheffler, K., and Schuh, M. (2018). Assembly and positioning of the oocyte meiotic spindle. Annu. Rev. Cell Dev. Biol. *34*, 381–403.

Moyer, T.C., and Holland, A.J. (2019). PLK4 promotes centriole duplication by phosphorylating STIL to link the procentriole cartwheel to the microtubule wall. Elife *8*.

Myer, D.L., Robbins, S.B., Yin, M., Boivin, G.P., Liu, Y., Greis, K.D., Bahassi, E.M., and Stambrook, P.J. (2011). Absence of polo-like kinase 3 in mice stabilizes Cdc25A after DNA damage but is not sufficient to produce tumors. Mutat. Res. *714*, 1–10.

Nagaoka, S.I., Hassold, T.J., and Hunt, P.A. (2012). Human aneuploidy: mechanisms and new insights into an age-old problem. Nat. Rev. Genet. *13*, 493–504.

Namgoong, S., and Kim, N.-H. (2018). Meiotic spindle formation in mammalian oocytes: implications for human infertility. Biol. Reprod. *98*, 153–161.

Pahlavan, G., Polanski, Z., Kalab, P., Golsteyn, R., Nigg, E.A., and Maro, B. (2000). Characterization of polo-like kinase 1 during meiotic maturation of the mouse oocyte. Dev. Biol. *220*, 392–400.

Prosser, S.L., and Pelletier, L. (2017). Mitotic spindle assembly in animal cells: a fine balancing act. Nat. Rev. Mol. Cell Biol. *18*, 187–201.

Rosario, C.O., Ko, M.A., Haffani, Y.Z., Gladdy, R.A., Paderova, J., Pollett, A., Squire, J.A., Dennis, J.W., and Swallow, C.J. (2010). Plk4 is required for cytokinesis and maintenance of chromosomal stability. Proc. Natl. Acad. Sci. USA *107*, 6888–6893.

Schatten, H., and Sun, Q.-Y. (2015). Centrosome and microtubule functions and dysfunctions in meiosis: implications for age-related infertility and developmental disorders. Reprod Fertil Dev *27*, 934–943.

So, C., Seres, K.B., Steyer, A.M., Mönnich, E., Clift, D., Pejkovska, A., Möbius, W., and Schuh, M. (2019). A liquid-like spindle domain promotes acentrosomal spindle assembly in mammalian oocytes. Science *364*.

Solc, P., Kitajima, T.S., Yoshida, S., Brzakova, A., Kaido, M., Baran, V., Mayer, A., Samalova, P., Motlik, J., and Ellenberg, J. (2015). Multiple requirements of PLK1 during mouse oocyte maturation. PLoS One *10*, e0116783.

Sonn, S., Oh, G.T., and Rhee, K. (2011). Nek2 and its substrate, centrobin/Nip2, are required for proper meiotic spindle formation of the mouse oocytes. Zygote *19*, 15–20.

Sun, S.-C., Liu, H.-L., and Sun, Q.-Y. (2012). Survivin regulates Plk1 localization to kinetochore in mouse oocyte meiosis. Biochem. Biophys. Res. Commun. *421*, 797–800.

Torosantucci, L., De Luca, M., Guarguaglini, G., Lavia, P., and Degrassi, F. (2008). Localized RanGTP accumulation promotes microtubule nucleation at kinetochores in somatic mammalian cells. Mol. Biol. Cell *19*, 1873–1882.

Vlijm, R., Li, X., Panic, M., Rüthnick, D., Hata, S., Herrmannsdörfer, F., Kuner, T., Heilemann, M., Engelhardt, J., Hell, S.W., et al. (2018). STED nanoscopy of the centrosome linker reveals a CEP68-organized, periodic rootletin network anchored to a C-Nap1 ring at centrioles. Proc. Natl. Acad. Sci. USA *115*, E2246–E2253.

Wang, H., Choe, M.H., Lee, I.-W., Namgoong, S., Kim, J.-S., Kim, N.-H., and Oh, J.S. (2017). CIP2A acts as a scaffold for CEP192-mediated microtubule organizing center assembly by recruiting Plk1 and aurora A during meiotic maturation. Development *144*, 3829–3839.

Webster, A., and Schuh, M. (2017). Mechanisms of aneuploidy in human eggs. Trends Cell Biol. *27*, 55–68.

Xie, S., Wu, H., Wang, Q., Cogswell, J.P., Husain, I., Conn, C., Stambrook, P., Jhanwar-Uniyal, M., and Dai, W. (2001). Plk3 functionally links DNA damage to cell cycle arrest and apoptosis at least in part via the p53 pathway. J. Biol. Chem. *276*, 43305–43312.

Xiong, B., Sun, S.-C., Lin, S.-L., Li, M., Xu, B.-Z., OuYang, Y.-C., Hou, Y., Chen, D.-Y., and Sun, Q.-Y. (2008). Involvement of Polo-like kinase 1 in MEK1/2-regulated spindle formation during mouse oocyte meiosis. Cell Cycle *7*, 1804–1809.

Zhang, X., Chen, Q., Feng, J., Hou, J., Yang, F., Liu, J., Jiang, Q., and Zhang, C. (2009). Sequential phosphorylation of Nedd1 by Cdk1 and Plk1 is required for targeting of the gammaTuRC to the centrosome. J. Cell Sci. *122*, 2240–2251.

Zhang, Y., Wang, Y., Wei, Y., Ma, J., Peng, J., Wumaier, R., Shen, S., Zhang, P., and Yu, L. (2015). The tumor suppressor proteins ASPP1 and ASPP2 interact with C-Nap1 and regulate centrosome linker reassembly. Biochem. Biophys. Res. Commun. *458*, 494–500.

Zhang, Z., Chen, C., Ma, L., Yu, Q., Li, S., Abbasi, B., Yang, J., Rui, R., and Ju, S. (2017). Plk1 is essential for proper chromosome segregation during meiosis I/meiosis II transition in pig oocytes. Reprod Biol Endocrinol *15*, 69.

Chapter II

PLK4 localizes to the centrioles in mouse spermatocytes

Tara M. Little, Jingwen Xu and Philip W. Jordan

Abstract

The principal goal of meiosis is to divide the genome of one diploid cell into four haploid gametes. To accomplish this, eukaryotic organisms have evolved to utilize a complex set of centriolar proteins. The centrosomes are responsible for initiating microtubule nucleation and driving the division of chromatin. In mammals, oocytes undergo acentriolar meiosis and instead rely on microtubule organizing centers (MTOCs) to control division. Polo-Like Kinase 4 (PLK4) is known to be critical for centriole formation in mammalian mitosis. Prior studies of both spermatocytes and oocytes have implied that PLK4 functions during meiosis, although its role in this context remains unknown. In oocytes, prior work has shown that PLK4 localizes to the MTOCs. To further assess PLK4's localization in spermatocytes, we utilized a *mCherry-Plk4* conditional overexpression mouse. This tagged transgenic protein allowed us to visualize PLK4 localizing to the centrioles of spermatocytes starting in prophase and continuing into metaphase. This observation further supports the belief that PLK4 plays a role in centriole regulation in meiosis.

Introduction

Centrosomes, which drive microtubule organization during cellular division, consist of a pair of centrioles surrounded by a pericentriolar matrix. Pairs of centrioles are held together by linker proteins. Mitotic centriole biogenesis is temporally coordinated with the cell cycle (Figure II.1A) (Arquint et al., 2012; Riparbelli et al., 2020; Rodrigues-Martins et al., 2008).

Mitotic centriole biogenesis is initiated at the start of S phase. A cartwheel structure consisting of nine spokes is assembled at the proximal end of the mother centriole (Arquint and Nigg, 2016). This initial structure will then serve as a scaffold on which the highly conserved nine-fold centriole structure is built on during both S and G2 phases. It is critical that this early cartwheel scaffold is correctly anchored to the mother centriole. Polo-like kinase 4 (PLK4) has been shown to phosphorylate STIL, which in turn anchors the forming cartwheel to the correct site. (Arquint and Nigg, 2016; Arquint *et al.*, 2012; Moyer and Holland, 2019).

PLK4 activity is critical in mitosis. PLK4 overexpression results in excessive centriole formation (Habedanck *et al.*, 2005), while depletion results in cells failing to duplicate their centrioles (Bettencourt-Dias *et al.*, 2005). Prior research has shown that the homozygous expression of a point mutation in the kinase domain of *Plk4* results in embryonic lethality (Harris et al., 2011).

Figure II.1: Centriole duplication is aligned with the cell cycle. Centrosomes consist of a linked pair of centrioles (green) surrounded by a pericentriolar matrix (pink). (A) In mitotic cells, each centriole pair will begin to separate in G1 as the centriolar linker starts to dissolve. In S phase, new daughter centrioles are nucleated at the base of each original mother centriole. The daughter centrioles are extended in G2, and the linker between the original two mother centrioles is fully dissolved. At metaphase, the fully matured centrosomes have migrated to the two spindle poles. (B) At the start of meiosis, centrosomes consist of tightly linked centrioles. In leptonema, these centrioles begin to separate. Each of the original mother centrioles serves as a nucleation site for the formation of a daughter centriole. Throughout the remainder of prophase, the daughter centrioles are extended. By prometaphase, the linker between the two mother centrioles is fully dissolved, and the now-separate centrosomes can migrate to opposite sides of the cell.

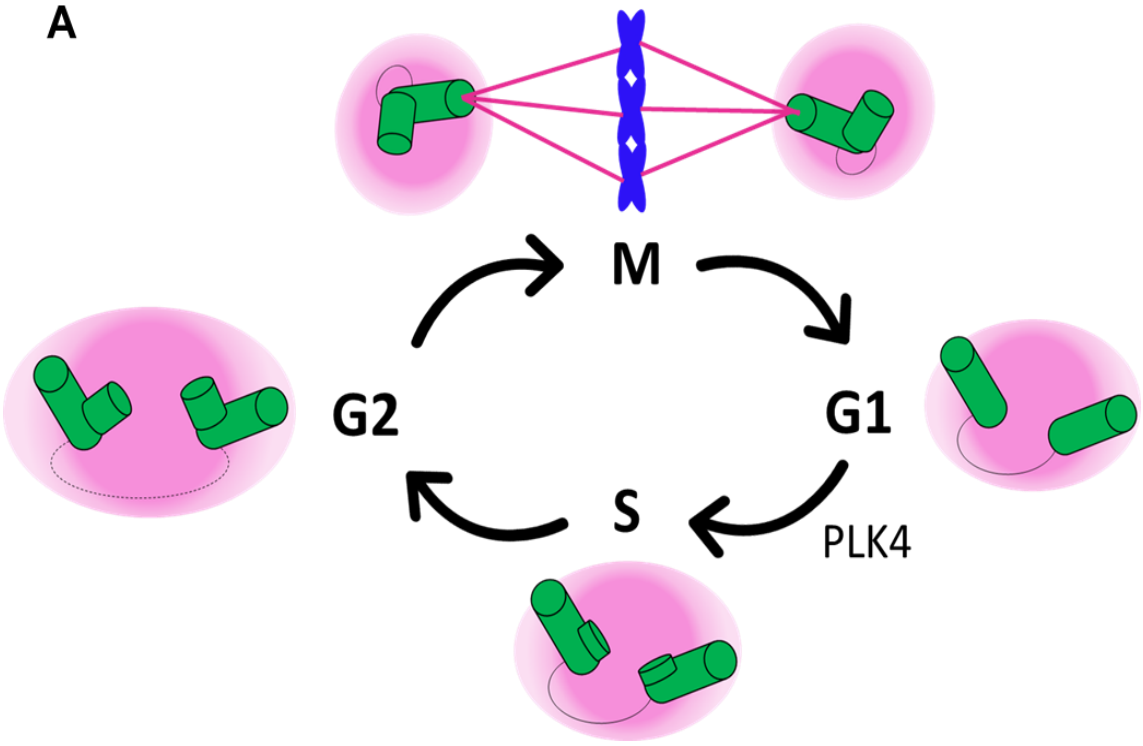
A
M
G1
S
G2
PLK4

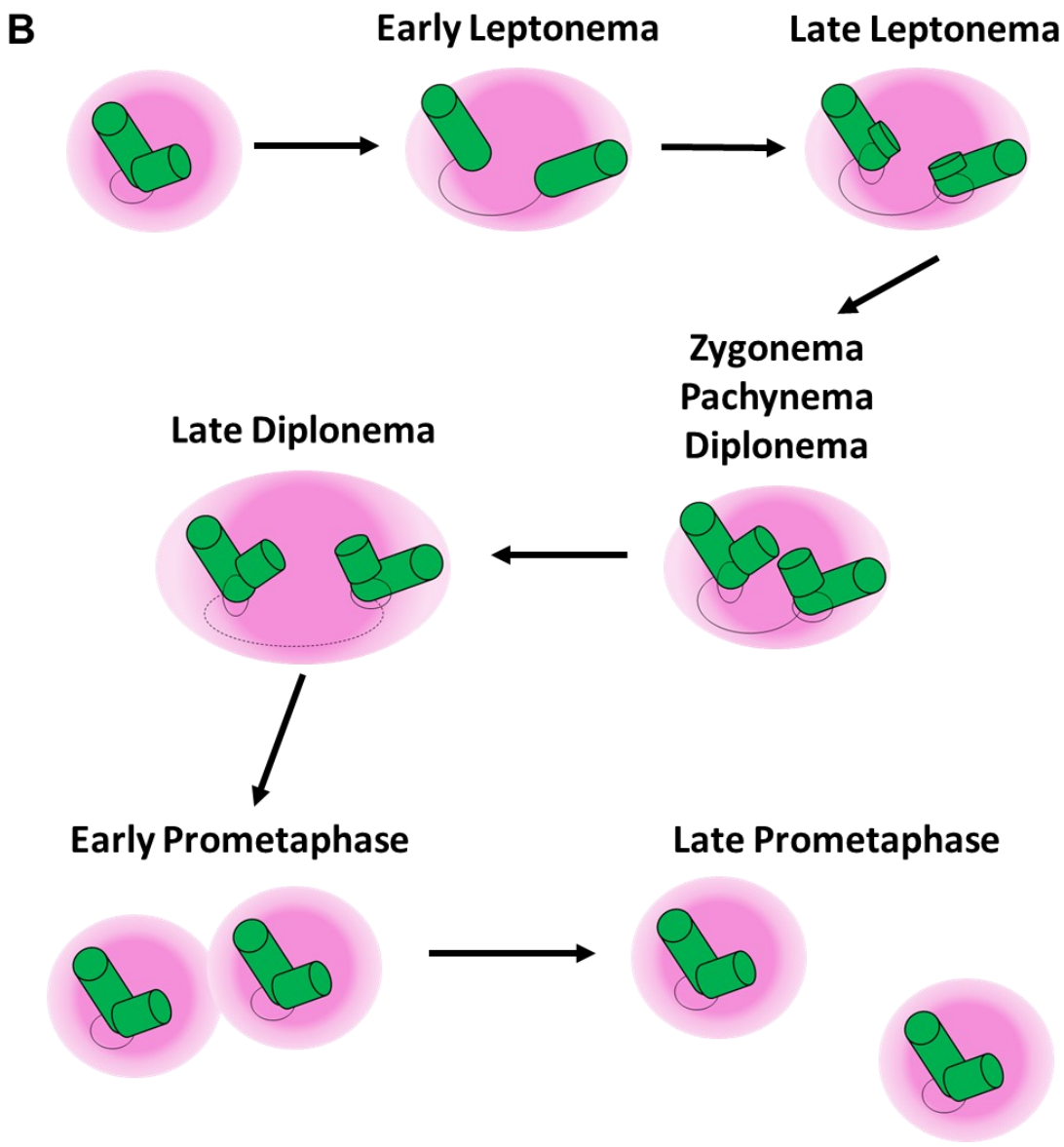
B
Early Leptonema
Late Leptonema
Zygonema
Pachynema
Diplonema
Late Diplonema
Early Prometaphase
Late Prometaphase

The steps of centriole biogenesis in spermatocytes are similar to those in mitosis, but the timing is different (Figure II.1B). Spermatocyte centrioles must duplicate twice to accommodate both meiotic divisions (Gall, 1961; Loncarek et al., 2007). Meiotic centrioles are nucleated as spermatocytes transition from late leptonema into zygonema. The daughter centrioles are extended in pachynema. By late prometaphase, the centrosomes are fully matured and begin migrating to the spindle poles.

Spermatocytes also face a unique challenge involving the X-Y sex chromosomes. Spermatocytes confine the X and Y chromosomes separately from the autosomal chromosomes, creating a heterochromatin domain known as the sex body (Handel, 2004). By tightly regulating this subcellular domain, spermatocytes can prevent transcriptional activity and better manage X-Y pairing and DNA repair.

The roles of PLK4 in meiosis have not been as well-studied as in mitosis. Prior research has utilized an ENU-induced PLK4 mutation, consisting of a single point mutation in the kinase domain (Harris et al., 2011). Heterozygous male mice harboring this mutation undergo partial germ cell loss, suggesting a role in early spermatogenesis.

Mammalian meiosis is unique due to its sexual dimorphism, in both timing and organization. Oocytes maintain a prolonged dictyate arrest, during which meiotic proteins must be maintained (Nagaoka *et al.*, 2012; Schatten and Sun, 2015; Webster and Schuh, 2017). While spermatogenesis utilizes canonical centrioles, mammalian oocytes instead rely on MTOCs consisting of

pericentrosomal proteins (Baumann *et al.*, 2017; Clift and Schuh, 2015; Lee *et al.*, 2017; Ma *et al.*, 2017). Oocytes also utilize a LISD, a complex of proteins that stabilize the acentriolar spindle (So et al., 2019). This dimorphism suggests that mammalian PLK4 may having differing roles in spermatocytes compared to oocytes.

Anti-PLK4 antibodies are often inconsistent and unreliable for immunofluorescence microscopy and protein expression studies. Prior research into the role of PLK4 in mammalian meiosis have relied on localization studies using either tagged mRNA or lab-developed antibodies. These studies have shown that PLK4 localizes to the cytoplasm and to the MTOCs in oocytes (Bury *et al.*, 2017; Luo and Kim, 2015). Prior studies of mouse spermatocytes have shown that PLK4 localizes to the centrioles and sex body (Jordan et al., 2012).

The development of an *mCherry-Plk4* overexpression transgenic mouse line has allowed for further research into the localization and roles of PLK4 (Basto *et al.*, 2006). This line was initially used to report on the impact of PLK4 overexpression in mouse brain development. More recently, it has been shown that the mCherry-PLK4 protein localizes to MTOCs during oogenesis (Manil-Ségalen *et al.*, 2018).

To further study the localization of PLK4, we utilized the *mCherry-Plk4* overexpression transgenic mouse line in both oocytes and spermatocytes. We confirm the localization of the overexpressed mCherry-PLK4 to oocyte MTOCs, and present novel findings of its localization to centrioles in spermatocytes.

Materials and Methods

Ethics Statement

All mice were bred at Johns Hopkins University (JHU, Baltimore, MD) in accordance with the National Institutes of Health and U.S. Department of Agriculture criteria. Protocols for their care and use were approved by the Institutional Animal Care and Use Committees of JHU.

Mice

Tg(mChPlk4) mice were acquired from the Curie Institute (Paris, France) (Marthiens *et al.*, 2013).

Hemizygous *Tg(mChPlk4)* male mice were bred to mice harboring the Cre transgenes that are specifically expressed in germ cells – *Spo11-Cre* (C57BL/6-Tg Spo11-cre)1Rsw/PecoJ) and *Hspa2-Cre* (C57BL/6-Tg Hspa2-Cre)1Eddy). This resulted in progeny hemizygous for both the *mCherry-Plk4* transgene and the germ cell-specific Cre transgene.

PCR genotyping

Primers used are described in Supplemental Table II.1. PCR conditions: 90°C for 2 min; 30 cycles of 90°C for 20 s, 58°C for annealing, 72°C for 1 min.

Oocyte harvesting and culture

Oocytes were prepared as previously described in Chapter I of this thesis.

Histological analyses

For testes to bodyweight ratio measurements, male mice were weighed prior to dissection. After the body weight measurement was recorded, testes were harvested. The fat surrounding the testes was trimmed as much as possible

without damaging the testes tissue. Both testes were weighed separately, and those weights were averaged for each mouse.

Tubule squash preparation

Tubule squashes were performed as previously described (Wellard *et al.*, 2018). Briefly, minced seminiferous tubules were fixed in a 2% paraformaldehyde solution. Tubule fragments were placed on a slide and squashed, then frozen in liquid nitrogen. Slides were washed in PBS and immediately immunostained.

Chromatin spread analyses

Spermatocyte chromatin spreads were prepared as previously described Briefly, spermatocytes were incubated in a hypotonic solution and then burst open by being dropped onto slides.

Microscopy and analyses

Immunofluorescence microscopy slide preparations and analyses were performed as previously described (Hwang *et al.*, 2018b). Primary and secondary antibodies used, and dilutions are listed in Supplemental Table II.2.

Meiotic substages of spermatocyte chromatin spreads were determined visually using SYCP3 morphology.

Graph preparation and statistical analysis was performed using GraphPad Prism (GraphPad Software). The number of samples used for each quantification is included in the corresponding figure legend.

Results and Discussion

mCherry-PLK4 localizes to the MTOCs of oocytes

To determine the localization of PLK4, we used a conditional overexpression *Tg(mChPlk4)* allele (Figure II.2A, see *Materials and Methods*). Breeding hemizygous *Tg(mChPlk4)* mice to mice expressing a Cre recombinase resulted in offspring with constitutive overexpression of the *mCherry-Plk4* allele. We used *Spo11-Cre,* a germ cell-specific Cre transgene. *Spo11-Cre* is expressed in early prophase, as previously described in Chapter I.

We first assessed the localization of mCherry-PLK4 in oocytes. As previously reported (Manil-Ségalen *et al.*, 2018), mCherry-PLK4 localizes to the chromosomes and MTOCs in prophase I (after meiotic resumption) and metaphase I, respectively (Figure II.2B). mCherry-PLK4 forms a disperse localization pattern around the chromatin in prometaphase following meiotic resumption. By metaphase I, mCherry-PLK4 has condensed to either side of the metaphase plate at the spindle poles. Notably, *mCherry-Plk4; Spo11-Cre* oocytes were frequently appeared to have more than one metaphase plate in metaphase I, with four mCherry-PLK4 foci. This is likely due to the overexpression of PLK4 resulting in the overduplication of MTOCs.

mCherry-PLK4 localizes to the centrioles of spermatocytes

We next assessed the localization of mCherry-PLK4 in spermatocytes. Pairing the *mCherry-Plk4* allele with *Spo11-Cre* was not appropriate to study PLK4 localization in spermatocytes. *mCherry-Plk4; Spo11-Cre* males developed testes that were smaller than control littermates by 16 dpp, indicating an arrest in early

Figure II.2: mCherry-PLK4 localizes to the MTOCs in oocytes. (A) Schematic of *mCherry-Plk4* transgene before and after Cre recombinase expression. A stop codon directly upstream of the transgene, flanked by loxP sites, is excised in the presence of a Cre. (B) Control and *mCherry-Plk4* oocytes immunolabeled with antibodies against mCherry (green) and counterstained with DAPI (DNA, blue). Scale bar: 10 μm.

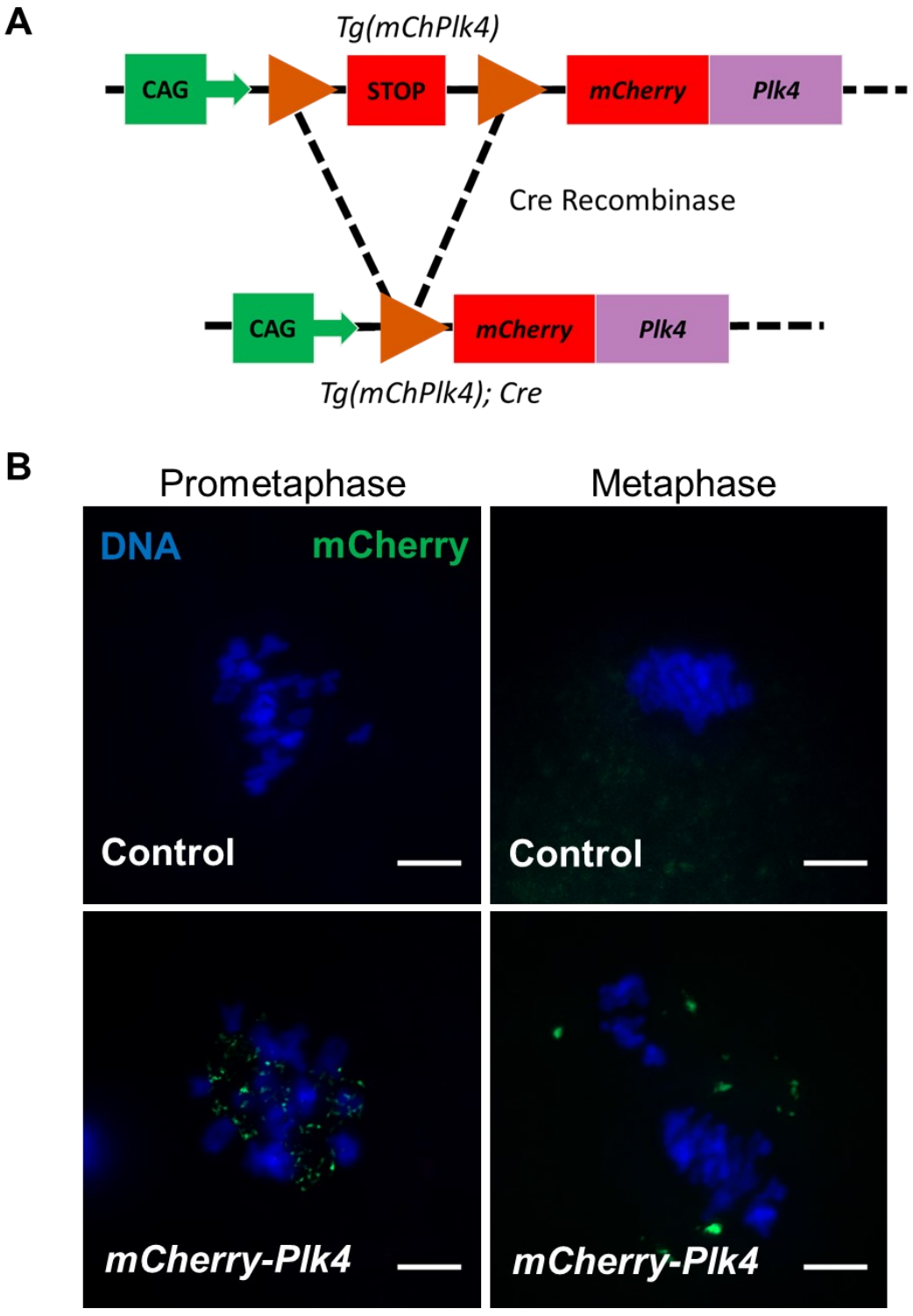
A
Tg(mChPlk4)
CAG
STOP
mCherry
Plk4
Cre Recombinase
CAG
mCherry
Plk4
Tg(mChPlk4); Cre
B
Prometaphase
Metaphase
DNA
mCherry
Control
Control
mCherry-Plk4
mCherry-Plk4

prophase (Figure II.3A). Further analysis of chromosome spreads taken from these males revealed that the spermatocytes were not progressing past leptotene stage (Figure II.3B and C). We attributed this early arrest to the overexpression of mCherry-PLK4 starting in early leptotene stage. It is likely that higher levels of PLK4 resulted in the premature duplication of centrioles, triggering an arrest.

To solve this problem, we instead utilized *Hspa2-Cre. Hspa2-Cre* is a male-specific Cre expressed in mid-prophase (Hwang *et al.*, 2018a; Inselman *et al.*, 2010).Tubule squashes from *mCherry-Plk4; Hspa2-Cre* males revealed that mCherry-PLK4 localizes as pairs of foci that migrate to the spindle poles in metaphase I (Figure II.4). Based on the localization of these foci, we hypothesized that mCherry-PLK4 is localizing to the centrioles. The co-localization of mCherry to CEP192, a known centrosomal protein, supports this hypothesis. In prophase, mCherry-PLK4 is visible on each of the two centrioles. By metaphase I, those centrioles have undergone a round of duplication, with mCherry-PLK4 localizing to each pair at the spindle poles.

Future Directions and Preliminary Conclusions

Future Directions

We will continue to evaluate the localization of mCherry-PLK4 in these mice. Preliminary results suggest that PLK4 may be localizing to the centrioles in prophase I and metaphase I spermatocytes. Further analysis is needed to confirm this localization. We plan to utilize additional centriole-specific antibodies to

Figure II.3: (A) Quantification of testes to body weight ratio of control and *mCherry-Plk4; Spo11-Cre* males. Mean and SD of each column are represented by the black bars. Numbers at the base of each bar indicate the number of mice counted for each genotype. (B) Chromosome spreads of control and *mCherry-Plk4; Spo11-Cre* spermatocytes, immunolabeled with antibodies against centromeres/kinetochores (CEN, purple) and SYCP3 (green), counterstained with DAPI (DNA, blue). Scale bars: 10 μm. (C) Quantification of meiosis I stages of spermatocytes harvested from 16 dpp males. One control mouse and 2 *mCherry-Plk4; Spo11-Cre* mice were assessed, with 100 spermatocytes counted per mouse. Mean and SD of each column are represented by the black bars.

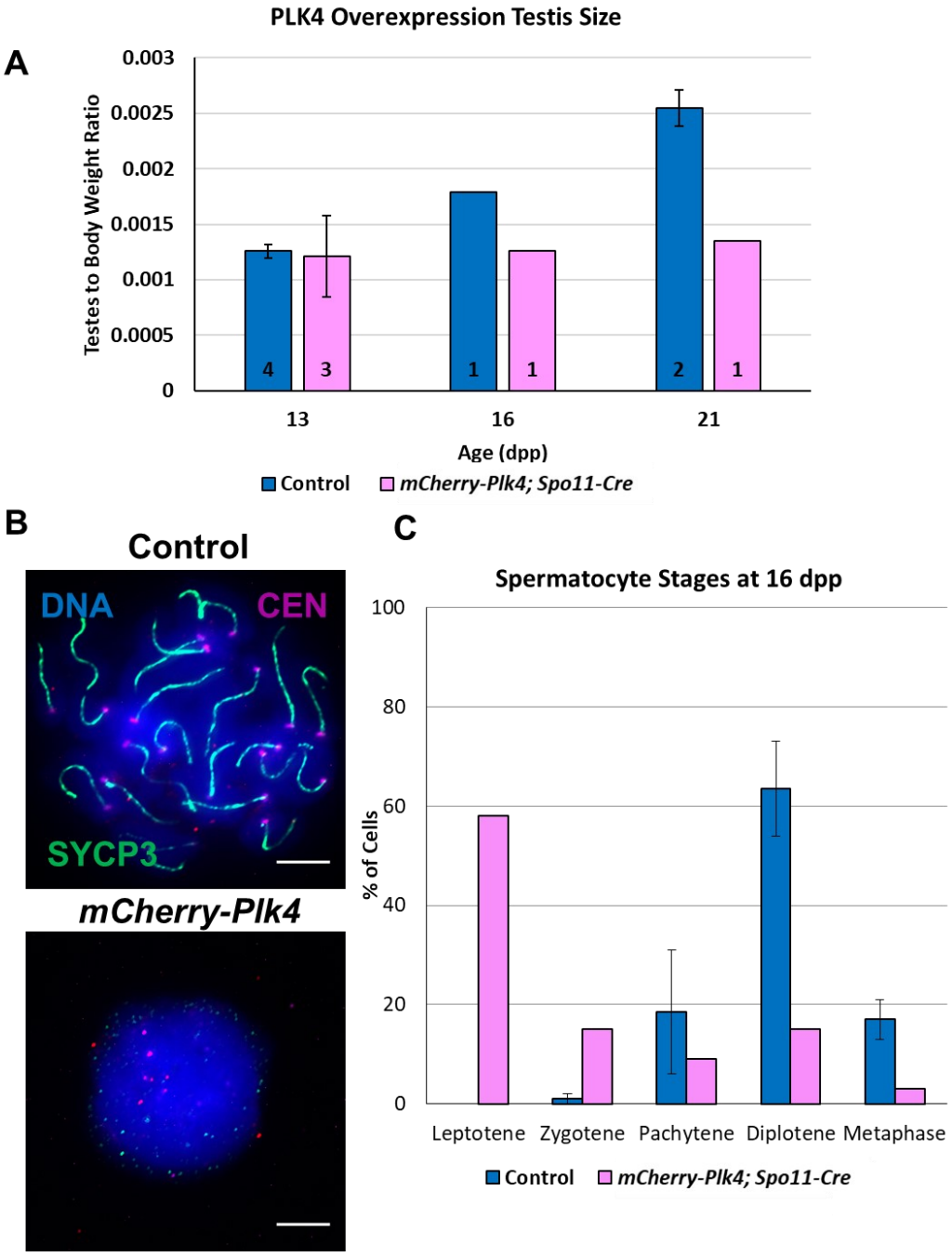
A
PLK4 Overexpression Testis Size
Testes to Body Weight Ratio
0.003
0.0025
0.002
0.0015
0.001
0.0005
0
4
3
1
1
2
1
13
16
21
Age (dpp)
Control
mCherry-Plk4; Spo11-Cre
B
Control
DNA
CEN
SYCP3
mCherry-Plk4
C
Spermatocyte Stages at 16 dpp
% of Cells
100
80
60
40
20
0
Leptotene
Zygotene
Pachytene
Diplotene
Metaphase
Control
mCherry-Plk4; Spo11-Cre

visually confirm that mCherry-PLK4 is colocalizing with centriolar machinery. While previous research has suggested that PLK4 localizes to spermatocyte centrioles (Harris et al., 2011; Jordan et al., 2012), this will be the first work to conclusively show colocalization of PLK4 and centriolar components.

Spermatocytes face the unique challenge of transcriptionally silencing the X-Y chromosome pair during meiosis. This is done by compartmentalizing the sex chromosomes into a nuclear subdomain, known as the sex body (Fernandez-Capetillo et al., 2003; Handel, 2004). Analysis of wildtype spermatocytes using anti-PLK4 antibodies has indicated that PLK4 localizes to the sex body (Jordan et al., 2012). We plan to utilize these *mCherry-Plk4* males to further investigate this localization, independently of anti-PLK4 antibodies.

Moving forward, we also plan to assess *mCherry-Plk4; Hspa2-Cre* males for meiotic defects. Any abnormal phenotype found in these mice may be informative as to what role PLK4 has during spermatogenesis. To accomplish this, we first plan to carry out fertility tests of these males. This will inform us whether spermatogenesis is progressing through to completion. We will also assess testes development by measuring testis to bodyweight ratios at varying ages. Any decrease in testes size compared to control littermates is indicative of meiotic defects, and the age at which that size difference begins can indicate when those defects are occurring. Histological analysis of testes cross-sections may also reveal the occurrence and timing of any defects.

We plan to utilize the tagged PLK4 protein to further determine interacting proteins. mCherry-tagged proteins have previously been used to study interactions

Figure II.4: mCherry-PLK4 localizes to the centrioles of spermatocytes throughout meiosis I. Tubule squashes of control and *mCherry-Plk4* spermatocytes immunolabeled with antibodies against mCherry (red), SYCP3 (green), CEP192 (white), and counterstained with DAPI (DNA, blue). Boxes indicate centrosomes in zoomed images below. Arrows indicate the other centriolar pair after centriole duplication.

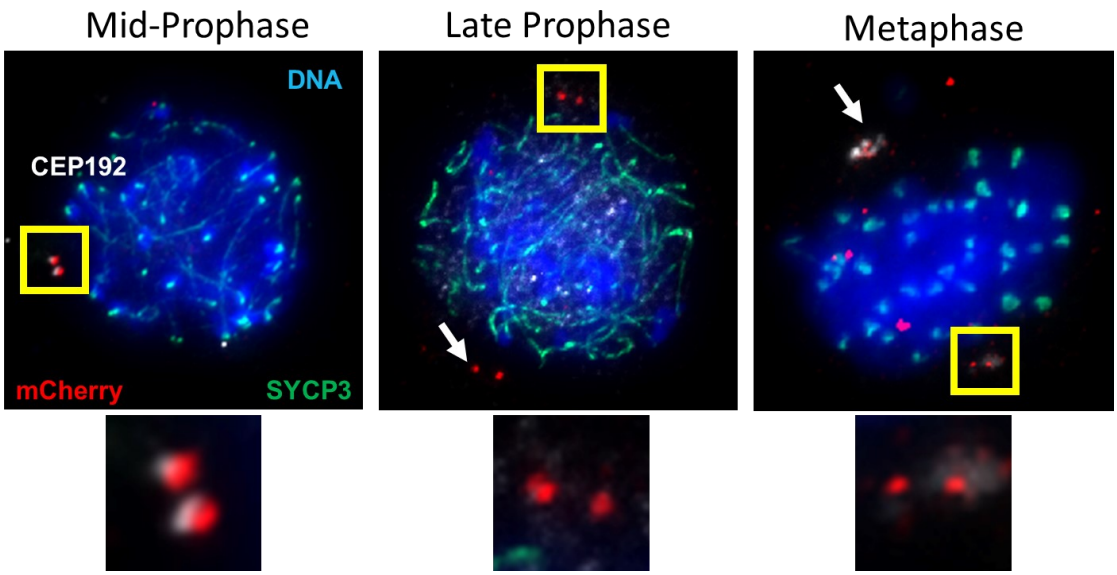
Mid-Prophase
Late Prophase
Metaphase
DNA
CEP192
mCherry
SYCP3

via mCherry-based immunoprecipitation (MacLennan et al., 2017; Willett et al., 2017). We plan to utilize a similar approach in combination with mass spectrometry to identify proteins that are co-immunoprecipitated with mCherry-PLK4.

The mCherry-PLK4 transgene can also be used to determine PLK4's later meiotic localization. Anti-mCherry antibodies will be used to track PLK4 localization throughout the later stages of both spermatogenesis and oogenesis, as well as immediately after fertilization. Based on the data presented here, we anticipate that PLK4 will continue to localize to the centrioles and MTOCs during meiosis II in spermatocytes and oocytes, respectively.

A caveat to this experimental approach is that the constitutive overexpression of mCherry-PLK4 may result in localization outside of what would be seen in a cell with wildtype PLK4 levels. To determine whether this is the case, we will be quantifying PLK4 levels in *mCherry-Plk4* mice compared to controls. Additionally, any localization or proposed roles resulting from this model will be confirmed using a *Plk4* cKO approach.

Preliminary Conclusions

PLK4 is known to play a vital role in mitotic centriolar cartwheel formation (Arquint and Nigg, 2016; Arquint et al., 2012; Harris et al., 2011; Moyer and Holland, 2019). Prior meiotic studies have shown that PLK4 localizes to the MTOCs of oocytes (Bury *et al.*, 2017; Luo and Kim, 2015; Manil-Ségalen *et al.*, 2018). Our work independently confirms these results. Our observation of multiple spindles in *mCherry-Plk4; Spo11-Cre* oocytes additionally implies that PLK4 influences MTOC duplication and organization.

The localization of PLK4 in spermatocytes has not been well-studied in previous research. Our preliminary results indicate that mCherry-PLK4 localizes to the centrioles starting in prophase and continuing into metaphase I. Prior research has shown that the mutation of *Plk4* results in spermatocyte death (Harris *et al.*, 2011). However, more work is needed to determine the role of PLK4 in spermatogenesis.

Acknowledgements

We thank Renata Basto for providing the *Tg(mChPlk4)* mice, and Stephen Wellard, Jessica Hopkins, and Christopher Shults for technical help.

Gene	Forward Primer (5'-…..-3')	Reverse Primer (5'-…..-3')	Product Size (bp)
mCherry-Plk4	AGGACGGCGAGTTCATCTAC	TGGTGTAGTCCTCGTTGTGG	*Flox*: 1174 *Del*: 341
mCherry-Plk4 Internal Control	CAAATGTTGCTTGTCTGGTG	GTCAGTCGAGTGCACAGTTT	1012
Cre Transgene	CCATCTGCCACCAGCCAG	TCGCCATCTTCCAGCAGG	420
Cre Internal Control	ACTGGGATCTTCGAACTCTTTGGAC	GATGTTGGGGCACTGCTCATTCACC	281

Table II.1: Primers used in this study.

Primary Antibodies				
Antibody	**Host**	**Source**	**Cat. Number**	**IF Dilution**
centromere	Human	Antibodies Inc.	15-235	1:100
mCherry	Mouse	Sigma-Aldrich	SAB2702291	1:500
SYCP3	Mouse	Santa Cruz Biotech	sc-74569	1:50
SYCP3	Rabbit	Novus Biologicals	NB300-231	1:1000
Secondary Antibodies				
Antibody	**Host**	**Source**	**Cat. Number**	**IF Dilution**
Mouse IgG (H+L), Alexa Fluor 488	Goat	Invitrogen	A-11001	1:500
Mouse IgG (H+L), Alexa Fluor 568	Goat	Invitrogen	A-11031	1:500
Rabbit IgG (H+L), Alexa Fluor 488	Goat	Invitrogen	A-11008	1:500
Rabbit IgG (H+L), Alexa Fluor 568	Goat	Invitrogen	A-11011	1:500
Human IgG (H+L), Alexa Fluor 633	Goat	Invitrogen	A-21091	1:500
Goat IgG (H+L) Alexa Fluor 488	Donkey	Invitrogen	A-11055	1:500
Goat IgG (H+L) Alexa Fluor 568	Donkey	Invitrogen	A-11057	1:500
Goat IgG (H+L) Alexa Fluor 633	Donkey	Invitrogen	A-21082	1:500

Table II.2: Antibodies used in this study.

References

Arquint, C., and Nigg, E.A. (2016). The PLK4-STIL-SAS-6 module at the core of centriole duplication. Biochem. Soc. Trans. *44*, 1253–1263.

Arquint, C., Sonnen, K.F., Stierhof, Y.-D., and Nigg, E.A. (2012). Cell-cycle-regulated expression of STIL controls centriole number in human cells. J. Cell Sci. *125*, 1342–1352.

Basto, R., Lau, J., Vinogradova, T., Gardiol, A., Woods, C.G., Khodjakov, A., and Raff, J.W. (2006). Flies without centrioles. Cell *125*, 1375–1386.

Baumann, C., Wang, X., Yang, L., and Viveiros, M.M. (2017). Error-prone meiotic division and subfertility in mice with oocyte-conditional knockdown of pericentrin. J. Cell Sci. *130*, 1251–1262.

Bettencourt-Dias, M., Rodrigues-Martins, A., Carpenter, L., Riparbelli, M., Lehmann, L., Gatt, M.K., Carmo, N., Balloux, F., Callaini, G., and Glover, D.M. (2005). SAK/PLK4 is required for centriole duplication and flagella development. Curr. Biol. *15*, 2199–2207.

Bury, L., Coelho, P.A., Simeone, A., Ferries, S., Eyers, C.E., Eyers, P.A., Zernicka-Goetz, M., and Glover, D.M. (2017). Plk4 and Aurora A cooperate in the initiation of acentriolar spindle assembly in mammalian oocytes. J. Cell Biol. *216*, 3571–3590.

Clift, D., and Schuh, M. (2015). A three-step MTOC fragmentation mechanism facilitates bipolar spindle assembly in mouse oocytes. Nat. Commun. *6*, 7217.

Fernandez-Capetillo, O., Mahadevaiah, S.K., Celeste, A., Romanienko, P.J., Camerini-Otero, R.D., Bonner, W.M., Manova, K., Burgoyne, P., and Nussenzweig, A. (2003). H2AX is required for chromatin remodeling and inactivation of sex chromosomes in male mouse meiosis. Dev. Cell *4*, 497–508.

Gall, J.G. (1961). Centriole replication. A study of spermatogenesis in the snail Viviparus. J Biophys Biochem Cytol *10*, 163–193.

Habedanck, R., Stierhof, Y.-D., Wilkinson, C.J., and Nigg, E.A. (2005). The Polo kinase Plk4 functions in centriole duplication. Nat. Cell Biol. *7*, 1140–1146.

Handel, M.A. (2004). The XY body: a specialized meiotic chromatin domain. Exp. Cell Res. *296*, 57–63.

Harris, R.M., Weiss, J., and Jameson, J.L. (2011). Male hypogonadism and germ cell loss caused by a mutation in Polo-like kinase 4. Endocrinology *152*, 3975–3985.

Hwang, G., Verver, D.E., Handel, M.A., Hamer, G., and Jordan, P.W. (2018a). Depletion of SMC5/6 sensitizes male germ cells to DNA damage. Mol. Biol. Cell *29*, 3003–3016.

Hwang, G.H., Hopkins, J.L., and Jordan, P.W. (2018b). Chromatin Spread Preparations for the Analysis of Mouse Oocyte Progression from Prophase to Metaphase II. J. Vis. Exp. *132*, e56736.

Inselman, A.L., Nakamura, N., Brown, P.R., Willis, W.D., Goulding, E.H., and Eddy, E.M. (2010). Heat shock protein 2 promoter drives Cre expression in spermatocytes of transgenic mice. Genesis *48*, 114–120.

Jordan, P.W., Karppinen, J., and Handel, M.A. (2012). Polo-like kinase is required for synaptonemal complex disassembly and phosphorylation in mouse spermatocytes. J. Cell Sci. *125*, 5061–5072.

Lee, I.-W., Jo, Y.-J., Jung, S.-M., Wang, H.-Y., Kim, N.-H., and Namgoong, S. (2017). Distinct roles of Cep192 and Cep152 in acentriolar MTOCs and spindle formation during mouse oocyte maturation. FASEB J.

Loncarek, J., Sluder, G., and Khodjakov, A. (2007). Centriole biogenesis: a tale of two pathways. Nat. Cell Biol. *9*, 736–738.

Luo, Y.-B., and Kim, N.-H. (2015). PLK4 is essential for meiotic resumption in mouse oocytes. Biol. Reprod. *92*, 101.

Ma, H., Marti-Gutierrez, N., Park, S.-W., Wu, J., Lee, Y., Suzuki, K., Koski, A., Ji, D., Hayama, T., Ahmed, R., et al. (2017). Correction of a pathogenic gene mutation in human embryos. Nature *548*, 413–419.

MacLennan, M., García-Cañadas, M., Reichmann, J., Khazina, E., Wagner, G., Playfoot, C.J., Salvador-Palomeque, C., Mann, A.R., Peressini, P., Sanchez, L., et al. (2017). Mobilization of LINE-1 retrotransposons is restricted by Tex19.1 in mouse embryonic stem cells. Elife *6*.

Manil-Ségalen, M., Łuksza, M., Kanaan, J., Marthiens, V., Lane, S.I.R., Jones, K.T., Terret, M.-E., Basto, R., and Verlhac, M.-H. (2018). Chromosome structural anomalies due to aberrant spindle forces exerted at gene editing sites in meiosis. J. Cell Biol. *217*, 3416–3430.

Marthiens, V., Rujano, M.A., Pennetier, C., Tessier, S., Paul-Gilloteaux, P., and Basto, R. (2013). Centrosome amplification causes microcephaly. Nat. Cell Biol. *15*, 731–740.

Moyer, T.C., and Holland, A.J. (2019). PLK4 promotes centriole duplication by phosphorylating STIL to link the procentriole cartwheel to the microtubule wall. Elife *8*.

Nagaoka, S.I., Hassold, T.J., and Hunt, P.A. (2012). Human aneuploidy: mechanisms and new insights into an age-old problem. Nat. Rev. Genet. *13*, 493–504.

Riparbelli, M.G., Persico, V., Dallai, R., and Callaini, G. (2020). Centrioles and Ciliary Structures during Male Gametogenesis in Hexapoda: Discovery of New Models. Cells *9*.

Rodrigues-Martins, A., Riparbelli, M., Callaini, G., Glover, D.M., and Bettencourt-Dias, M. (2008). From centriole biogenesis to cellular function: centrioles are essential for cell division at critical developmental stages. Cell Cycle *7*, 11–16.

Schatten, H., and Sun, Q.-Y. (2015). Centrosome and microtubule functions and dysfunctions in meiosis: implications for age-related infertility and developmental disorders. Reprod Fertil Dev *27*, 934–943.

So, C., Seres, K.B., Steyer, A.M., Mönnich, E., Clift, D., Pejkovska, A., Möbius, W., and Schuh, M. (2019). A liquid-like spindle domain promotes acentrosomal spindle assembly in mammalian oocytes. Science *364*.

Webster, A., and Schuh, M. (2017). Mechanisms of aneuploidy in human eggs. Trends Cell Biol. *27*, 55–68.

Wellard, S.R., Hopkins, J., and Jordan, P.W. (2018). A seminiferous tubule squash technique for the cytological analysis of spermatogenesis using the mouse model. J. Vis. Exp. *132*, e56453.

Willett, R., Martina, J.A., Zewe, J.P., Wills, R., Hammond, G.R.V., and Puertollano, R. (2017). TFEB regulates lysosomal positioning by modulating TMEM55B expression and JIP4 recruitment to lysosomes. Nat. Commun. *8*, 1580.

Chapter III

The roles of PLK4 and SAS4 in mammalian meiosis

Tara M. Little, Jingwen Xu and Philip W. Jordan

Abstract

The tightly controlled duplication of centrioles is a critical step in cell division. Both Polo-Like Kinase 4 (PLK4) and SAS4 (also known as CENPJ or CPAP) are known to be essential for the proper regulation of centriole biogenesis in mitosis. Preliminary studies have shown that PLK4 localizes to both the centrioles and microtubule organizing centers (MTOCs) in mammalian germ cells, although its role in meiosis is not clearly understood. SAS4 is known to be a critical structural component of mitotic centrioles but has not been as well studied in mammalian meiosis. To better understand the roles of PLK4 and SAS4, we utilized *Plk4* and *Sas4* conditional knockout (cKO) mouse lines. This approach allows us to evaluate the effects of PLK4 and SAS4 depletion on mammalian oocytes and spermatocytes. Our results indicate that *Plk4* cKO testes are undersized, while *Sas4* cKO spermatocytes fail to properly duplicate their centrioles. Preliminary results indicate that *Plk4* and *Sas4* cKO oocytes successfully organize their MTOCs through prometaphase.

Introduction

In most cell types, centrioles are responsible for driving the formation of the metaphase spindle. Therefore, the proper regulation of centrioles is critical to ensure that division occurs correctly. Mitotic centrosome defects can lead to genome instability, microcephaly, or cancer (Bazzi and Anderson, 2014; Marjanović et al., 2015; Marthiens et al., 2013; Pihan, 2013; Rodrigues-Martins et al., 2008). Centriolar components and regulators have been shown to be essential for spermatogenesis in both *Drosophila melanogaster* and mouse models (Bettencourt-Dias et al., 2005; Harris et al., 2011).

As described in Chapter 2, centriole duplication and division is temporally regulated with the meiotic cell cycle (Nigg, 2007; Rodrigues-Martins *et al.*, 2008; Sumiyoshi *et al.*, 2002). The ways in which this process is regulated in spermatocytes are not well understood.

Mammalian oocytes are unique in that they undergo acentriolar division (Simerly et al., 2018). Oocytes instead rely on microtubule organizing centers (MTOCs) consisting of pericentrosomal material and a liquid-like spindle domain (LISD) that stabilizes the acentriolar spindle (So et al., 2019). MTOCs are linked together during the dictyate arrest, and separate following nuclear envelope breakdown. Once freed, the MTOCs organize themselves into two poles, from which the microtubules will emanate during metaphase (Baumann *et al.*, 2017; Clift and Schuh, 2015; Lee *et al.*, 2017; Ma *et al.*, 2017). As described in Chapter II, spermatocytes must reconcile the challenge of regulating the sex body. The

difference in mechanisms between oogenesis and spermatogenesis present the possibility of unique regulation pathways.

A symmetrical cartwheel structure, consisting of scaffolding proteins, forms the basis of centrioles (Hirono, 2014; Yoshiba *et al.*, 2019). At the start of centriole biogenesis, this cartwheel is constructed at the base of the original mother centriole. PLK4 has been shown to regulate this process during mitosis by phosphorylating STIL, which in turn initiates cartwheel assembly and attaches the forming cartwheel structure to the centriole wall (Arquint and Nigg, 2016; Arquint et al., 2012; Moyer and Holland, 2019). PLK4 has been shown to localize to the centriole in mouse spermatocytes (Jordan *et al.*, 2012), as well as to MTOCs in oocytes (Bury *et al.*, 2017).

Previous research has shown that a single homozygous missense mutation in the kinase domain of PLK4 is embryonically lethal (Harris et al., 2011). In heterozygous males, this I242N mutation results in reduced testes weight beginning at 10 dpp. Histological analysis revealed that this weight reduction was due to patchy germ cell loss, with some tubules containing only Sertoli cells. At this age, the first wave of spermatocytes are undergoing prophase I (Oakberg, 1956). Germ cell loss at this stage suggests defects in the initial stages of prophase – possibly in DNA repair, chromosome condensation, synapsis, or early centriole biogenesis. Despite these findings, PLK4's roles in mammalian meiosis are not fully understood.

SAS4, named for its spindle assembly phenotype, was initially discovered in *Saccharomyces cerevisiae* (Xu et al., 1999). Later studies showed that SAS4

was required for centriole duplication in *Caenorhabditis elegans* (Kirkham et al., 2003). SAS4 depletion in *Drosophila melanogaster*, resulted in successful, acentriolar mitosis but failed meiosis (Riparbelli and Callaini, 2011). In humans, *Sas4* mutations can result in microcephaly from mitotic defects during neurogenesis (Verloes et al., 1993). SAS4 mutations have also been attributed to the development of cancer phenotypes (Leidel and Gönczy, 2003; Xu *et al.*, 1999). Mitotic SAS4 depletion is embryonically lethal due to a failure to properly organize tubulin, resulting in apoptosis (Bazzi and Anderson, 2014). SAS4 is a critical regulator of mammalian centriole formation. At the start of mitotic centriole biogenesis, the initial cartwheel base of the daughter centriole must be docked at the base of the mature mother centriole. SAS4 serves as a scaffolding protein that builds on the new centriole base immediately after docking. SAS4 localizes on the outside of the cartwheel structure and recruits outer centriole components which in turn will organize tubulin (Gopalakrishnan *et al.*, 2011; Kuriyama, 2009; Leidel and Gönczy, 2003). SAS4 has not been previously studied within the context of mammalian meiosis.

To better understand the roles of PLK4 and SAS4 in mammalian meiosis, we plan to utilize *Plk4* cKO and *Sas4* cKO mouse models. By using these germ cell-specific models, we will be able to examine the effects of PLK4 and SAS4 depletion in both oocytes and spermatocytes. We hope that this approach reveals the mechanisms through which these proteins regulate meiosis. Our preliminary results confirm that both PLK4 and SAS4 are essential for spermatogenesis.

Further studies are needed to evaluate potential roles in oogenesis, although SAS4 does not appear to be essential for acentriolar division.

Materials and Methods

Ethics Statement

All mice were bred at Johns Hopkins University (JHU, Baltimore, MD) in accordance with the National Institutes of Health and U.S. Department of Agriculture criteria. Protocols for their care and use were approved by the Institutional Animal Care and Use Committees of JHU.

Mice

Plk4 flox mice were generated using CRISPR/Cas9-mediated editing. Guide DNA sequencings targeting either end of exon 5 of *Plk4* were used for mESC injection, along with a loxP repair template. mESCs were then microinjected into C57BL/6JN blastocysts and transferred into pseudo-pregnant females. Heterozygous *Plk4 flox* progeny were confirmed by sequencing. Heterozygous *Plk4 flox* males and females were bred together to produce *Plk4 flox/flox* offspring.*Plk4 flox/flox* mice were bred to mice harboring germ-cell specific Cre transgenes - *Spo11-Cre* (C57BL/6-Tg Spo11-cre)1Rsw/PecoJ), *Stra8-Cre* (C57BL/6-Tg Stra8-cre)1Reb/LguJ), and *Zp3-Cre* (C57BL/6-Tg Zp3-cre)93Knw to produce *Plk4 +/flox; Cre* offspring. These mice were then bred to *Plk4 flox/flox* mice, resulting in *Plk4* cKO (*Plk4 flox/del; Cre*) and control (*Plk4 +/flox*) genotypes.

Sas4 flox mice were acquired from the Memorial Sloan-Kettering Cancer Center (New York, NY) (Bazzi and Anderson, 2014).

Heterozygous *Sas4 flox* mice were mated to produce homozygous *Sas4 flox/flox* mice. These homozygous offspring were then mated to mice harboring meiotic-specific Cre transgenes - *Spo11-Cre* (C57BL/6-Tg(Spo11-cre)1Rsw/PecoJ), *Stra8-Cre* (C57BL/6-Tg(Stra8-icre)1Reb), and *Zp3-Cre* (C57BL/6-Tg Zp3-cre)93Knw - to produce *Sas4 +/flox; Cre* offspring. These mice were then bred to *Sas4 flox/flox* mice to produce *Sas4* cKO (*Sas4 flox/del; Cre)* and control (*Sas4 +/flox*) genotypes.

PCR genotyping

Primers used are described in Supplemental Table III.1. PCR conditions: 90°C for 2 min; 30 cycles of 90°C for 20 s, 58°C for annealing, 72°C for 1 min.

Histological analyses

Testes to bodyweight ratio measurements were obtained as described in Chapter II. For H&E staining, testis tissues were fixed in bouins fixative, then embedded in paraffin. Sections were cut to a thickness of 5 microns and placed onto slides. Slides were then stained with hematoxylin and eosin.

Tubule squash preparation

Tubule squashes were performed as previously described in Chapter II (Wellard *et al.*, 2018).

Chromatin spread analyses

Spermatocyte chromatin spreads were prepared as previously described in Chapter 2.

Oocyte harvesting and culture

Oocytes were collected as described in Chapter 1.

Microscopy and analyses

Immunofluorescence microscopy slide preparations and analyses were performed as previously described (Hwang *et al.*, 2018b). Primary and secondary antibodies used, and dilutions are listed in Supplemental Table III.2.

Graph preparation and statistical analysis was performed using GraphPad Prism (GraphPad Software). The number of samples used for each quantification is included in the corresponding figure legend.

Preliminary Results

Sas4 cKO; Spo11-Cre males fail to develop mature spermatozoa

We utilized a previously published *Sas4* cKO mouse line (Bazzi and Anderson, 2014) to assess the effects of SAS4 depletion in meiosis (Figure III.1A, see *Materials and Methods*). Homozygous *Sas4 flox* mice were mated to *Sas4 +/flox* mice harboring a germ cell-specific Cre transgene to produce *Sas4* cKO (*Sas4 flox/del; Cre*) offspring.

Initially, we paired the *Sas4* cKO genotype with *Spo11-Cre* to deplete SAS4 in early prophase (Hwang *et al.*, 2018a; Lyndaker *et al.*, 2013). We measured testes to body weight ratios of *Sas4* cKO; *Spo11-Cre* and control males at varying ages (Figure III.1B). Surprisingly, *Sas4* cKO; *Spo11-Cre* males did not show any size difference compared to their control littermates at any age.

We then prepared tubule squashes from *Sas4* cKO; *Spo11-Cre* males to assess the integrity of the centrioles (Figure III.2A and B). While control mice have 2 centrioles at both spindle poles in metaphase I, *Sas4* cKO; *Spo11-Cre* spermatocytes only had 1 centriole at either pole (Figure III.2A). In control

spermatocytes, CEP164 staining marks the mature mother centriole, while the newly formed daughter centriole is free of CEP164 (Graser *et al.*, 2007). CEP164 localized to the singular centrioles in *Sas4* cKO; *Spo11-Cre* spermatocytes, indicating a failure in daughter centriole biogenesis. Despite the failure of spermatocytes to properly duplicate their centrioles, *Sas4* cKO; *Spo11-Cre* spermatocytes did appear to undergo meiosis I normally. We anticipated that this lack of centriole biogenesis would result in errors in the next round of division. This was confirmed by pericentriolar matrix staining (PCM) of MII spermatocytes, which indicated that the single centriole is fully matured (Figure III.2B).

To determine if *Sas4* cKO; *Spo11-Cre* spermatocytes completed meiosis successfully, we assessed cross sections of tubules harvested from adult mice (Figure III.3A). While mature spermatozoa were clearly visible in the lumen of control tubules, mature spermatozoa were absent in *Sas4* cKO; *Spo11-Cre* tubules. *Sas4* cKO; *Spo11-Cre* primary spermatids had a larger diameter compared to controls, indicating either potential apoptotic cells or cells containing an incorrect amount of genetic material (Figure III.3B). Sperm counts from epididymis samples confirmed that *Sas4* cKO; *Spo11-Cre* males were likely infertile, with very low sperm density compared to controls (Figure III.3C). Closer analysis of the sperm collected from these mice revealed that *Sas4* cKO; *Spo11-Cre* spermatozoa lacked flagella (Figure III.3D). Prior research has demonstrated that mitotic cells fail to develop cilia when SAS4 expression is depleted (Gopalakrishnan *et al.*, 2011). This mobility role of centrioles likely explains the lack of flagella in *Sas4* cKO; *Spo11-Cre* spermatocytes.

Figure III.1: *Sas4* cKO; *Spo11-Cre* males develop normally sized testes. (A) Schematic of mouse *Sas4* floxed allele containing loxP sites (orange triangle), flanking exon 12 (gray box), and the resulting *Sas4* deletion allele after excision of exon 12 by Cre recombinase in early prophase. (B) Quantification of testes to body weight ratio of control and *Sas4* cKO; *Spo11-Cre* males. Mean and SD of each column are represented by the black bars. Numbers at the base of each bar indicate the number of mice counted for each genotype.

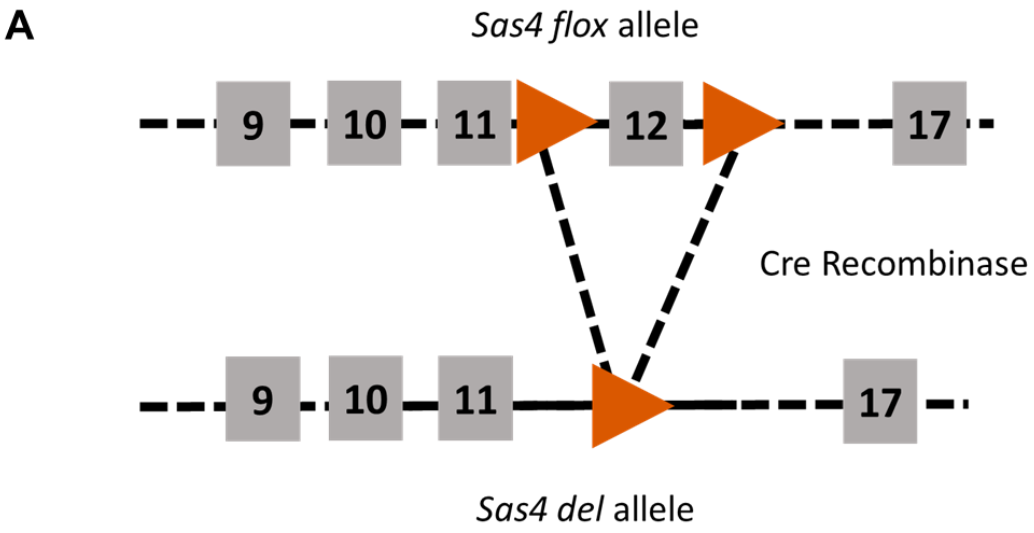
A
Sas4 flox allele
9
10
11
12
17
Cre Recombinase
9
10
11
17
Sas4 del allele

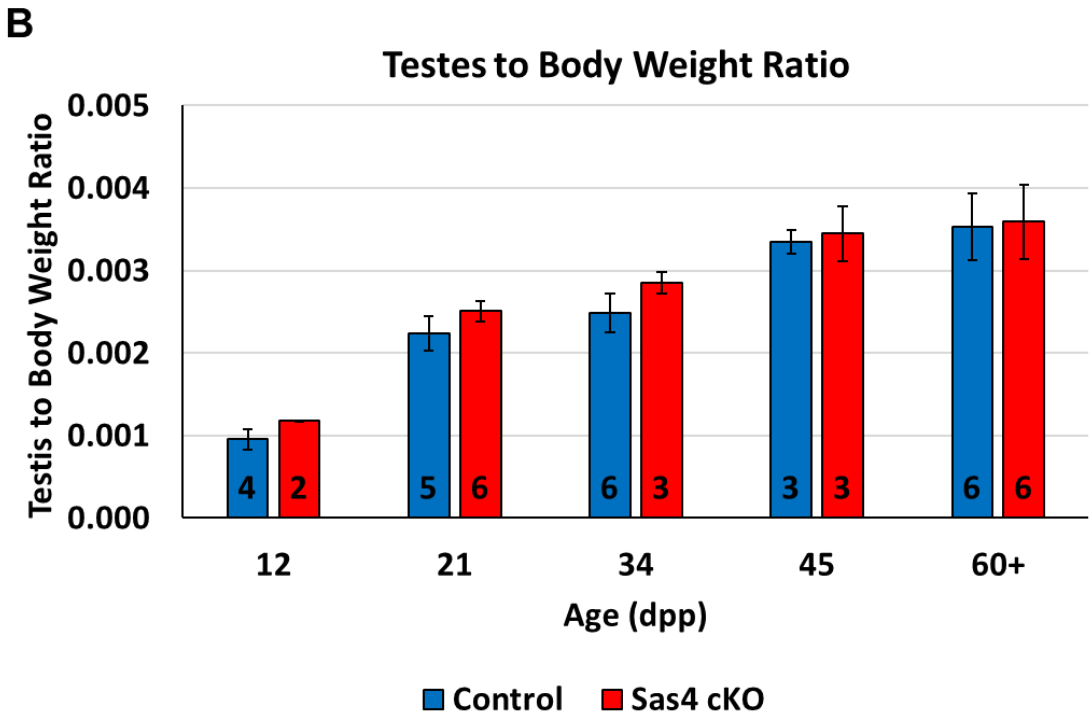
B
Testes to Body Weight Ratio
Testis to Body Weight Ratio
0.005
0.004
0.003
0.002
0.001
0.000
4
2
5
6
6
3
3
3
6
6
12
21
34
45
60+
Age (dpp)
Control
Sas4 cKO

Sas4 cKO; Stra8-Cre spermatocytes undergo apoptosis in prophase

While the *Sas4* cKO; *Spo11-Cre* phenotype confirms SAS4's critical roles in centriole duplication and flagella formation, it does not serve as a source of information on SAS4's role in the earlier stages of meiosis. To better assess this, we moved to using a *Stra8-Cre* transgene. Compared to *Spo11-Cre* expression in early meiosis, *Stra8-Cre* is expressed earlier, in the pre-meiotic stage (Hwang *et al.*, 2018a; Sadate-Ngatchou *et al.*, 2008). We hoped that an earlier depletion of SAS4 would result in an earlier, meiosis I phenotype.

Testes to body weight ratios of *Sas4* cKO; *Stra8-Cre* males were smaller than control littermates beginning at 16 dpp (Figure III.4A). At this age, the first wave of spermatogenesis should be in mid- to late-prophase I (Zindy *et al.*, 2001). Cross sections of *Sas4* cKO; *Stra8-Cre* tubules revealed an enrichment of primary spermatocytes with compact chromatin, indicative of an arrest in prophase (Figure III.4B). To investigate the exact timing of this arrest, we performed prophase-stage chromosome spreads to look at yH2AX localization (Supplemental Text III.1 and Supplemental Figure III.1). yH2AX is a marker for the DNA damage repair that occurs at the start of prophase during chromatin remodeling (Fernandez-Capetillo et al., 2003; Hamer et al., 2003; Hunter et al., 2001). yH2AX localization was resolved normally in *Sas4* cKO; *Stra8-Cre* spermatocytes, indicating that the observed arrest is due to a defect occurring in later prophase, after double-strand breaks are repaired.

Sas4 cKO females are fertile

We also wanted to evaluate the role of SAS4 in mammalian oogenesis. To accomplish this, we paired the *Sas4* cKO model with the female-specific *Zp3-Cre*

Figure III.2: *Sas4* cKO; *Spo11-Cre* spermatocytes do not duplicate their centrioles. (A) Examples of metaphase I control and *Sas4* cKO; *Spo11-Cre* spermatocytes stained for alpha-tubulin (α-TUB, red), centrin 3 (CETN3, green), CEP164 (purple) and DNA (DAPI, blue). Lower images are enlarged views of centrioles on either side of the spindle. (B) Example of a metaphase I *Sas4* cKO; *Spo11-Cre* spermatocyte stained for alpha-tubulin (α-TUB, red), centrin 3 (CETN3, green), pericentrin (PCM, purple), and (DNA (DAPI, blue). Lower image is an enlarged view of the single centriole.

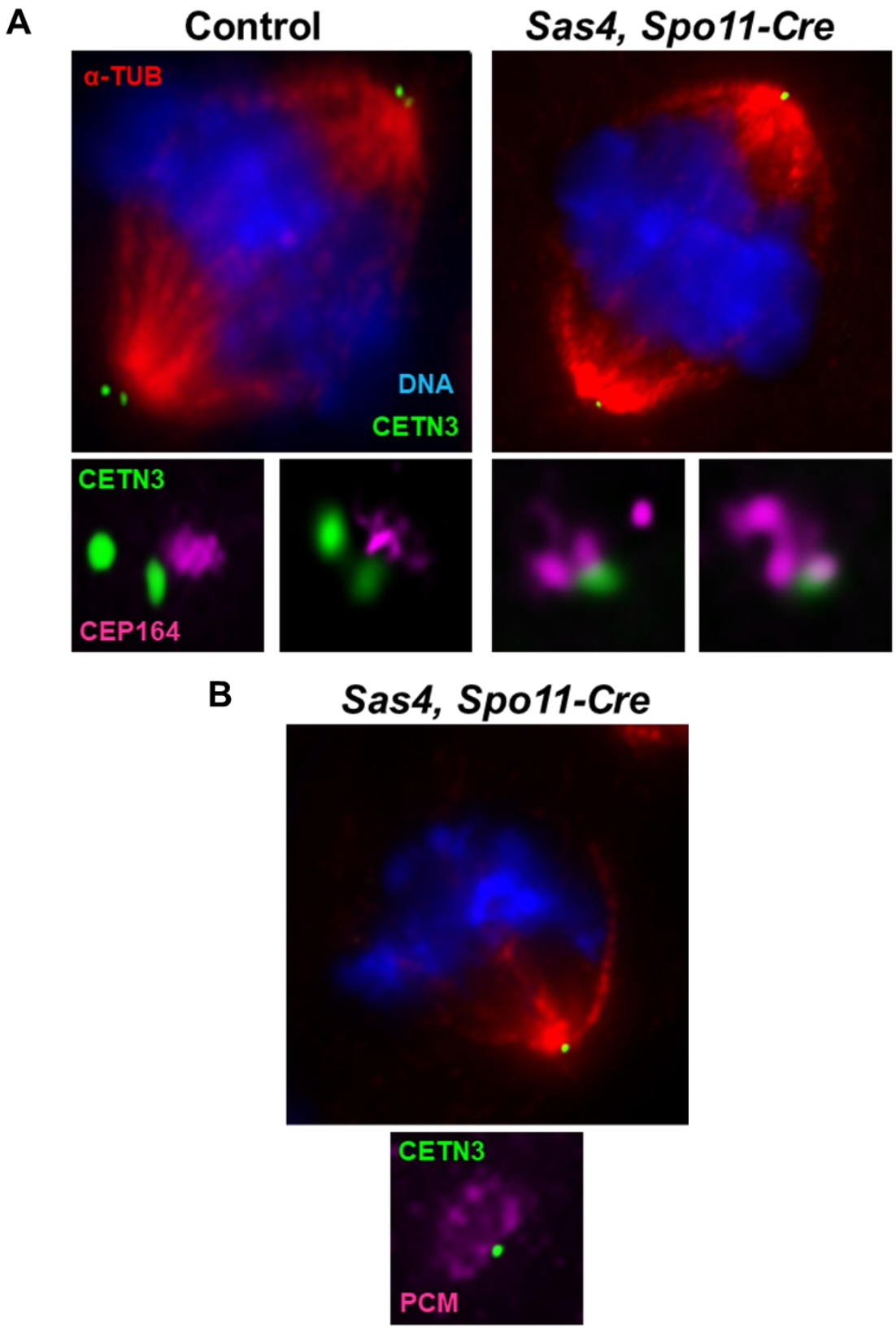
A
Control
Sas4, Spo11-Cre
α-TUB
DNA
CETN3
CETN3
CEP164
B
Sas4, Spo11-Cre
CETN3
PCM

Figure III.3: *Sas4* cKO; *Spo11-Cre* males do not produce mature spermatozoa. (A) Cross sections of H&E stained testes tubules from control and *Sas4* cKO; *Spo11-Cre* adult males. (B) Quantification of round spermatid diameter measured from adult control and *Sas4* cKO; *Spo11-Cre* males. (C) Quantification of sperm density counted from epididymis samples of adult control and *Sas4* cKO; *Spo11-Cre* males. Mean and SD of each column are represented by the black bars. Numbers at the base of each bar indicate the number of mice counted for each genotype. (D) Images of spermatozoa taken from adult control and *Sas4* cKO; *Spo11-Cre* males.

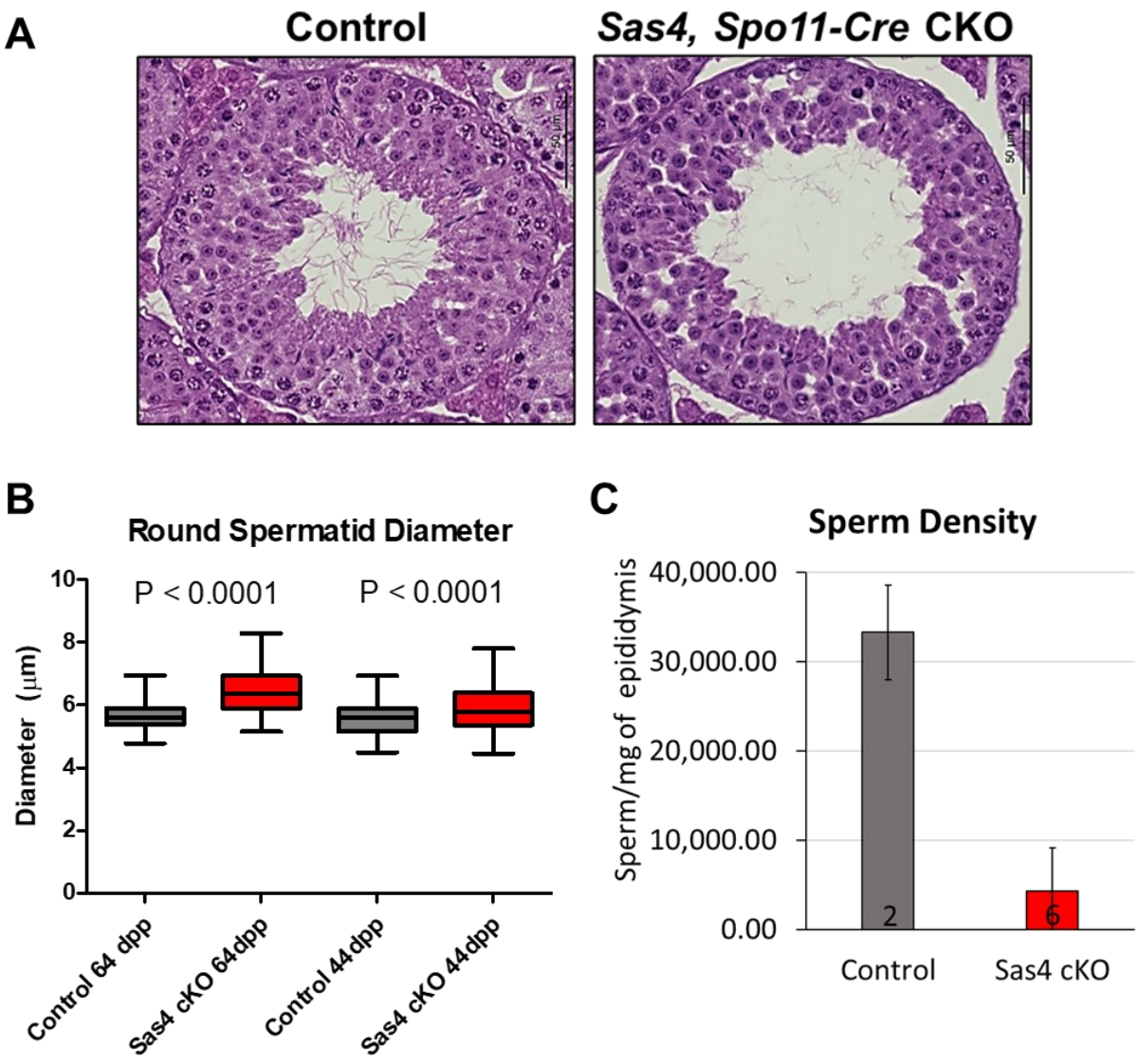
A
Control
Sas4, Spo11-Cre CKO
B
Round Spermatid Diameter
P < 0.0001
P < 0.0001
Diameter (μm)
10
8
6
4
2
0
Control 64 dpp
Sas4 cKO 64dpp
Control 44dpp
Sas4 cKO 44dpp
C
Sperm Density
Sperm/mg of epididymis
40,000.00
30,000.00
20,000.00
10,000.00
0.00
2
6
Control
Sas4 cKO
D
Control
Sas4 cKO

transgene, which results in SAS4 depletion at the primary follicle stage prior to meiotic resumption (Lan *et al.*, 2004).

Fertility tests have shown that *Sas4* cKO; *Zp3-Cre* females are fertile and deliver healthy litters (*N*=2). *Sas4* cKO; *Zp3-Cre* and control oocytes were collected and assessed via immunofluorescence microscopy. *Sas4* cKO; *Zp3-Cre* oocytes underwent NEBD and achieved a bipolar metaphase I spindle at the same rate as controls (Figure III.5 A and B). All of the observed *Sas4* cKO; *Zp3-Cre* oocytes had similar NEDD1 localization compared to controls, indicating normal MTOC organization. These results indicate that SAS4 is not essential for oogenesis.

Plk4 cKO males develop undersized testes

We developed a floxed *Plk4* allele (*Plk4 flox*) to evaluate the roles of PLK4 in mammalian meiosis (Figure III.6A; see *Materials and Methods*). By breeding homozygous *Plk4 flox/flox* mice to mice expressing a Cre recombinase transgene, we were able to obtain *Plk4 +/flox; Cre* offspring. These mice were bred to *Plk4 flox/flox* mice to produce *Plk4* cKO (*Plk4 flox/del; Cre*) mice. (Figure III.6A). We utilized *Spo11-Cre*, which is specifically expressed in early meiotic prophase (Hwang *et al.*, 2018a; Lyndaker *et al.*, 2013).

We first assessed the effect of conditional PLK4 depletion in adult (65 dpp) males by quantifying testes to body weight ratios (Figure III.6B). At 65 dpp, the first wave of spermatogenesis should have reached its completion. *Plk4 Spo11-Cre* cKO males had a significantly smaller testes to body weight ratio compared to control littermates. This defect was confirmed using a *Stra8-Cre* transgene (Figure

Figure III.4: *Sas4* cKO; *Stra8-Cre* spermatocytes arrest in prophase I. (A) Quantification of testes to body weight ratio of 16 dpp control and *Sas4* cKO; *Stra8-Cre* males. Mean and SD of each column are represented by the black bars. Numbers at the base of each bar indicate the number of mice counted for each genotype. (B) Cross sections of an H&E stained testes from a 16 dpp *Sas4* cKO; *Stra8-Cre* adult male. Zoomed images on the right include a cross section of a control 16 dpp littermate.

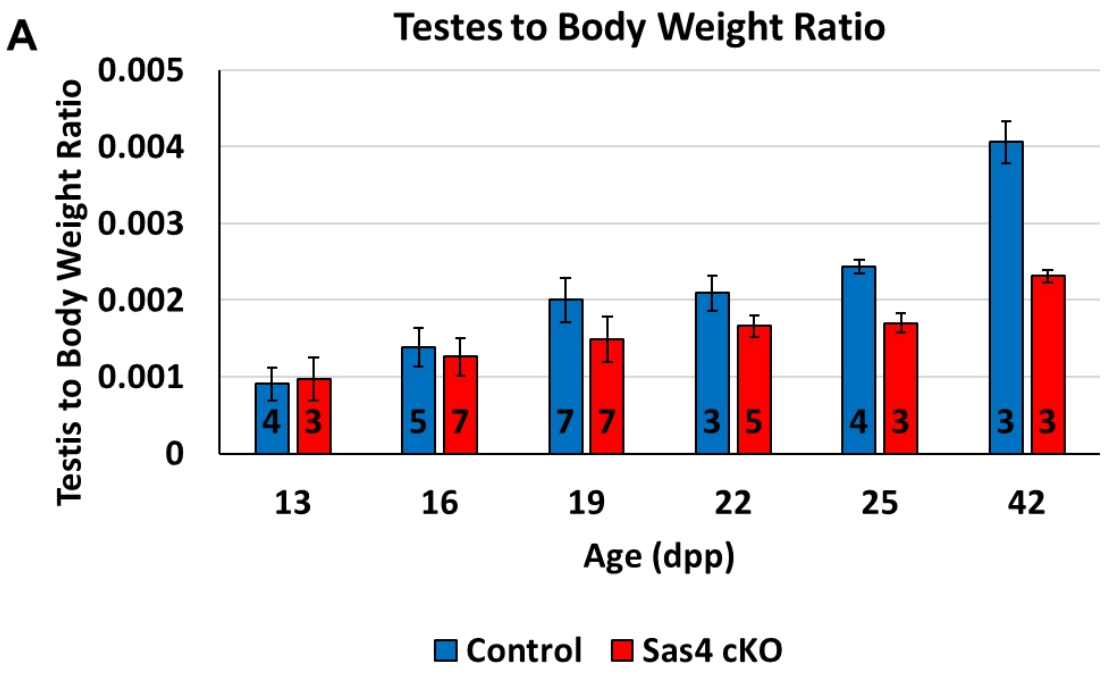
A
Testes to Body Weight Ratio
Testis to Body Weight Ratio
0.005
0.004
0.003
0.002
0.001
0
4 3
5 7
7 7
3 5
4 3
3 3
13
16
19
22
25
42
Age (dpp)
Control
Sas4 cKO

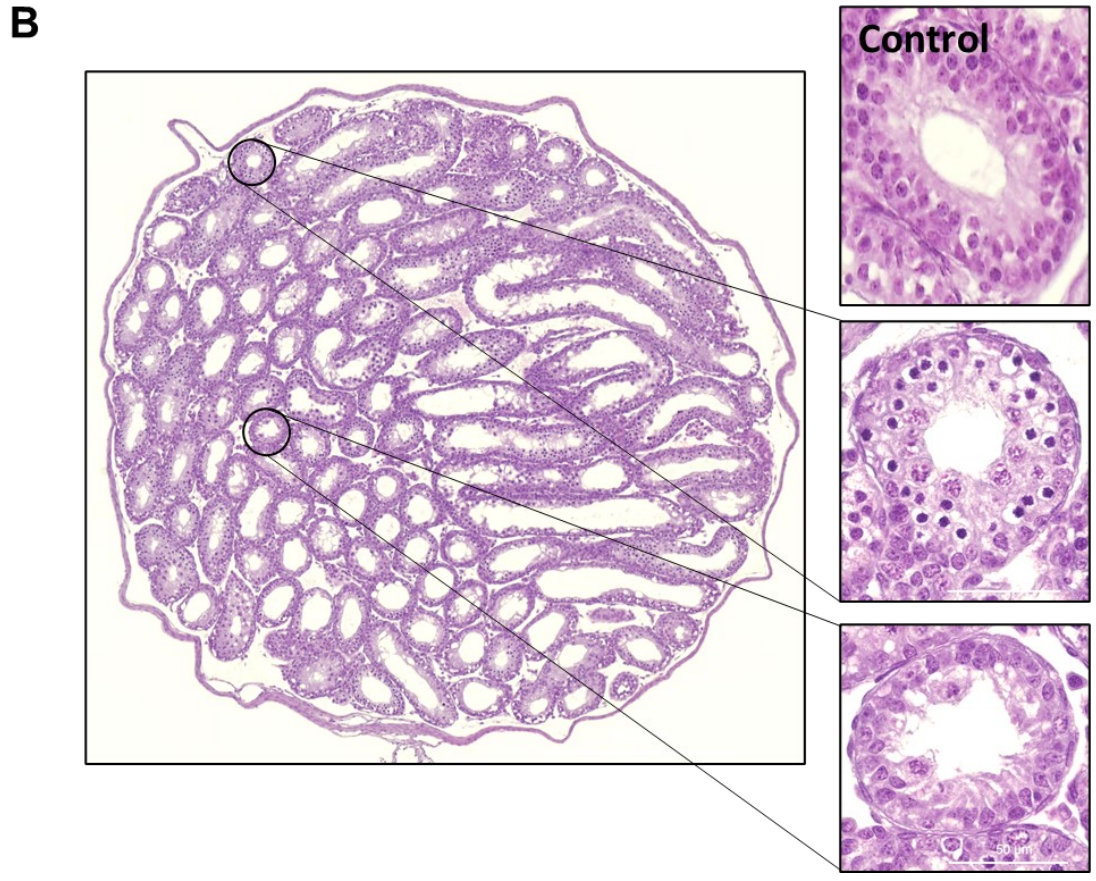
B
Control

III.6C). This size difference is indicative of germ cell arrest and apoptosis, although further experiments are needed to determine the exact timing.

Plk4 cKO oocytes successfully form a bipolar metaphase I spindle

To assess the role of PLK4 in oogenesis, we collected and assessed oocytes from control and *Plk4* cKO females. We utilized *Zp3-Cre* and *Spo11-Cre* transgenes, which will deplete PLK4 in the primary follicle stage and in early prophase, respectively. Both *Plk4* cKO; *Zp3-Cre* and *Plk4* cKO; *Spo11-Cre* oocytes underwent NEBD at a similar rate as controls (Figure III.7A and B). Preliminary analysis of these oocytes indicated that they successfully organize their MTOCs in prometaphase (Figure III.7C). Additionally, *Plk4* cKO oocytes underwent normal chromosome condensation processes to form bivalents by prometaphase.

Discussion

Both PLK4 and SAS4 play critical roles in mammalian mitosis. PLK4 has been shown to recruit downstream regulators and structural components to the base of the mother centriole at the start of centriole biogenesis (Arquint and Nigg, 2016; Bettencourt-Dias et al., 2005; Habedanck et al., 2005; Kuriyama, 2009; Moyer and Holland, 2019). Prior research has shown that PLK4 phosphorylates STIL at two separate sites, which allows STIL to form a bridge between the mother centriole and the newly-formed cartwheel (Moyer and Holland, 2019).

The roles of PLK4 in mammalian meiosis are not fully understood. PLK4 has been shown to localize to centrioles in spermatocytes and to MTOCs in oocytes (Bury et al., 2017; Coelho et al., 2013; Gopalakrishnan et al., 2011; Jordan

et al., 2012). Since PLK4 depletion is embryonically lethal due to its mitotic roles, functional studies in meiosis have been limited to heterozygous point mutations, RNA inhibition and overexpression studies. Mutations in the kinase domain of PLK4 has been shown to cause partial germ cell loss during the first wave of spermatogenesis (Harris et al., 2011). In oocytes, PLK4 has previously been shown to regulate the assembly of MTOCs (Bury et al., 2017; Luo and Kim, 2015; Severance and Latham, 2018).

SAS4 is also known to be essential for centriole biogenesis. SAS4 serves as a scaffold for the initial centriolar cartwheel, and therefore must be recruited to the base of the mother centriole for nucleation to occur (Kuriyama, 2009; McLamarrah et al., 2018). Complete knockouts of SAS4 are embryonically lethal due to a failure to organize tubulin (Bazzi and Anderson, 2014; Leidel and Gönczy, 2003).

Meiotic studies of SAS4 have been limited to non-mammalian models. In *Drosophila melanogaster,* SAS4 depletion results in the acentriolar mitosis of germline stem cells (Riparbelli et al., 2020). The meiotically-dividing spermatocytes downstream of these stem cells undergo apoptosis due to a lack of spindle organization. This contrast between mitosis and meiosis implies a divergence of roles for SAS4.

The embryonic lethality of PLK4 and SAS4 depletion have limited our current understanding of their roles in mammalian meiosis. To better address these needs, we utilized meiosis-specific conditional knockouts of both PLK4 and

SAS4. The results presented here are the first to examine the effects of PLK4 and SAS4 depletion using a meiosis specific knockout model.

Our preliminary results indicate that SAS4 is essential for spermatogenesis, but not oogenesis. The ability of *Sas4* cKO oocytes to undergo successful meiosis I is unsurprising, given that oocytes do not rely on a canonical centriole structure. Prior research has shown that SAS4 localizes to oocyte MTOCs prior to NEBD, but not after (So et al., 2019). Interestingly, we observed that *Sas4* cKO spermatocytes arrest in prophase I or metaphase II, depending on the timing of SAS4 depletion. This indicates a dual role for SAS4 in spermatogenesis. Our data confirms that SAS4 is required for centriole duplication in meiosis, similarly to its known mitotic roles. However, the early prophase I arrest of *Sas4* cKO; *Stra8-Cre* spermatocytes indicate that SAS4 has a previously unreported role in the initial stages of meiosis.

Plk4 Stra8-Cre cKO males develop undersized testes by 24 dpp. This indicates an arrest in the first wave of spermatogenesis. This finding aligns with previous reports of early spermatocyte arrest in mice harboring PLK4 mutations (Harris et al., 2011). Surprisingly, we did not observe a notable difference between control and *Plk4* cKO oocytes at prometaphase. This contrasts previous reports of a role for PLK4 in MTOC assembly (Bury et al., 2017; Luo and Kim, 2015). Further analysis is needed to confirm that the targeted proteins are being depleted as expected, and to determine whether these oocytes develop defects at later stages.

Figure III.5: (A) Timing of NEBD in oocytes from control and *Sas4* cKO mice. 52 oocytes from 1 control mouse and 43 oocytes from 1 *Sas4* cKO mouse were assessed. (B) Examples of metaphase I control and *Sas4* cKO oocytes stained for alpha-tubulin (α-TUB, red), NEDD1 (green) and DNA (DAPI, blue). Scale bar: 10 μm.

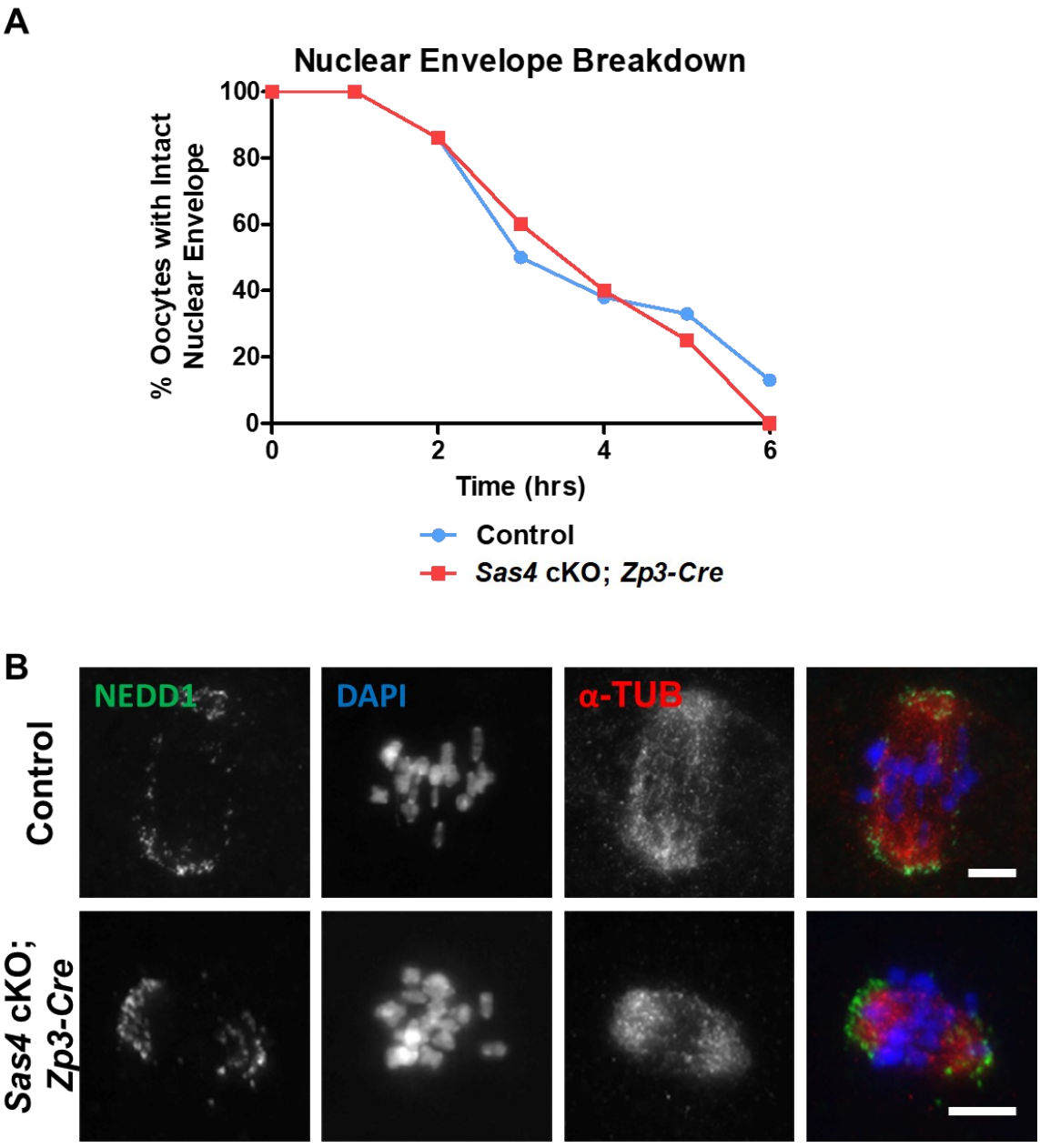
A
Nuclear Envelope Breakdown
% Oocytes with Intact Nuclear Envelope
100
80
60
40
20
0
0
2
4
6
Time (hrs)
Control
Sas4 cKO; Zp3-Cre
B
Control
Sas4 cKO; Zp3-Cre
NEDD1
DAPI
α-TUB

Figure III.6: PLK4 depletion results in decreased testes size. (A) Schematic of mouse *Plk4* floxed allele containing loxP sites (orange triangle), flanking exon 5 (gray box), and the resulting *Plk4* deletion allele after excision of exon 5 by Cre recombinase in early prophase. (B) Quantification of testes to body weight ratio of control and *Plk4* cKO; *Spo11-Cre* males. Mean and SD of each column are represented by the black bars. Numbers at the base of each bar indicate the number of mice counted for each genotype. The *P* value (Mann-Whitney, two-tailed) for the indicated comparison is significant (*P*=0.005). (C) Quantification of testes to body weight ratio of control and *Plk4* cKO; *Stra8-Cre* males. Mean and SD of each column are represented by the black bars. Numbers at the base of each bar indicate the number of mice counted for each genotype.

A

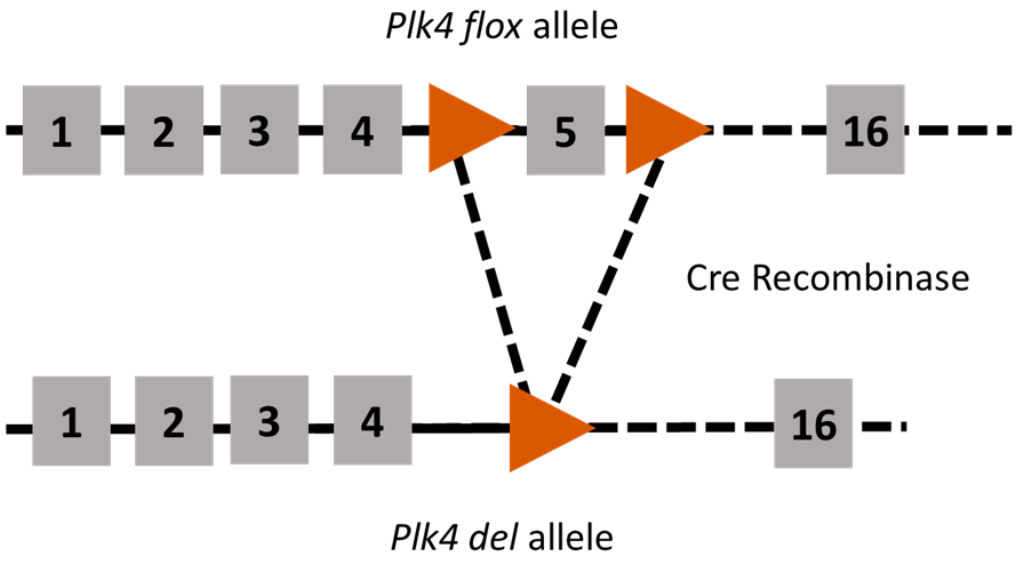
Plk4 flox allele
1
2
3
4
5
16
Cre Recombinase
1
2
3
4
16
Plk4 del allele

B

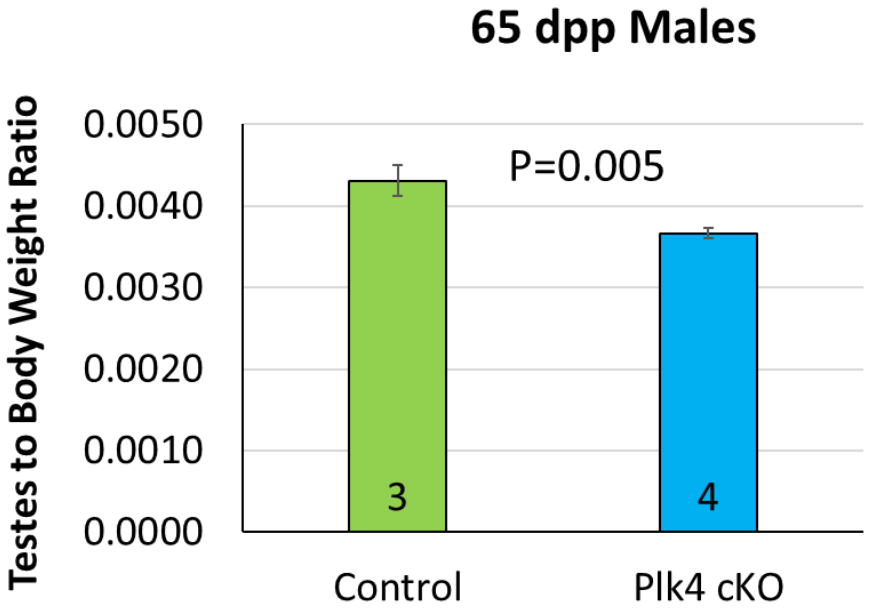
65 dpp Males
Testes to Body Weight Ratio
0.0050
0.0040
0.0030
0.0020
0.0010
0.0000
P=0.005
3
4
Control
Plk4 cKO

C

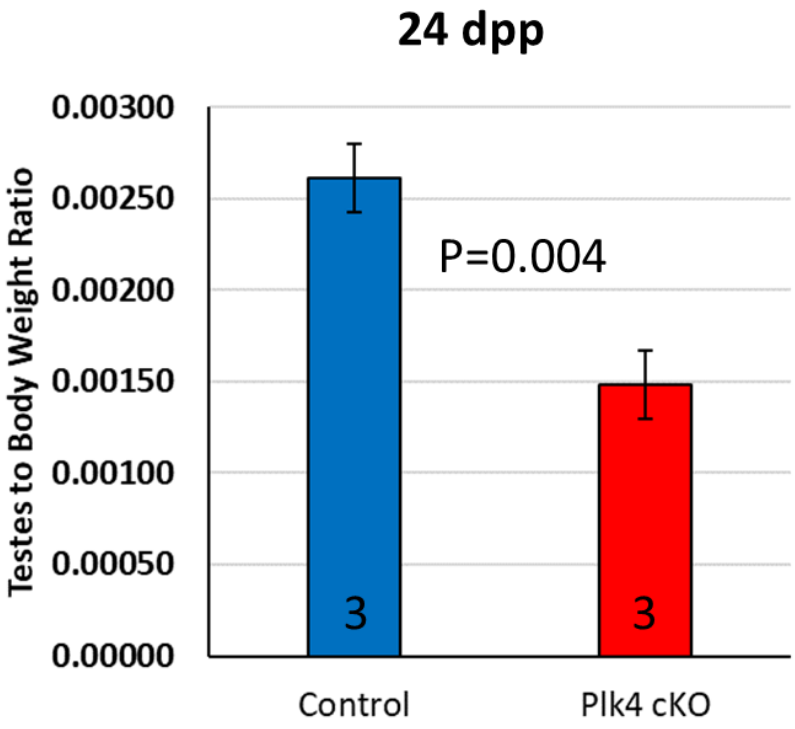
24 dpp
Testes to Body Weight Ratio
0.00300
0.00250
0.00200
0.00150
0.00100
0.00050
0.00000
P=0.004
3
3
Control
Plk4 cKO

Figure III.7: (A) Timing of NEBD in oocytes from control and *Plk4* cKO; *Zp3-Cre* mice. 152 oocytes from 5 control mice and 103 oocytes from 4 *Plk4* cKO: *Zp3-Cre* mice were assessed. Mean and SD of the columns of each graph are represented by the blue circles (control), pink squares (*Plk4* cKO), and corresponding bars. (B) Timing of NEBD in oocytes from control and *Plk4* cKO; *Spo11-Cre* mice. 86 oocytes from 3 control mice and 79 oocytes from 3 *Plk4* cKO: *Spo11-Cre* mice were assessed. Mean and SD of the columns of each graph are represented by the blue circles (control), pink squares (*Plk4* cKO), and corresponding bars. (C) Examples of prometaphase I control and *Plk4* cKO oocytes stained for NEDD1 (green) and DNA (DAPI, blue). Scale bar: 10 μm.

A

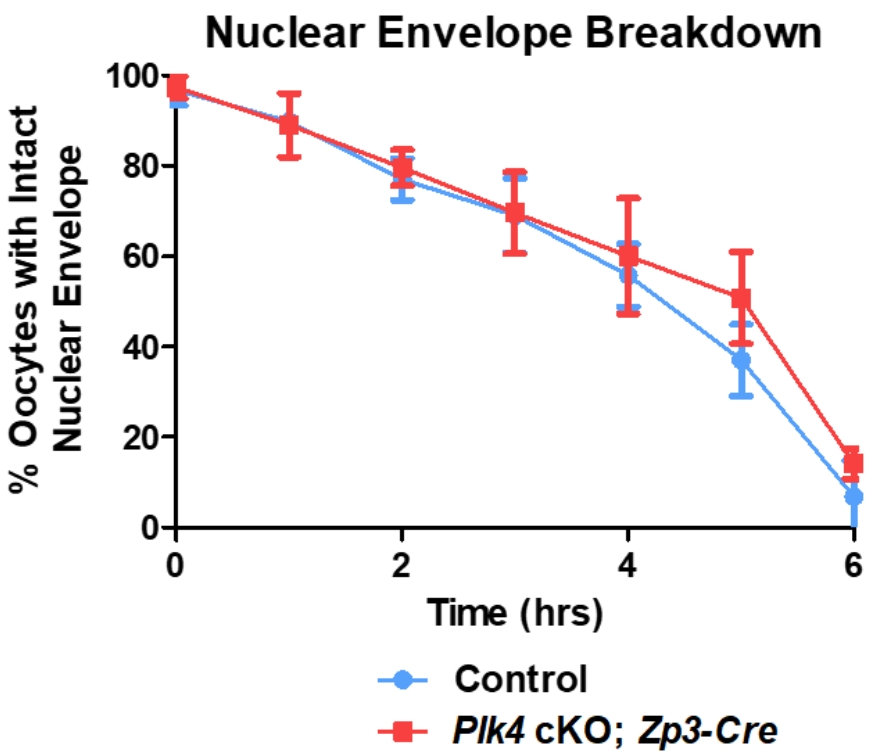
Nuclear Envelope Breakdown
% Oocytes with Intact Nuclear Envelope
100
80
60
40
20
0
0
2
4
6
Time (hrs)
Control
Plk4 cKO; Zp3-Cre

B

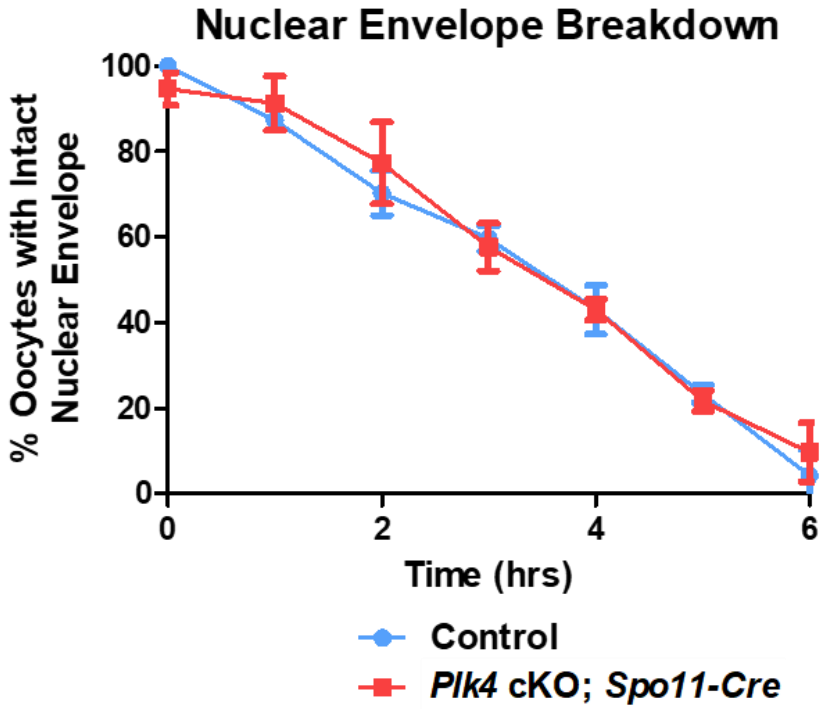
Nuclear Envelope Breakdown
% Oocytes with Intact Nuclear Envelope
100
80
60
40
20
0
0
2
4
6
Time (hrs)
Control
Plk4 cKO; Spo11-Cre

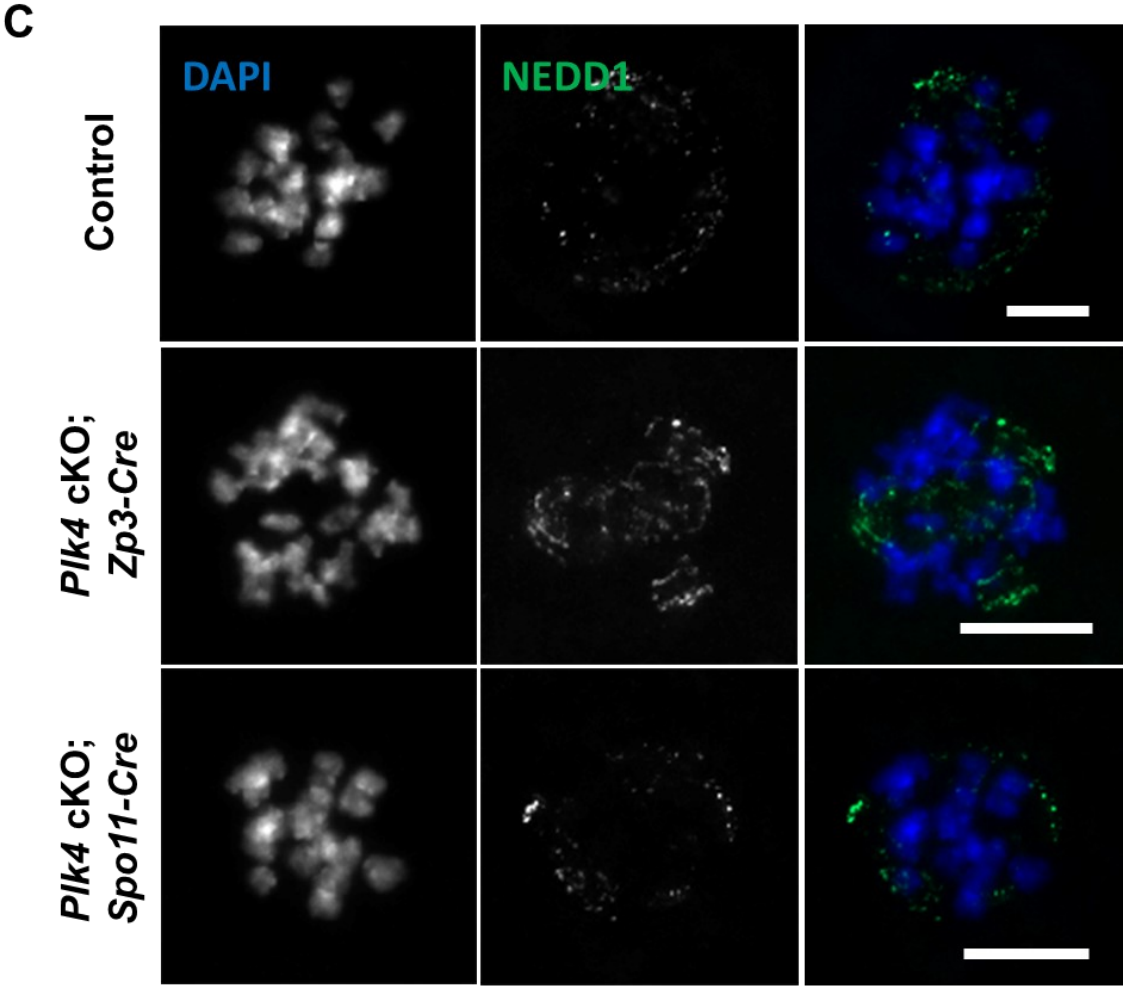
C
DAPI
NEDD1
Control
Plk4 cKO; Zp3-Cre
Plk4 cKO; Spo11-Cre

Future Directions and Concluding Remarks

Further experiments are needed to elucidate the specific roles of PLK4 and SAS4 in mammalian meiosis. First, we plan to confirm the depletion of these proteins by Western blot analysis of both oocytes and spermatocytes. This will inform us whether the Cre transgenes are depleting the target proteins as expected. Based on our preliminary results, we expect to see significant levels of PLK4 and SAS4 depletion in the cKO spermatocytes. In contrast, both *Sas4* and *Plk4* cKO oocytes appear to successfully reach metaphase I. This may be due to these proteins being unnecessary for oogenesis, or it may be a result of the conditional depletion being inefficient.

Our results indicate that *Plk4* cKO oocytes reach prometaphase I successfully. It is possible that defects occur in the later stages of meiosis. To determine this, we will be performing fertility tests where *Plk4* cKO females are mated with wildtype males. If the *Plk4* cKO females are infertile, this will indicate that there is are defects occurring in later stages of meiosis. Depending on the results of the fertility tests, we can perform immunofluorescence staining to observe MTOC organization at metaphase I and metaphase II. Certain genes, referred to as maternal effect genes, must be expressed by the oocyte for early stages of embryogenesis to occur (Li et al., 2010; Zhang and Smith, 2015). IVF studies with *Plk4* cKO oocytes and control spermatocytes can be used to determine if *Plk4* is a maternal effect gene.

Additional experiments are also needed to better understand the observed phenotypes of *Plk4* and *Sas4* cKO males. In the case of *Plk4 Stra8-Cre* cKO

males, spermatocytes appear to be arresting during the first wave of spermatogenesis. We plan to prepare tubule squashes and chromosome spreads throughout the first wave of spermatogenesis to track centriole duplication and migration and pinpoint the onset of this arrest. Additionally, we plan to assess both lines for defects in chromosome synapsis and chromosome segregation.

Based on our current data, we believe that both the *Plk4* and *Sas4* cKO mouse lines will provide insight into currently unknown roles of PLK4 and SAS4. While much work remains, we have demonstrated that these proteins may have differing roles in the sexually dimorphic processes of spermatogenesis and oogenesis.

Supplementary Text III.1: yH2AX localization in *Sas4* cKO males

At the start of meiotic prophase, I, double strand breaks are created and repaired to induce the interaction of homologous chromosomes. Spermatocytes, which have the unique challenge of an XY chromosome pairing, must also compartmentalize the sex body separately from the autosomal chromatin. yH2AX has been shown to be critical for both of these processes (Fernandez-Capetillo *et al.*, 2003; Hamer *et al.*, 2003; Hunter *et al.*, 2001).

Preliminary chromosome spreads of *Sas4* cKO spermatocytes show normal yH2AX localization (Supplemental Figure III.1). In early prophase I-stage spermatocytes, yH2AX localizes to double-strand breaks throughout the chromatin. By late prophase, these breaks have been resolved, leaving yH2AX only at the sex body. Based on the observed yH2AX localization, *Sas4* cKO spermatocytes successfully resolve DNA breaks by late prophase. Based on these observations, we concluded that the defects resulting in a prophase arrest must be occurring in later prophase, after DNA damage has been repaired.

Supplemental Figure III.1: yH2AX localization in *Sas4* cKO males. Examples of chromosome spreads prepared from control and *Sas4* cKO; *Stra8-Cre* spermatocytes stained for SYCP3 (red) and yH2AX (green). Scale bar: 10 μm.

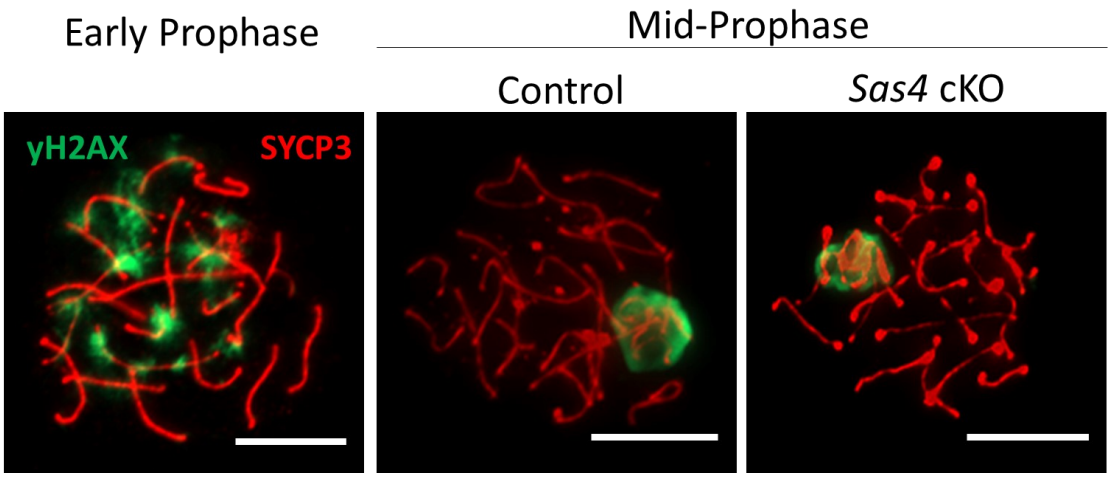
Early Prophase
Mid-Prophase
Control
Sas4 cKO
γH2AX
SYCP3

Gene	Forward Primer (5'-…..-3')	Reverse Primer (5'-…..-3')	Product Size (bp)
Plk4^{del}	TCTTGAGGGGAATTAGATAGCA	CTCACTCAGCCCCAGATAAC	618
Plk4^{flox} and *Plk4*^{Wt}	TCTTGAGGGGAATTAGATAGCA	TGCAATATGCCATGAGAATGA	*Flox*: 1800 *WT*: 1700
Sas4^{flox} and *Sas4*^{Wt}	TGCTTGCTTGTCTCTCCTGA	TGCTTGCTTGTCTCTCCTGA	*Flox*: 286 *WT*: 316
Cre Transgene	CCATCTGCCACCAGCCAG	TCGCCATCTTCCAGCAGG	420
Cre Internal Control	ACTGGGATCTTCGAACTCTTTGGAC	GATGTTGGGGCACTGCTCATTCACC	281

Supplemental Table III.1: Primers used in this study.

Primary Antibodies				
Antibody	**Host**	**Source**	**Cat. Number**	**IF Dilution**
alpha-tubulin	Goat	LS Bio	LS-C24216	1:500
alpha-tubulin	Mouse	Sigma-Aldrich	T9025	1:1000
alpha-tubulin	Rabbit	Thermo Scientific	PA5-29444	1:500
CEP164	Rabbit	Millipore Sigma	ABE2621	1:1000
CETN3	Mouse	Abnova	H00001070-M01	1:200
NEDD1	Mouse	Abcam	ab57336	1:750
Pericentrin	Mouse	Abcam	ab4448	1:200
Secondary Antibodies				
Antibody	**Host**	**Source**	**Cat. Number**	**IF Dilution**
Mouse IgG (H+L), Alexa Fluor 488	Goat	Invitrogen	A-11001	1:500
Mouse IgG (H+L), Alexa Fluor 568	Goat	Invitrogen	A-11031	1:500
Rabbit IgG (H+L), Alexa Fluor 488	Goat	Invitrogen	A-11008	1:500
Rabbit IgG (H+L), Alexa Fluor 568	Goat	Invitrogen	A-11011	1:500
Human IgG (H+L), Alexa Fluor 633	Goat	Invitrogen	A-21091	1:500
Goat IgG (H+L) Alexa Fluor 488	Donkey	Invitrogen	A-11055	1:500
Goat IgG (H+L) Alexa Fluor 568	Donkey	Invitrogen	A-11057	1:500
Goat IgG (H+L) Alexa Fluor 633	Donkey	Invitrogen	A-21082	1:500
Mouse IgG (H+L), HRP	Rabbit	Invitrogen	31450	
Rabbit IgG (H+L), HRP	Goat	Invitrogen	31466	

Supplemental Table III.2: Antibodies used in this study.

References

Arquint, C., and Nigg, E.A. (2016). The PLK4-STIL-SAS-6 module at the core of centriole duplication. Biochem. Soc. Trans. *44*, 1253–1263.

Arquint, C., Sonnen, K.F., Stierhof, Y.-D., and Nigg, E.A. (2012). Cell-cycle-regulated expression of STIL controls centriole number in human cells. J. Cell Sci. *125*, 1342–1352.

Baumann, C., Wang, X., Yang, L., and Viveiros, M.M. (2017). Error-prone meiotic division and subfertility in mice with oocyte-conditional knockdown of pericentrin. J. Cell Sci. *130*, 1251–1262.

Bazzi, H., and Anderson, K.V. (2014). Acentriolar mitosis activates a p53-dependent apoptosis pathway in the mouse embryo. Proc. Natl. Acad. Sci. USA *111*, E1491–500.

Bettencourt-Dias, M., Rodrigues-Martins, A., Carpenter, L., Riparbelli, M., Lehmann, L., Gatt, M.K., Carmo, N., Balloux, F., Callaini, G., and Glover, D.M. (2005). SAK/PLK4 is required for centriole duplication and flagella development. Curr. Biol. *15*, 2199–2207.

Bury, L., Coelho, P.A., Simeone, A., Ferries, S., Eyers, C.E., Eyers, P.A., Zernicka-Goetz, M., and Glover, D.M. (2017). Plk4 and Aurora A cooperate in the initiation of acentriolar spindle assembly in mammalian oocytes. J. Cell Biol. *216*, 3571–3590.

Clift, D., and Schuh, M. (2015). A three-step MTOC fragmentation mechanism facilitates bipolar spindle assembly in mouse oocytes. Nat. Commun. *6*, 7217.

Coelho, P.A., Bury, L., Sharif, B., Riparbelli, M.G., Fu, J., Callaini, G., Glover, D.M., and Zernicka-Goetz, M. (2013). Spindle formation in the mouse embryo requires Plk4 in the absence of centrioles. Dev. Cell *27*, 586–597.

Fernandez-Capetillo, O., Mahadevaiah, S.K., Celeste, A., Romanienko, P.J., Camerini-Otero, R.D., Bonner, W.M., Manova, K., Burgoyne, P., and Nussenzweig, A. (2003). H2AX is required for chromatin remodeling and inactivation of sex chromosomes in male mouse meiosis. Dev. Cell *4*, 497–508.

Gopalakrishnan, J., Mennella, V., Blachon, S., Zhai, B., Smith, A.H., Megraw, T.L., Nicastro, D., Gygi, S.P., Agard, D.A., and Avidor-Reiss, T. (2011). Sas-4 provides a scaffold for cytoplasmic complexes and tethers them in a centrosome. Nat. Commun. *2*, 359.

Graser, S., Stierhof, Y.-D., Lavoie, S.B., Gassner, O.S., Lamla, S., Le Clech, M., and Nigg, E.A. (2007). Cep164, a novel centriole appendage protein required for primary cilium formation. J. Cell Biol. *179*, 321–330.

Habedanck, R., Stierhof, Y.-D., Wilkinson, C.J., and Nigg, E.A. (2005). The Polo kinase Plk4 functions in centriole duplication. Nat. Cell Biol. *7*, 1140–1146.

Hamer, G., Roepers-Gajadien, H.L., van Duyn-Goedhart, A., Gademan, I.S., Kal, H.B., van Buul, P.P.W., and de Rooij, D.G. (2003). DNA Double-Strand Breaks and γ-H2AX Signaling in the Testis1. Biol. Reprod. *68*, 628–634.

Harris, R.M., Weiss, J., and Jameson, J.L. (2011). Male hypogonadism and germ cell loss caused by a mutation in Polo-like kinase 4. Endocrinology *152*, 3975–3985.

Hirono, M. (2014). Cartwheel assembly. Philos. Trans. R. Soc. Lond. B, Biol. Sci. *369*.

Hunter, N., Börner, G.V., Lichten, M., and Kleckner, N. (2001). Gamma-H2AX illuminates meiosis. Nat. Genet. *27*, 236–238.

Hwang, G., Verver, D.E., Handel, M.A., Hamer, G., and Jordan, P.W. (2018a). Depletion of SMC5/6 sensitizes male germ cells to DNA damage. Mol. Biol. Cell *29*, 3003–3016.

Hwang, G.H., Hopkins, J.L., and Jordan, P.W. (2018b). Chromatin Spread Preparations for the Analysis of Mouse Oocyte Progression from Prophase to Metaphase II. J. Vis. Exp. *132*, e56736.

Jordan, P.W., Karppinen, J., and Handel, M.A. (2012). Polo-like kinase is required for synaptonemal complex disassembly and phosphorylation in mouse spermatocytes. J. Cell Sci. *125*, 5061–5072.

Kirkham, M., Müller-Reichert, T., Oegema, K., Grill, S., and Hyman, A.A. (2003). SAS-4 is a C. elegans centriolar protein that controls centrosome size. Cell *112*, 575–587.

Kuriyama, R. (2009). Centriole assembly in CHO cells expressing Plk4/SAS6/SAS4 is similar to centriogenesis in ciliated epithelial cells. Cell Motil. Cytoskeleton *66*, 588–596.

Lan, Z.-J., Xu, X., and Cooney, A.J. (2004). Differential oocyte-specific expression of Cre recombinase activity in GDF-9-iCre, Zp3cre, and Msx2Cre transgenic mice. Biol. Reprod. *71*, 1469–1474.

Lee, I.-W., Jo, Y.-J., Jung, S.-M., Wang, H.-Y., Kim, N.-H., and Namgoong, S. (2017). Distinct roles of Cep192 and Cep152 in acentriolar MTOCs and spindle formation during mouse oocyte maturation. FASEB J.

Leidel, S., and Gönczy, P. (2003). SAS-4 is essential for centrosome duplication in C elegans and is recruited to daughter centrioles once per cell cycle. Dev. Cell *4*, 431–439.

Li, L., Zheng, P., and Dean, J. (2010). Maternal control of early mouse development. Development *137*, 859–870.

Luo, Y.-B., and Kim, N.-H. (2015). PLK4 is essential for meiotic resumption in mouse oocytes. Biol. Reprod. *92*, 101.

Lyndaker, A.M., Lim, P.X., Mleczko, J.M., Diggins, C.E., Holloway, J.K., Holmes, R.J., Kan, R., Schlafer, D.H., Freire, R., Cohen, P.E., et al. (2013). Conditional inactivation of the DNA damage response gene Hus1 in mouse testis reveals separable roles for components of the RAD9-RAD1-HUS1 complex in meiotic chromosome maintenance. PLoS Genet. *9*, e1003320.

Ma, H., Marti-Gutierrez, N., Park, S.-W., Wu, J., Lee, Y., Suzuki, K., Koski, A., Ji, D., Hayama, T., Ahmed, R., et al. (2017). Correction of a pathogenic gene mutation in human embryos. Nature *548*, 413–419.

Marjanović, M., Sánchez-Huertas, C., Terré, B., Gómez, R., Scheel, J.F., Pacheco, S., Knobel, P.A., Martínez-Marchal, A., Aivio, S., Palenzuela, L., et al. (2015). CEP63 deficiency promotes p53-dependent microcephaly and reveals a role for the centrosome in meiotic recombination. Nat. Commun. *6*, 7676.

Marthiens, V., Rujano, M.A., Pennetier, C., Tessier, S., Paul-Gilloteaux, P., and Basto, R. (2013). Centrosome amplification causes microcephaly. Nat. Cell Biol. *15*, 731–740.

McLamarrah, T.A., Buster, D.W., Galletta, B.J., Boese, C.J., Ryniawec, J.M., Hollingsworth, N.A., Byrnes, A.E., Brownlee, C.W., Slep, K.C., Rusan, N.M., et al. (2018). An ordered pattern of Ana2 phosphorylation by Plk4 is required for centriole assembly. J. Cell Biol. *217*, 1217–1231.

Moyer, T.C., and Holland, A.J. (2019). PLK4 promotes centriole duplication by phosphorylating STIL to link the procentriole cartwheel to the microtubule wall. Elife *8*.

Nigg, E.A. (2007). Centrosome duplication: of rules and licenses. Trends Cell Biol. *17*, 215–221.

Oakberg, E.F. (1956). Duration of spermatogenesis in the mouse and timing of stages of the cycle of the seminiferous epithelium. Am J. Anat. *99*, 507–516.

Pihan, G.A. (2013). Centrosome dysfunction contributes to chromosome instability, chromoanagenesis, and genome reprograming in cancer. Front. Oncol. *3*, 277.

Riparbelli, M.G., and Callaini, G. (2011). Male gametogenesis without centrioles. Dev. Biol. *349*, 427–439.

Riparbelli, M.G., Persico, V., Dallai, R., and Callaini, G. (2020). Centrioles and Ciliary Structures during Male Gametogenesis in Hexapoda: Discovery of New Models. Cells *9*.

Rodrigues-Martins, A., Riparbelli, M., Callaini, G., Glover, D.M., and Bettencourt-Dias, M. (2008). From centriole biogenesis to cellular function: centrioles are essential for cell division at critical developmental stages. Cell Cycle *7*, 11–16.

Sadate-Ngatchou, P.I., Payne, C.J., Dearth, A.T., and Braun, R.E. (2008). Cre recombinase activity specific to postnatal, premeiotic male germ cells in transgenic mice. Genesis *46*, 738–742.

Severance, A.L., and Latham, K.E. (2018). Meeting the meiotic challenge: Specializations in mammalian oocyte spindle formation. Mol. Reprod. Dev. *85*, 178–187.

Simerly, C., Manil-Ségalen, M., Castro, C., Hartnett, C., Kong, D., Verlhac, M.-H., Loncarek, J., and Schatten, G. (2018). Separation and loss of centrioles from primordidal germ cells to mature oocytes in the mouse. Sci. Rep. *8*, 12791.

So, C., Seres, K.B., Steyer, A.M., Mönnich, E., Clift, D., Pejkovska, A., Möbius, W., and Schuh, M. (2019). A liquid-like spindle domain promotes acentrosomal spindle assembly in mammalian oocytes. Science *364*.

Sumiyoshi, E., Sugimoto, A., and Yamamoto, M. (2002). Protein phosphatase 4 is required for centrosome maturation in mitosis and sperm meiosis in C. elegans. J. Cell Sci. *115*, 1403–1410.

Verloes, A., Drunat, S., Gressens, P., and Passemard, S. (1993). Primary Autosomal Recessive Microcephalies and Seckel Syndrome Spectrum Disorders. In GeneReviews, R.A. Pagon, M.P. Adam, H.H. Ardinger, S.E. Wallace, A. Amemiya, L.J. Bean, T.D. Bird, C.-T. Fong, H.C. Mefford, R.J. Smith, et al., eds. (Seattle (WA): University of Washington, Seattle),.

Wellard, S.R., Hopkins, J., and Jordan, P.W. (2018). A seminiferous tubule squash technique for the cytological analysis of spermatogenesis using the mouse model. J. Vis. Exp. *132*, e56453.

Xu, E.Y., Kim, S., Replogle, K., Rine, J., and Rivier, D.H. (1999). Identification of SAS4 and SAS5, two genes that regulate silencing in Saccharomyces cerevisiae. Genetics *153*, 13–23.

Yoshiba, S., Tsuchiya, Y., Ohta, M., Gupta, A., Shiratsuchi, G., Nozaki, Y., Ashikawa, T., Fujiwara, T., Natsume, T., Kanemaki, M.T., et al. (2019). HsSAS-6-dependent cartwheel assembly ensures stabilization of centriole intermediates. J. Cell Sci. *132*.

Zhang, K., and Smith, G.W. (2015). Maternal control of early embryogenesis in mammals. Reprod Fertil Dev *27*, 880–896.

Zindy, F., den Besten, W., Chen, B., Rehg, J.E., Latres, E., Barbacid, M., Pollard, J.W., Sherr, C.J., Cohen, P.E., and Roussel, M.F. (2001). Control of spermatogenesis in mice by the cyclin D-dependent kinase inhibitors p18(Ink4c) and p19(Ink4d). Mol. Cell. Biol. *21*, 3244–3255.

Master List of References

Abe, S., Nagasaka, K., Hirayama, Y., Kozuka-Hata, H., Oyama, M., Aoyagi, Y., Obuse, C., and Hirota, T. (2011). The initial phase of chromosome condensation requires Cdk1-mediated phosphorylation of the CAP-D3 subunit of condensin II. Genes Dev. *25*, 863–874.

Almawi, A.W., Langlois-Lemay, L., Boulton, S., Rodríguez González, J., Melacini, G., D'Amours, D., and Guarné, A. (2020). Distinct surfaces on Cdc5/PLK Polo-box domain orchestrate combinatorial substrate recognition during cell division. Sci. Rep. *10*, 3379.

Aquino Perez, C., Palek, M., Stolarova, L., von Morgen, P., and Macurek, L. (2020). Phosphorylation of PLK3 is controlled by protein phosphatase 6. Cells *9*.

Arquint, C., and Nigg, E.A. (2016). The PLK4-STIL-SAS-6 module at the core of centriole duplication. Biochem. Soc. Trans. *44*, 1253–1263.

Arquint, C., Sonnen, K.F., Stierhof, Y.-D., and Nigg, E.A. (2012). Cell-cycle-regulated expression of STIL controls centriole number in human cells. J. Cell Sci. *125*, 1342–1352.

Asteriti, I.A., De Mattia, F., and Guarguaglini, G. (2015). Cross-Talk between AURKA and Plk1 in Mitotic Entry and Spindle Assembly. Front. Oncol. *5*, 283.

Attner, M.A., Miller, M.P., Ee, L., Elkin, S.K., and Amon, A. (2013). Polo kinase Cdc5 is a central regulator of meiosis I. Proc. Natl. Acad. Sci. USA *110*, 14278–14283.

Bahassi, E.M., Myer, D.L., McKenney, R.J., Hennigan, R.F., and Stambrook, P.J. (2006). Priming phosphorylation of Chk2 by polo-like kinase 3 (Plk3) mediates its full activation by ATM and a downstream checkpoint in response to DNA damage. Mutat. Res. *596*, 166–176.

Basto, R., Lau, J., Vinogradova, T., Gardiol, A., Woods, C.G., Khodjakov, A., and Raff, J.W. (2006). Flies without centrioles. Cell *125*, 1375–1386.

Baumann, C., Wang, X., Yang, L., and Viveiros, M.M. (2017). Error-prone meiotic division and subfertility in mice with oocyte-conditional knockdown of pericentrin. J. Cell Sci. *130*, 1251–1262.

Bazzi, H., and Anderson, K.V. (2014). Acentriolar mitosis activates a p53-dependent apoptosis pathway in the mouse embryo. Proc. Natl. Acad. Sci. USA *111*, E1491–500.

Bettencourt-Dias, M., Rodrigues-Martins, A., Carpenter, L., Riparbelli, M., Lehmann, L., Gatt, M.K., Carmo, N., Balloux, F., Callaini, G., and Glover, D.M. (2005). SAK/PLK4 is required for centriole duplication and flagella development. Curr. Biol. *15*, 2199–2207.

Burkhardt, S., Borsos, M., Szydlowska, A., Godwin, J., Williams, S.A., Cohen, P.E., Hirota, T., Saitou, M., and Tachibana-Konwalski, K. (2016). Chromosome cohesion established by REC8-cohesin in fetal oocytes is maintained without detectable turnover in oocytes arrested for months in mice. Curr. Biol. *26*, 678–685.

Bury, L., Coelho, P.A., Simeone, A., Ferries, S., Eyers, C.E., Eyers, P.A., Zernicka-Goetz, M., and Glover, D.M. (2017). Plk4 and Aurora A cooperate in the initiation of acentriolar spindle assembly in mammalian oocytes. J. Cell Biol. *216*, 3571–3590.

Challa, K., Fajish V, G., Shinohara, M., Klein, F., Gasser, S.M., and Shinohara, A. (2019). Meiosis-specific prophase-like pathway controls cleavage-independent release of cohesin by Wapl phosphorylation. PLoS Genet. *15*, e1007851.

Champion, L., Linder, M.I., and Kutay, U. (2017). Cellular Reorganization during Mitotic Entry. Trends Cell Biol. *27*, 26–41.

Cizmecioglu, O., Warnke, S., Arnold, M., Duensing, S., and Hoffmann, I. (2008). Plk2 regulated centriole duplication is dependent on its localization to the centrioles and a functional polo-box domain. Cell Cycle *7*, 3548–3555.

Clift, D., and Schuh, M. (2015). A three-step MTOC fragmentation mechanism facilitates bipolar spindle assembly in mouse oocytes. Nat. Commun. *6*, 7217.

Coelho, P.A., Bury, L., Sharif, B., Riparbelli, M.G., Fu, J., Callaini, G., Glover, D.M., and Zernicka-Goetz, M. (2013). Spindle formation in the mouse embryo requires Plk4 in the absence of centrioles. Dev. Cell *27*, 586–597.

Cozza, G., and Salvi, M. (2018). The acidophilic kinases PLK2 and PLK3: structure, substrate targeting and inhibition. Curr Protein Pept Sci *19*, 728–745.

de Cárcer, G., Manning, G., and Malumbres, M. (2011a). From Plk1 to Plk5: functional evolution of polo-like kinases. Cell Cycle *10*, 2255–2262.

de Cárcer, G., Escobar, B., Higuero, A.M., García, L., Ansón, A., Pérez, G., Mollejo, M., Manning, G., Meléndez, B., Abad-Rodríguez, J., et al. (2011b). Plk5, a polo box domain-only protein with specific roles in neuron differentiation and glioblastoma suppression. Mol. Cell. Biol. *31*, 1225–1239.

de Castro, I.J., Gil, R.S., Ligammari, L., Di Giacinto, M.L., and Vagnarelli, P. (2018). CDK1 and PLK1 coordinate the disassembly and reassembly of the nuclear envelope in vertebrate mitosis. Oncotarget *9*, 7763–7773.

Elia, A.E.H., Rellos, P., Haire, L.F., Chao, J.W., Ivins, F.J., Hoepker, K., Mohammad, D., Cantley, L.C., Smerdon, S.J., and Yaffe, M.B. (2003). The molecular basis for phosphodependent substrate targeting and regulation of Plks by the Polo-box domain. Cell *115*, 83–95.

Fernandez-Capetillo, O., Mahadevaiah, S.K., Celeste, A., Romanienko, P.J., Camerini-Otero, R.D., Bonner, W.M., Manova, K., Burgoyne, P., and Nussenzweig, A. (2003). H2AX is required for chromatin remodeling and inactivation of sex chromosomes in male mouse meiosis. Dev. Cell *4*, 497–508.

Fu, W., Chen, H., Wang, G., Luo, J., Deng, Z., Xin, G., Xu, N., Guo, X., Lei, J., Jiang, Q., et al. (2013). Self-assembly and sorting of acentrosomal microtubules by TACC3 facilitate kinetochore capture during the mitotic spindle assembly. Proc. Natl. Acad. Sci. USA *110*, 15295–15300.

Gall, J.G. (1961). Centriole replication. A study of spermatogenesis in the snail Viviparus. J Biophys Biochem Cytol *10*, 163–193.

Gheghiani, L., Loew, D., Lombard, B., Mansfeld, J., and Gavet, O. (2017). PLK1 activation in late G2 sets up commitment to mitosis. Cell Rep. *19*, 2060–2073.

Gopalakrishnan, J., Mennella, V., Blachon, S., Zhai, B., Smith, A.H., Megraw, T.L., Nicastro, D., Gygi, S.P., Agard, D.A., and Avidor-Reiss, T. (2011). Sas-4 provides a scaffold for cytoplasmic complexes and tethers them in a centrosome. Nat. Commun. *2*, 359.

Graser, S., Stierhof, Y.-D., Lavoie, S.B., Gassner, O.S., Lamla, S., Le Clech, M., and Nigg, E.A. (2007). Cep164, a novel centriole appendage protein required for primary cilium formation. J. Cell Biol. *179*, 321–330.

Gray, S., and Cohen, P.E. (2016). Control of meiotic crossovers: from double-strand break formation to designation. Annu. Rev. Genet. *50*, 175–210.

Haarhuis, J.H.I., Elbatsh, A.M.O., and Rowland, B.D. (2014). Cohesin and its regulation: on the logic of X-shaped chromosomes. Dev. Cell *31*, 7–18.

Habedanck, R., Stierhof, Y.-D., Wilkinson, C.J., and Nigg, E.A. (2005). The Polo kinase Plk4 functions in centriole duplication. Nat. Cell Biol. *7*, 1140–1146.

Hamer, G., Roepers-Gajadien, H.L., van Duyn-Goedhart, A., Gademan, I.S., Kal, H.B., van Buul, P.P.W., and de Rooij, D.G. (2003). DNA Double-Strand Breaks and γ-H2AX Signaling in the Testis1. Biol. Reprod. *68*, 628–634.

Handel, M.A. (2004). The XY body: a specialized meiotic chromatin domain. Exp. Cell Res. *296*, 57–63.

Harris, R.M., Weiss, J., and Jameson, J.L. (2011). Male hypogonadism and germ cell loss caused by a mutation in Polo-like kinase 4. Endocrinology *152*, 3975–3985.

Hirono, M. (2014). Cartwheel assembly. Philos. Trans. R. Soc. Lond. B, Biol. Sci. *369*.

Hunter, N., Börner, G.V., Lichten, M., and Kleckner, N. (2001). Gamma-H2AX illuminates meiosis. Nat. Genet. *27*, 236–238.

Hwang, G., Sun, F., O'Brien, M., Eppig, J.J., Handel, M.A., and Jordan, P.W. (2017). SMC5/6 is required for the formation of segregation-competent bivalent chromosomes during meiosis I in mouse oocytes. Development *144*, 1648–1660.

Hwang, G., Verver, D.E., Handel, M.A., Hamer, G., and Jordan, P.W. (2018a). Depletion of SMC5/6 sensitizes male germ cells to DNA damage. Mol. Biol. Cell *29*, 3003–3016.

Hwang, G.H., Hopkins, J.L., and Jordan, P.W. (2018b). Chromatin Spread Preparations for the Analysis of Mouse Oocyte Progression from Prophase to Metaphase II. J. Vis. Exp. *132*, e56736.

Inselman, A.L., Nakamura, N., Brown, P.R., Willis, W.D., Goulding, E.H., and Eddy, E.M. (2010). Heat shock protein 2 promoter drives Cre expression in spermatocytes of transgenic mice. Genesis *48*, 114–120.

Jackman, M., Lindon, C., Nigg, E.A., and Pines, J. (2003). Active cyclin B1-Cdk1 first appears on centrosomes in prophase. Nat. Cell Biol. *5*, 143–148.

Jessberger, R. (2012). Age-related aneuploidy through cohesion exhaustion. EMBO Rep. *13*, 539–546.

Jordan, P.W., Karppinen, J., and Handel, M.A. (2012). Polo-like kinase is required for synaptonemal complex disassembly and phosphorylation in mouse spermatocytes. J. Cell Sci. *125*, 5061–5072.

Joukov, V., and De Nicolo, A. (2018). Aurora-PLK1 cascades as key signaling modules in the regulation of mitosis. Sci. Signal. *11*.

Kim, J.H., Shim, J., Ji, M.-J., Jung, Y., Bong, S.M., Jang, Y.-J., Yoon, E.-K., Lee, S.-J., Kim, K.G., Kim, Y.H., et al. (2014). The condensin component NCAPG2 regulates microtubule-kinetochore attachment through recruitment of Polo-like kinase 1 to kinetochores. Nat. Commun. *5*, 4588.

Kirkham, M., Müller-Reichert, T., Oegema, K., Grill, S., and Hyman, A.A. (2003). SAS-4 is a C. elegans centriolar protein that controls centrosome size. Cell *112*, 575–587.

Ko, M.A., Rosario, C.O., Hudson, J.W., Kulkarni, S., Pollett, A., Dennis, J.W., and Swallow, C.J. (2005). Plk4 haploinsufficiency causes mitotic infidelity and carcinogenesis. Nat. Genet. *37*, 883–888.

Kuriyama, R. (2009). Centriole assembly in CHO cells expressing Plk4/SAS6/SAS4 is similar to centriogenesis in ciliated epithelial cells. Cell Motil. Cytoskeleton *66*, 588–596.

Lan, Z.-J., Xu, X., and Cooney, A.J. (2004). Differential oocyte-specific expression of Cre recombinase activity in GDF-9-iCre, Zp3cre, and Msx2Cre transgenic mice. Biol. Reprod. *71*, 1469–1474.

Lee, B.H., and Amon, A. (2003). Role of Polo-like kinase CDC5 in programming meiosis I chromosome segregation. Science *300*, 482–486.

Lee, K., and Rhee, K. (2011). PLK1 phosphorylation of pericentrin initiates centrosome maturation at the onset of mitosis. J. Cell Biol. *195*, 1093–1101.

Lee, I.-W., Jo, Y.-J., Jung, S.-M., Wang, H.-Y., Kim, N.-H., and Namgoong, S. (2017). Distinct roles of Cep192 and Cep152 in acentriolar MTOCs and spindle formation during mouse oocyte maturation. FASEB J.

Leidel, S., and Gönczy, P. (2003). SAS-4 is essential for centrosome duplication in C elegans and is recruited to daughter centrioles once per cell cycle. Dev. Cell *4*, 431–439.

Li, L., Zheng, P., and Dean, J. (2010). Maternal control of early mouse development. Development *137*, 859–870.

Liao, Y., Lin, D., Cui, P., Abbasi, B., Chen, C., Zhang, Z., Zhang, Y., Dong, Y., Rui, R., and Ju, S. (2018). Polo-like kinase 1 inhibition results in misaligned chromosomes and aberrant spindles in porcine oocytes during the first meiotic division. Reprod. Domest. Anim. *53*, 256–265.

Linder, M.I., Köhler, M., Boersema, P., Weberruss, M., Wandke, C., Marino, J., Ashiono, C., Picotti, P., Antonin, W., and Kutay, U. (2017). Mitotic Disassembly of Nuclear Pore Complexes Involves CDK1- and PLK1-Mediated Phosphorylation of Key Interconnecting Nucleoporins. Dev. Cell *43*, 141–156.e7.

Little, T.M. and Jordan, P.W. (2020). PLK1 is required for chromosome compaction and microtubule organization in mouse oocytes. Mol. Biol. Cell. *31* (12), 1201-1313.

Loncarek, J., Sluder, G., and Khodjakov, A. (2007). Centriole biogenesis: a tale of two pathways. Nat. Cell Biol. *9*, 736–738.

Lu, L.-Y., Wood, J.L., Minter-Dykhouse, K., Ye, L., Saunders, T.L., Yu, X., and Chen, J. (2008). Polo-like kinase 1 is essential for early embryonic development and tumor suppression. Mol. Cell. Biol. *28*, 6870–6876.

Luo, Y.-B., and Kim, N.-H. (2015). PLK4 is essential for meiotic resumption in mouse oocytes. Biol. Reprod. *92*, 101.

Lyndaker, A.M., Lim, P.X., Mleczko, J.M., Diggins, C.E., Holloway, J.K., Holmes, R.J., Kan, R., Schlafer, D.H., Freire, R., Cohen, P.E., et al. (2013). Conditional inactivation of the DNA damage response gene Hus1 in mouse testis reveals

separable roles for components of the RAD9-RAD1-HUS1 complex in meiotic chromosome maintenance. PLoS Genet. *9*, e1003320.

Ma, H., Marti-Gutierrez, N., Park, S.-W., Wu, J., Lee, Y., Suzuki, K., Koski, A., Ji, D., Hayama, T., Ahmed, R., et al. (2017). Correction of a pathogenic gene mutation in human embryos. Nature *548*, 413–419.

Ma, S., Charron, J., and Erikson, R.L. (2003). Role of Plk2 (Snk) in mouse development and cell proliferation. Mol. Cell. Biol. *23*, 6936–6943.

MacLennan, M., Crichton, J.H., Playfoot, C.J., and Adams, I.R. (2015). Oocyte development, meiosis and aneuploidy. Semin. Cell Dev. Biol. *45*, 68–76.

Manil-Ségalen, M., Łuksza, M., Kanaan, J., Marthiens, V., Lane, S.I.R., Jones, K.T., Terret, M.-E., Basto, R., and Verlhac, M.-H. (2018). Chromosome structural anomalies due to aberrant spindle forces exerted at gene editing sites in meiosis. J. Cell Biol. *217*, 3416–3430.

Mardin, B., Agircan, F., Lange, C., and Schiebel, E. (2011). Plk1 Controls the Nek2A-PP1[gamma] Antagonism in Centrosome Disjunction. Curr. Biol. *21*, 1145–1151.

Marjanović, M., Sánchez-Huertas, C., Terré, B., Gómez, R., Scheel, J.F., Pacheco, S., Knobel, P.A., Martínez-Marchal, A., Aivio, S., Palenzuela, L., et al. (2015). CEP63 deficiency promotes p53-dependent microcephaly and reveals a role for the centrosome in meiotic recombination. Nat. Commun. *6*, 7676.

Marthiens, V., Rujano, M.A., Pennetier, C., Tessier, S., Paul-Gilloteaux, P., and Basto, R. (2013). Centrosome amplification causes microcephaly. Nat. Cell Biol. *15*, 731–740.

Martino, L., Morchoisne-Bolhy, S., Cheerambathur, D.K., Van Hove, L., Dumont, J., Joly, N., Desai, A., Doye, V., and Pintard, L. (2017). Channel Nucleoporins Recruit PLK-1 to Nuclear Pore Complexes to Direct Nuclear Envelope Breakdown in C. elegans. Dev. Cell *43*, 157–171.e7.

McLamarrah, T.A., Buster, D.W., Galletta, B.J., Boese, C.J., Ryniawec, J.M., Hollingsworth, N.A., Byrnes, A.E., Brownlee, C.W., Slep, K.C., Rusan, N.M., et al. (2018). An ordered pattern of Ana2 phosphorylation by Plk4 is required for centriole assembly. J. Cell Biol. *217*, 1217–1231.

Mishra, R.K., Chakraborty, P., Arnaoutov, A., Fontoura, B.M.A., and Dasso, M. (2010). The Nup107-160 complex and gamma-TuRC regulate microtubule polymerization at kinetochores. Nat. Cell Biol. *12*, 164–169.

Mogessie, B., Scheffler, K., and Schuh, M. (2018). Assembly and positioning of the oocyte meiotic spindle. Annu. Rev. Cell Dev. Biol. *34*, 381–403.

Moyer, T.C., and Holland, A.J. (2019). PLK4 promotes centriole duplication by phosphorylating STIL to link the procentriole cartwheel to the microtubule wall. Elife *8*.

Myer, D.L., Robbins, S.B., Yin, M., Boivin, G.P., Liu, Y., Greis, K.D., Bahassi, E.M., and Stambrook, P.J. (2011). Absence of polo-like kinase 3 in mice stabilizes Cdc25A after DNA damage but is not sufficient to produce tumors. Mutat. Res. *714*, 1–10.

Nagaoka, S.I., Hassold, T.J., and Hunt, P.A. (2012). Human aneuploidy: mechanisms and new insights into an age-old problem. Nat. Rev. Genet. *13*, 493–504.

Namgoong, S., and Kim, N.-H. (2018). Meiotic spindle formation in mammalian oocytes: implications for human infertility. Biol. Reprod. *98*, 153–161.

Nigg, E.A. (2007). Centrosome duplication: of rules and licenses. Trends Cell Biol. *17*, 215–221.

Oakberg, E.F. (1956). Duration of spermatogenesis in the mouse and timing of stages of the cycle of the seminiferous epithelium. Am J. Anat. *99*, 507–516.

Pahlavan, G., Polanski, Z., Kalab, P., Golsteyn, R., Nigg, E.A., and Maro, B. (2000). Characterization of polo-like kinase 1 during meiotic maturation of the mouse oocyte. Dev. Biol. *220*, 392–400.

Pihan, G.A. (2013). Centrosome dysfunction contributes to chromosome instability, chromoanagenesis, and genome reprograming in cancer. Front. Oncol. *3*, 277.

Prosser, S.L., and Pelletier, L. (2017). Mitotic spindle assembly in animal cells: a fine balancing act. Nat. Rev. Mol. Cell Biol. *18*, 187–201.

Riparbelli, M.G., and Callaini, G. (2011). Male gametogenesis without centrioles. Dev. Biol. *349*, 427–439.

Riparbelli, M.G., Persico, V., Dallai, R., and Callaini, G. (2020). Centrioles and Ciliary Structures during Male Gametogenesis in Hexapoda: Discovery of New Models. Cells *9*.

Rodrigues-Martins, A., Riparbelli, M., Callaini, G., Glover, D.M., and Bettencourt-Dias, M. (2008). From centriole biogenesis to cellular function: centrioles are essential for cell division at critical developmental stages. Cell Cycle *7*, 11–16.

Rosario, C.O., Ko, M.A., Haffani, Y.Z., Gladdy, R.A., Paderova, J., Pollett, A., Squire, J.A., Dennis, J.W., and Swallow, C.J. (2010). Plk4 is required for cytokinesis and maintenance of chromosomal stability. Proc. Natl. Acad. Sci. USA *107*, 6888–6893.

Sadate-Ngatchou, P.I., Payne, C.J., Dearth, A.T., and Braun, R.E. (2008). Cre recombinase activity specific to postnatal, premeiotic male germ cells in transgenic mice. Genesis *46*, 738–742.

Schatten, H., and Sun, Q.-Y. (2015). Centrosome and microtubule functions and dysfunctions in meiosis: implications for age-related infertility and developmental disorders. Reprod Fertil Dev *27*, 934–943.

Severance, A.L., and Latham, K.E. (2018). Meeting the meiotic challenge: Specializations in mammalian oocyte spindle formation. Mol. Reprod. Dev. *85*, 178–187.

Simerly, C., Manil-Ségalen, M., Castro, C., Hartnett, C., Kong, D., Verlhac, M.-H., Loncarek, J., and Schatten, G. (2018). Separation and loss of centrioles from primordidal germ cells to mature oocytes in the mouse. Sci. Rep. *8*, 12791.

So, C., Seres, K.B., Steyer, A.M., Mönnich, E., Clift, D., Pejkovska, A., Möbius, W., and Schuh, M. (2019). A liquid-like spindle domain promotes acentrosomal spindle assembly in mammalian oocytes. Science *364*.

Solc, P., Kitajima, T.S., Yoshida, S., Brzakova, A., Kaido, M., Baran, V., Mayer, A., Samalova, P., Motlik, J., and Ellenberg, J. (2015). Multiple requirements of PLK1 during mouse oocyte maturation. PLoS One *10*, e0116783.

Sonn, S., Oh, G.T., and Rhee, K. (2011). Nek2 and its substrate, centrobin/Nip2, are required for proper meiotic spindle formation of the mouse oocytes. Zygote *19*, 15–20.

Sumiyoshi, E., Sugimoto, A., and Yamamoto, M. (2002). Protein phosphatase 4 is required for centrosome maturation in mitosis and sperm meiosis in C. elegans. J. Cell Sci. *115*, 1403–1410.

Sun, S.-C., Liu, H.-L., and Sun, Q.-Y. (2012). Survivin regulates Plk1 localization to kinetochore in mouse oocyte meiosis. Biochem. Biophys. Res. Commun. *421*, 797–800.

Torosantucci, L., De Luca, M., Guarguaglini, G., Lavia, P., and Degrassi, F. (2008). Localized RanGTP accumulation promotes microtubule nucleation at kinetochores in somatic mammalian cells. Mol. Biol. Cell *19*, 1873–1882.

Verloes, A., Drunat, S., Gressens, P., and Passemard, S. (1993). Primary Autosomal Recessive Microcephalies and Seckel Syndrome Spectrum Disorders. In GeneReviews, R.A. Pagon, M.P. Adam, H.H. Ardinger, S.E. Wallace, A. Amemiya, L.J. Bean, T.D. Bird, C.-T. Fong, H.C. Mefford, R.J. Smith, et al., eds. (Seattle (WA): University of Washington, Seattle).

Vlijm, R., Li, X., Panic, M., Rüthnick, D., Hata, S., Herrmannsdörfer, F., Kuner, T., Heilemann, M., Engelhardt, J., Hell, S.W., et al. (2018). STED nanoscopy of the

centrosome linker reveals a CEP68-organized, periodic rootletin network anchored to a C-Nap1 ring at centrioles. Proc. Natl. Acad. Sci. USA *115*, E2246–E2253.

Wang, H., Choe, M.H., Lee, I.-W., Namgoong, S., Kim, J.-S., Kim, N.-H., and Oh, J.S. (2017). CIP2A acts as a scaffold for CEP192-mediated microtubule organizing center assembly by recruiting Plk1 and aurora A during meiotic maturation. Development *144*, 3829–3839.

Webster, A., and Schuh, M. (2017). Mechanisms of aneuploidy in human eggs. Trends Cell Biol. *27*, 55–68.

Wellard, S.R., Hopkins, J., and Jordan, P.W. (2018). A seminiferous tubule squash technique for the cytological analysis of spermatogenesis using the mouse model. J. Vis. Exp. *132*, e56453.

Willett, R., Martina, J.A., Zewe, J.P., Wills, R., Hammond, G.R.V., and Puertollano, R. (2017). TFEB regulates lysosomal positioning by modulating TMEM55B expression and JIP4 recruitment to lysosomes. Nat. Commun. *8*, 1580.

Xie, S., Wu, H., Wang, Q., Cogswell, J.P., Husain, I., Conn, C., Stambrook, P., Jhanwar-Uniyal, M., and Dai, W. (2001). Plk3 functionally links DNA damage to cell cycle arrest and apoptosis at least in part via the p53 pathway. J. Biol. Chem. *276*, 43305–43312.

Xiong, B., Sun, S.-C., Lin, S.-L., Li, M., Xu, B.-Z., OuYang, Y.-C., Hou, Y., Chen, D.-Y., and Sun, Q.-Y. (2008). Involvement of Polo-like kinase 1 in MEK1/2-regulated spindle formation during mouse oocyte meiosis. Cell Cycle *7*, 1804–1809.

Xu, E.Y., Kim, S., Replogle, K., Rine, J., and Rivier, D.H. (1999). Identification of SAS4 and SAS5, two genes that regulate silencing in Saccharomyces cerevisiae. Genetics *153*, 13–23.

Yoshiba, S., Tsuchiya, Y., Ohta, M., Gupta, A., Shiratsuchi, G., Nozaki, Y., Ashikawa, T., Fujiwara, T., Natsume, T., Kanemaki, M.T., et al. (2019). HsSAS-6-dependent cartwheel assembly ensures stabilization of centriole intermediates. J. Cell Sci. *132*.

Zhang, K., and Smith, G.W. (2015). Maternal control of early embryogenesis in mammals. Reprod Fertil Dev *27*, 880–896.

Zhang, X., Chen, Q., Feng, J., Hou, J., Yang, F., Liu, J., Jiang, Q., and Zhang, C. (2009). Sequential phosphorylation of Nedd1 by Cdk1 and Plk1 is required for targeting of the gammaTuRC to the centrosome. J. Cell Sci. *122*, 2240–2251.

Zhang, Y., Wang, Y., Wei, Y., Ma, J., Peng, J., Wumaier, R., Shen, S., Zhang, P., and Yu, L. (2015). The tumor suppressor proteins ASPP1 and ASPP2 interact with C-Nap1 and regulate centrosome linker reassembly. Biochem. Biophys. Res. Commun. *458*, 494–500.

Zhang, Z., Chen, C., Ma, L., Yu, Q., Li, S., Abbasi, B., Yang, J., Rui, R., and Ju, S. (2017). Plk1 is essential for proper chromosome segregation during meiosis I/meiosis II transition in pig oocytes. Reprod Biol Endocrinol *15*, 69.

Zindy, F., den Besten, W., Chen, B., Rehg, J.E., Latres, E., Barbacid, M., Pollard, J.W., Sherr, C.J., Cohen, P.E., and Roussel, M.F. (2001). Control of spermatogenesis in mice by the cyclin D-dependent kinase inhibitors p18(Ink4c) and p19(Ink4d). Mol. Cell. Biol. *21*, 3244–3255.

CURRICULUM VITAE
TARA MARIE LITTLE, B.A., Ph.D.

EDUCATION

JOHNS HOPKINS SCHOOL OF PUBLIC HEALTH (JHSPH)
Baltimore, MD
Doctor of Philosophy, Mentor: Dr. Philip Jordan
Sep. 2015-Aug. 2020

- Field of Study: Biochemistry and Molecular Biology
- Thesis Topic: *Regulators of Mammalian Meiosis*

HOOD COLLEGE
Frederick, MD
Bachelor of Arts
Sep. 2011-May 2015

- Major: Biochemistry, Final GPA: 3.48

SERVICE, AWARDS AND ACADEMIC ACHIEVEMENT

- 2019-2020 JHSPH Doctoral Student Council: *Representative*
- 2018-2020 JHSPH Dept. of Biochemistry and Molecular Biology *Diversity and Inclusion Committee*
- 2018-2020 NIH RTCD: *Training Grant Appointee*
- 2014 NIH Undergraduate Research Symposium: *Poster Award Winner*
- 2014 Mortar Board National College Honors Society
- 2013-2014 Hood College Academic Judicial Council: *Chair*
- 2013 Hood College Gamma Sigma Epsilon Chemistry Honors Society
- 2012-2015 Hood College Gender Equality Club: *Secretary*
- 2012 Hood College Ionic Society
- 2011-2015 Hood College Chemistry Club: *President*
- 2011-2015 Hood College: *Hodson Trust Scholarship Recipient*
- 2011-2015 Maryland Higher Education Commission: *Scholarship Recipient*
- 2011 Hood College Alpha Lambda Delta Honors Society

ACADEMIC SOCIETY MEMBERSHIPS

American Society of Cell Biology

SELECTED PUBLICATIONS

- **Little TM** and Jordan PW. PLK1 is required for chromosome compaction and microtubule organization in mouse oocytes. *MBoC*. 2020; 31.
- Meyer RL, Zhandosova AD, **Biser TM**, et al. Photochemical dynamics of a trimethyl-phosphine derivatized [FeFe]-hydrogenase model compound. *J Chem Phys*. 2018; 512: 135-145.
- Frey KG, **Biser TM**, et al. Bioinformatic characterization of mosquito viromes within the Eastern United States and Puerto Rico: Discovery of novel viruses. *Evol Bioinform.* 2016; 12 (Suppl 2): 1-12.

ORAL PRESENTATIONS

- ***Investigating the Role of PLK1 in Mammalian Meiosis***
  April 2019 – JHSPH Dept. of Biochemistry and Molecular Biology; Annual Retreat
  December 2018 – JHU Chromatin and Chromosomes Workshop
- ***Developing Mouse Models for Pachyonychia Congenita Type I***
  December 2016 – JHSPH & School of Medicine Keratin Joint Lab Meeting
- ***Conditional Mutation of Plk1 in Primary Spermatocytes***
  April 2016 – JHSPH Dept. of Biochemistry and Molecular Biology; Annual Retreat

POSTER PRESENTATIONS

- ***PLK1 is Required for Normal Chromosome Compaction and Microtubule Organization in Mouse Oocytes***
  December 2019 – American Society of Cell Biology Annual Meeting
- ***Investigating the Role of PLK1 in Mammalian Meiosis***
  April 2019 – JHU Women in STEM Symposium
  September 2018 – Cold Spring Harbor Germ Cells Meeting
- ***Investigating the Role of PLK1 in Mammalian Oogenesis***
  April 2018 – JHSPH Dept. of Biochemistry and Molecular Biology; Annual Retreat
- ***Developing Novel Mouse Models for Pachyonychia Congenita***
  April 2017 – JHSPH Dept. of Biochemistry and Molecular Biology; Annual Retreat
- ***Identification of Previously Unsequenced Viruses from Wild-Caught Mosquitoes by Metagenomic Sequencing***
  March 2015 – American Chemical Society National Meeting & Exposition
- ***Ultrafast Time-Resolved UV-Pump/IR-Probe Spectroscopy of [FeFe]-Hydrogenase Model Compounds***
  March 2014 – American Chemical Society National Meeting & Exposition

GRADUATE TEACHING AND MENTORING EXPERIENCE

- **Courses:** Fundamentals of Reproductive Biology (2017-2019)
- **Trainees:** Anagha Sadasivan (MPH, 2017-2018), Abhinaya Ganesan (MPH, 2018), Christopher Shults (MPH, 2018-2019), Jingwen Xu (Visiting Scholar, 2019-2020)

PAST EXPERIENCE AND EMPLOYMENT

- ***May 2016 – June 2017:*** Ph.D. Student, Coulombe Lab, JHSPH
- ***May 2014 – August 2015:*** Intern, Naval Medical Research Center
- ***August 2014 – May 2015:*** Volunteer, Alzheimer's Association
- ***August 2013 – May 2014:*** Volunteer, Frederick Memorial Hospital
- ***May 2013 – September 2013:*** Intern, Hood College Summer Research Program